RECONSTRUCTION OF METABOLIC BRAIN MODEL WITH THE AID OF PHYSIOLOGICALLY BASED PHARMACOKINETIC MODELLING IN THE PRESENCE OF AUTISM SPECTRUM DISORDER

by

Sena Erimli

B.S., Chemical Engineering, Boğaziçi University, 2018

Submitted to the Institute for Graduate Studies in
Science and Engineering in partial fulfillment of
the requirements for the degree of
Master of Science

Graduate Program in Chemical Engineering

Boğaziçi University

2022

ACKNOWLEDGEMENTS

I would like to acknowledge and offer my deepest thanks, respect, and gratitude to my supervisor Prof. Kutlu Ülgen. Without her and her guidance, I could not have finished my master's degree. I am grateful for her patience, understanding, and embracing despite all the surprises in my life. I will never forget how she supported me and gently guided me through safe "graduated" waters. I would also like to express my respect to my thesis committee members Assist. Prof. Betül Uralcan and Assist. Prof. Gülçin Tuğcu for devoting their precious time and effort to my thesis and providing guidance and recommendations.

I love, appreciate, and thank my beloved family. I always feel lucky to have people like you around me. My son, Can Deniz and my sister Ülke Neris. You are the first and only children I genuinely like and love. You are the real reasons I have never given up on my dreams. To show you daring to dream is extremely hard, but seeing those sparkles in your eyes is worth every challenge.

My beloved husband, Cemil. You deserve a parade of gratitude made of rainbows and the thousand sunny. You are my most significant support, mentor, and inspiration. Thank you for your belief in me and the miracles you create every single day. Without you studying with me by staying awake till morning, without you always giving me the best advice, life would not be this colorful and joyful.

I love to thank my mother, who always listens to me and be there for me. I refill with every hug, every call, every kiss from you. Thank you for being my emotional support; thank you for just being you. I appreciate every help from my father, Önder, my brother, Uğur, my mother-in-law and father-in-law, Şemse, and Mehmet. Thank you for showing up in my darkest times. I especially thank İlkay İrem Özbek for all her support and guidance through my thesis process. You are an exceptional and valuable person under the cape of a hero. I am also grateful for the help and guidance from Mustafa Sertbaş.

I acknowledge this thesis has been financially supported by TUSEB project 2324.

ABSTRACT

RECONSTRUCTION OF METABOLIC BRAIN MODEL WITH THE AID OF PHYSIOLOGICALLY BASED PHARMACOKINETIC MODELLING IN PRESENCE OF AUTISM SPECTRUM DISORDER

Autism spectrum disorder (ASD) is a neurodevelopmental disorder with only symptomatic medical treatment with increasing prevalence. This study aims to reconstruct a genome-scale metabolic brain model that is expanded via genes and reactions related to ASD and observe changes in dopamine D2 receptors in the presence of antipsychotics. For this aim, iMS570, iNL403, and MODEL1608180000 are merged. After standardization, duplicate reaction removals, deletion of zero flux reactions, and expanding model with ASD-related genes and reactions, the final model consists of 1638 reactions, 1358 metabolites, and 756 genes. For further investigations of the autism-specific brain model, transcriptome gene expression data GSE28475 is prepared and integrated. Autism-specific brain model shows mitochondrial and glutaminergic dysfunctions. Final 18360 unique genes are assigned as up-or down-regulated based on threshold determined by downregulated SHANK3 expression and 30% of averages of gene expression data. Additionally, the physiology-based pharmacokinetic (PBPK) model of risperidone and its metabolite paliperidone is simulated. Both drugs are antipsychotics that are used in ASD symptoms. First, simulations are performed to observe population density, CYP2D6 subtypes, ethnicity, total hepatic clearance, and P-gp concentration changes for 2 mg risperidone. PBPK simulation results of experimental articles were in the range of literature findings. Receptor occupancy simulations with chronic dosing underestimate plasma concentrations, but results are still in the range. With down-regulation of the SLC6A3 dopamine transporter gene, which is used to mimic DRD2 gene, proportional to receptor occupancy findings, the effect of risperidone on autism-specific brain model is investigated. Glutaminergic neurotransmission is decreased below healthy brain level, and mitochondrial dysfunction was relieved but still not in the healthy range. Reconstruction of ASD-specific brain model with PBPK modeling enhancement is promising work to better under disease mechanism.

ÖZET

OTİZM SPEKTRUM BOZUKLUĞU VARLIĞINDA BEYİN METABOLİK MODELİNİN FİZYOLOJİ BAZLI FARMAKOKİNETİK MODELİ YARDIMIYLA OLUŞTURULMASI

Otizm spektrum bozukluğu (OSB) medikal olarak sadece semptomatik tedavisi olan ve prevalansı her yıl artan nörogelişimsel bir bozukluktur. Bu çalışma, OSB ile ilişkilendirilen genler ve reaksiyonlar aracılığıyla genişletilmiş genom ölçekli beyin metabolik modelinin oluşturulmasını ve antipsikotiklerin varlığında dopamin D2 reseptörlerindeki değişiklikleri gözlemlemeyi amaçlar. Bu amaçla iMS570, iNL403 ve MODEL1608180000 birleştirildi. Standardizasyon, reaksiyon silinmesi ve ASD ile ilgili genler ve reaksiyonlarla beyin modeli geliştirildi. Nihai model 1638 reaksiyon, 1358 metabolit ve 756 genden oluşur. Otizme özgü beyin modelinde mitokondriyal ve glutamerjik disfonksiyon gözlemlendi. Modeli daha ayrıntılı incelemek için transkriptom gen ekspresyon verileri, GSE28475 hazırlandı. Hazırlanan 18360 benzersiz genin ekspresyon verileri, aşağı regüle edilmiş SHANK3 geninin ekspresyon verisi birinci eşik ve hazırlanan gen ekspresyon verilerinin ortalamalarının %30'u ikinci eşik olarak iki ayrı dosyaya atandı. Ek olarak, OSB semptomlarında kullanılan antipsikotik risperidon ve metaboliti paliperidonun PBPK modeli simüle edildi. İlk simülasyonlar, popülasyon yoğunluğu, CYP2D6 alt tipleri, etnik köken, toplam karaciğer klirensi ve P-gp konsantrasyon değişikliklerini gözlemlemek için 2 mg risperidone ile simüle edildi. Deneysel makalelerin PBPK simülasyonları literatür verileriyle uyumludur. Kronik doz alımıyla reseptör doluluk simülasyonları sonucu plazma konsantrasyonları daha düşük tahmin edilmiştir, ancak sonuçlar hala literatür aralığı içindedir. DRD2 genini taklit etmek için kullanılan SLC6A3 dopamin transport geninin reseptör doluluk bulgularıyla orantılı olarak aşağı regülasyonu ile risperidonun otizme özgü beyin modeline etkisi araştırıldı. Glutamaterjik nörotransmisyon, sağlıklı beyin seviyesinin altına düştü ve mitokondriyal disfonksiyon azaldı, ancak yine de sağlıklı aralıkta değildir. ASD'ye özgü beyin modelinin PBPK modeli verileriyle geliştirilmesi, hastalık mekanizmasını daha iyi anlamak için umut verici bir çalışmadır.

TABLE OF CONTENTS

LIST OF FIGURES

LIST OF TABLES

LIST OF ACRONYMS/ABBREVIATIONS

ASD	Autism Spectrum Disorder
GEMs	Genome-scale Metabolic Models
KEGG	Kyoto Encyclopedia of Genes and Genomes
PBPK	Physiology Based Pharmacokinetic Modelling
CYP	Cytochrome P450
BBB	Blood-Brain Barrier
RT-PCR	Reverse Transcription-Polymerase Chain Reaction
P-gp	P-glycoprotein
RO	Receptor occupancy
ADME	Absorption, Distribution, Metabolism, and Excretion
BMI	Body mass index
HMR	Human Metabolic Reaction
HMDB	Human Metabolome Database
FBA	Flux Balance Analysis
FVA	Flux Variability Analysis
c	Objective function
S	Stoichiometric matrix
k_{off}	Dissociation rate constant
K_d	Dissociation constant
$CL_{Hepatic}$	Hepatic clearance
CL_{Renal}	Renal clearance
K_m	Michaelis-Menten constant
V_{max}	The maximum rate of the enzyme
m	Metabolite vector
n	Reaction vector
v	Flux vector
Z	Objective function
x	Concentration vector

1. INTRODUCTION

Autism spectrum disorder (ASD) is a neurodevelopmental disorder that affects one child out of 54. Even the mechanism of the disorder is not well-known, there are possible culprits for the root of the disease: genetic factors, environmental factors, and biochemical factors. In the thesis, environmental factors, primarily genetic factors, ASD-related genes, and metabolisms, were investigated through reconstruction of the metabolic brain network. This study aims to reconstruct a genome-scale metabolic model in the presence of ASD-related genes and reactions and enhance the model with dopamine D2 receptor occupancy.

Genome-scale metabolic models (GEMs) allow researchers to computerize gene-protein-reaction relation and manipulate the model with certain constraints. Reconstruction of metabolic brain model is performed by merging and comparing three main brain GEMs, iMS570, iNL403, and MODEL1608180000. Combined model consists of five compartments: Astrocyte cytosol (_A[c]), neuron cytosol (_N[c]), astrocyte mitochondria (_A[m]), neuron mitochondria (_N[m]) and intercellular space ([s]). iMS570 by Sertbas et al., 2014 (630 reactions, 524 metabolites, 570 genes) is expanded to 1638 reactions, 1358 metabolites, and 756 genes. For this purpose, the Cobra Toolbox of MATLAB is used. Transcriptome data for integration is extracted from GSE28475 and prepared and analyzed by GIMME. Final autism-specific model is reconstructed after minimization of internal reactions fluxes.

One of the medical treatments of ASD, risperidone, is investigated through Physiology Based Pharmacokinetic (PBPK) Modelling. PBPK modeling helps predict the pharmacokinetics of a drug and drug-drug or drug-receptor relations. PBPK modeling is performed in PK-Sim. The effects of individual count in a population, ethnicity, CYP2D6 subtype enzyme kinetics, P-gp reference calculation, and hepatic clearance of paliperidone are investigated. Then, the data in seven experimental articles with three different ethnicities (European, White American, and Asian) are used to validate PBPK model simulations. Maximum plasma concentration, time passed when maximum concentration is achieved, and half-lives of risperidone and paliperidone are analyzed. Receptor occupancy studies with

eight schizophrenic patients are simulated, and plasma concentration and receptor occupancy trends are investigated. Receptor occupancy data is integrated into the autistic brain model.

A detailed explanation of the steps through the reconstructed metabolic brain model and risperidone PBPK model can be found in the “Methods” section. Examination of reconstructed autism-specific metabolic brain model, effects of population demographics, enzyme kinetics, transporter concentration on PBPK modeling of risperidone, investigation of 7 experimental articles and on the pharmacokinetics of risperidone and paliperidone, receptor occupancy observation in chronic dosing, and integration and analysis of receptor occupancy data to autism-specific brain model are thoroughly explained in the “Results and Discussion” section. Main simulation results, further development, and suggestions are detailed in “Conclusion and Recommendations.”

2. THEORETICAL BACKGROUND

2.1. Autism Spectrum Disorder

Autism Spectrum Disorder (ASD) was firstly described in 1943 by the American child psychiatrist Leo Kanner [1, 2], and the effects of the disorder were categorized under three criteria: Social communication; Interaction; Restrictive and repetitive behavior, interest or activities [1–3]. For 2014, ASD prevalence was one in 54 for 8-year-old children, by the American Centers for Disease Control and Prevention report. For 200, ASD prevalence was one in 150. In 14 years, prevalence increased approximately 150% [4].

Heterogenic distribution of the disorder and lack of effective biomarkers obstructs the diagnosis and treatment process. Currently, the best effective treatment is behavioral therapy. However, due to the difficulty of diagnosis and the cost of special education, there is a need for treatment methods for the cause of the disease. The annual expenditure of the USA, which provides the most comprehensive service in the field of ASD, is 236-262 billion dollars [5]. In Turkey, The Ministry of Family and Social Policies has founded a "National Action Plan for Individuals with Autism Spectrum Disorders." It has initiated the action plan for the diagnosis of ASD, informing individuals and families and helping individuals be active participants in daily life. The "Autism Screening Project," which was created with the European Union grant of the Ministry of Health to disseminate early diagnosis, is also becoming widespread. Tohum Autism Foundation and other similar foundations have educational and behavioral therapy centric projects. Current projects do not include pharmacological treatment or drug targets [6].

2.1.1. Genetic Factors

Hereditary factors have caused the main focus of research to be genetic studies. Gender-based prevalence difference strengthens this point of view. ASD prevalence of boys was one in 42, and girls were one in 189. However, when mental retardation is severe, the boy/girl ratio is close to one. Mental retardation is more common in girls with ASD [4, 7].

The incidence of this disorder in siblings of children with ASD is reported to be 3% [8]. It has been observed that if one of the identical twins has autism, the probability of the other having ASD is higher than that of fraternal twins [9, 10]. However, heterogeneity of the research results indicates that expression of the disorder may have occurred as a result of the interaction of multiple gene loci rather than one gene. Every gene interacts with other responsible genes and affects the disorder differently. When the risk in alleles reaches a certain threshold, the individual becomes susceptible to the occurrence of the disorder [11, 12].

Genes associated with ASD were collected from various articles [2, 13, 14–21, 22–30]. The reactions which are catalyzed by the proteins coded by those genes were gathered subcellular location-based from “The Human Protein Atlas” [31], “UniProt” [32], and “KEGG: Kyoto Encyclopedia of Genes and Genomes” [33]. The collection is given in Table 2.1.

Table 2.1. Genes associated with autism spectrum disorder.

Gene	**Subcellular Location**	**Biological Process**	**EC Number**
ACHE	Golgi apparatus, Vesicles	Neurotransmitter degradation	3.1.1.7
ASH1L	Nucleoplasm, Golgi apparatus	Transcription, Transcription regulation	2.1.1.354
B3GALNT2	Golgi apparatus	Glycosyltransferase, Transferase	2.4.1.313
B3GALT1	Intracellular	Glycosyltransferase, Transferase	2.4.1.86
B3GALT6	Intracellular	Glycosyltransferase, Transferase	2.4.1.134
B3GNT5	Nucleoli	Developmental protein, Glycosyltransferase, Transferase	2.4.1.206

Table 2.1. Genes associated with autism spectrum disorder. (cont.)

Gene	Subcellular Location	Biological Process	EC Number
CACNA1	Intracellular, Membrane	Calcium transport, Ion transport, Transport	-
CACNA2D3	Intracellular, Membrane	Calcium transport, Ion transport, Transport	-
CAPN12	Nucleoplasm, Focal adhesion sites	Hydrolase, Protease, Thiol protease	3.4.22.-
CHD2	Nucleoplasm	Myogenesis, Transcription, Transcription regulation	3.6.4.12
CHD8	Nucleoplasm	Transcription, Transcription regulation, Wnt signaling pathway	3.6.4.12
CNTN3	Intracellular	Cell adhesion	-
CNTN4	Intracellular	Cell adhesion	-
CNTNAP2	Intracellular, Membrane	Cell adhesion	-
CREBBP	Nucleoplasm, Nuclear bodies	Biological rhythms, Host-virus interaction, Transcription, Transcription regulation	2.3.1.48
CTNNB1	Plasma membrane	Cell adhesion, Host-virus interaction, Neurogenesis, Transcription, Transcription regulation, Wnt signaling pathway	-
DNMT3A	Nucleoplasm	Chromatin regulator, DNA-binding, Methyltransferase, Repressor, Transferase	

Table 2.1. Genes associated with autism spectrum disorder. (cont.)

Gene	Subcellular Location	Biological Process	EC Number
DYRK1A	Nucleoli fibrillar center, Cytosol	Host-virus interaction	2.7.12.1
EIF4E	Nucleoplasm, Cytosol, Cytoplasmic bodies	Host-virus interaction, Protein biosynthesis, Translation regulation	-
EXT1	Membrane	Glycosyltransferase, Transferase	2.4.1.224, 2.4.1.225
GABRA3	Nucleoplasm, Plasma membrane	Ion transport, Transport	-
GABRA5	Nucleoplasm, Plasma membrane	Ion transport, Transport	-
GABRB3	Membrane	Ion transport, Transport	-
GAL3ST2	Intracellular	Transferase	2.8.2.-
GALNT9	Vesicles	Glycosyltransferase, Transferase	2.4.1.41
GALNTL5	Membrane	Differentiation, Spermatogenesis	2.4.1.41
GCNT2	Golgi apparatus	Glycosyltransferase, Transferase	2.4.1.150
GLRA2	Intracellular, Membrane	Ion transport, Transport	-
GPC5	Nucleoplasm, Cytosol	Cell surface proteoglycan	-
GPC6	Golgi apparatus, Vesicles	Cell surface proteoglycan	-
GRIN2B	Intracellular, Membrane	Ion transport, Transport	-

Table 2.1. Genes associated with autism spectrum disorder. (cont.)

Gene	Subcellular Location	Biological Process	EC Number
HDAC4	Nucleoplasm, Nuclear speckles, Cytosol	Transcription, Transcription regulation	3.5.1.98
HECTD4	Nucleoplasm, Vesicles	Ubl conjugation pathway	2.3.2.26
HS3ST5	Intracellular	Transferase	2.8.2.23
KAT2B	Nucleoplasm, Cytosol	Biological rhythms, Cell cycle, Host-virus interaction, Transcription, Transcription regulation	2.3.1.48
KATNAL2	Nucleoplasm, Intermediate filaments	Isomerase	5.6.1.1
KDM5B	Nucleoplasm, Cytosol	Biological rhythms, Transcription, Transcription regulation	1.14.11.67
KDM6B	Nuclear speckles	Inflammatory response	1.14.11.68
KMT2C	Nucleoplasm	Transcription, Transcription regulation	2.1.1.354
KMT2E	Nucleoplasm, Nuclear bodies	Cell cycle, Growth arrest, Transcription, Transcription regulation	2.1.1.354
KMT5B	Nucleoplasm	Myogenesis, Transcription, Transcription regulation	2.1.1.362
LARGE1	Intracellular	Glycosyltransferase, Multifunctional enzyme, Transferase	2.4.2.-, 2.4.1.-

Table 2.1. Genes associated with autism spectrum disorder. (cont.)

Gene	Subcellular Location	Biological Process	EC Number
MECP2	Nucleoplasm	Transcription, Transcription regulation	-
MEF2C	Nucleoplasm, Vesicles	Apoptosis, Differentiation, Neurogenesis, Transcription, Transcription regulation	-
MIB1	Vesicles, Plasma membrane	Notch signaling pathway, Ubl conjugation pathway	2.3.2.27
NCOA1	Nucleoplasm, Plasma membrane, Cytosol	Transcription, Transcription regulation	2.3.1.48
NF1	Mitochondria	GTPase activation	-
NLGN3	Golgi apparatus, Cell junctions	Cell adhesion	-
NLGN4X	Intracellular, Membrane	Cell adhesion	-
NRCAM	Nucleoplasm, Vesicles, Plasma membrane	Cell adhesion	-
NRXN1	Plasma membrane	Angiogenesis, Cell adhesion	-
NSD1	Nucleoplasm, Plasma membrane	Transcription, Transcription regulation	2.1.1.357
PCDH10	Golgi apparatus, Nucleoplasm, Vesicles	Cell adhesion	-
PHF2	Nucleoplasm, Nucleoli rim	Transcription, Transcription regulation	1.14.11.-

Table 2.1. Genes associated with autism spectrum disorder. (cont.)

Gene	Subcellular Location	Biological Process	EC Number
POMGNT1	Membrane	Glycosyltransferase, Transferase	2.4.1.-
PPP5C	Vesicles, Cytosol	DNA damage, DNA repair	3.1.3.16
PTCHD1	Intracellular, Membrane	Unknown	-
PTEN	Nucleoplasm, Cytosol	Apoptosis, Lipid metabolism, Neurogenesis	3.1.3.16, 3.1.3.48, 3.1.3.67
RPL10	Endoplasmic Reticulum, Cytosol	Translation regulation	-
SCN7A	Plasma membrane	Ion transport, Sodium transport, Transport	-
SGSH	Intracellular	Hydrolase	3.10.1.1
SHANK2	Nuclear speckles, Vesicles, Plasma membrane	Receptor binding	-
SHANK3	Nucleoplasm, Plasma membrane	Actin-binding	-
SLC35A3	Membrane	Sugar transport, Transport	-
SLC9A9	Membrane	Antiport, Ion transport, Sodium transport, Transport	-

Table 2.1. Genes associated with autism spectrum disorder. (cont.)

Gene	Subcellular Location	Biological Process	EC Number
SMPDL3b	Golgi apparatus, Cytosol	Immunity, Inflammatory response, Innate immunity, Lipid degradation, Lipid metabolism	3.1.14.-
SPAST	Nucleoplasm, Cytosol	Cell cycle, Cell division, Differentiation, Neurogenesis	5.6.1.1
ST8SIA2	Nucleoplasm, Golgi apparatus, Cytosol	Glycosyltransferase, Transferase	2.4.99.-
SynGAP1	Nucleoplasm	GTPase activation	-
TAOK1	Vesicles	Apoptosis, DNA damage, DNA repair	2.7.11.1
TEK	Plasma membrane, Centriolar satellite	Angiogenesis	2.7.10.1
TLK2	Intracellular	Cell cycle, DNA damage	2.7.11.1
TMLHE	Mitochondria	Carnitine biosynthesis	1.14.11.8
TRAF7	Vesicles, Plasma membrane	Apoptosis, Transcription, Transcription regulation, Ubl conjugation pathway	2.3.2.27
TRIM23	Intracellular	Host-virus interaction, Immunity, Innate immunity, Ubl conjugation pathway	2.3.2.27
TRIO	Vesicles, Cytosol	Guanine-nucleotide releasing factor, Kinase, Serine/threonine-protein kinase, Transferase	2.7.11.1

Table 2.1. Genes associated with autism spectrum disorder. (cont.)

Gene	Subcellular Location	Biological Process	EC Number
TRIP12	Nuclear speckles	DNA damage, DNA repair, Ubl conjugation pathway	2.3.2.26
UBR1	Nucleoplasm, Vesicles, Cytosol	Ubl conjugation pathway	2.3.2.27
USP45	Nucleoplasm, Cytosol	Ubl conjugation pathway	3.4.19.12

2.1.2. Environmental Factors

New studies suggest environmental factors which negatively affect the immune function or transcriptome organization can trigger ASD [1, 2]. Maternal complications or medical conditions (bleedings after the first trimester, meconium aspiration, miscarriage possibility, obesity, celiac disease, immunological disorders, zinc, folic acid, vitamin B2, B6, B12 deficiency, maternal bleeding disorders, diabetes) or during birth complications (low birth weight, complicated birth) or radiation, immunotoxins (polychlorinated biphenyls (PCB), polybrominated diphenyl ether (PBDE), pesticide), viral infections (e.g., Rubella, Cytomegalovirus), advanced parental age, use of psychiatric drugs, the increased age gap between parents, familial autoimmune diseases, teratogenic factors, air pollution are also associated with ASD [34–42].

2.1.3. Biochemical Factors

It was found as patients with ASD have lower plasma oxytocin levels [43]. It is stated that regions of the brains of ASD patients that are thought to be problematic are rich in glutamate, and autistic symptoms are revealed with glutamate antagonists [44]. Another

study shows low carnitine levels and lactic acidosis are expected in ASD. Those findings suggest ASD as a mitochondrial disorder [45]. Mitochondrial disorder prevalence of the general population, 0.01%, is 500 times more than the prevalence of ASD patients, 5%. Additionally, 30% of ASD biomarkers are compatible with biomarkers of mitochondrial diseases [46]. The sensitivity of mitochondria to toxins and endo- or exo-induced stress factors increases the importance of the brain-gut relationship on ASD [47].

2.1.4. Risperidone treatment in autism spectrum disorder

Risperidone is an effective inhibitor of serotonin 2A and dopamine D2 receptors, and it is the most widely investigated antipsychotic agent for children with ASD [48, 49]. Most works of risperidone have focused on children with maladaptive symptoms. According to these studies, risperidone had the edge over placebo in decreasing behavioral issues such as aggression self-harm in more than half of the patients [50, 51]. In a study conducted by Won et al., in 70% of children participating in the study, at least six months of regular use of this drug resulted in a noticeable improvement in their behavioral disorders [49].

However, weight gain has also been observed in the patients due to Risperidone treatment. It was also found that risperidone is more effective in managing behavioral difficulties and enhancing language abilities and social interactions in short and long periods than haloperidol, which is also antipsychotic [52, 53]. In another recent study, the higher doses of risperidone and 9-hydroxyrisperidone plasma have increased prolactin quantity, sedation, and improvement in behavioral disruptions of children with ASD [54]. They found that the optimum dose might change based on the treatment length, patient's body mass index, and age at the beginning of risperidone treatment. For instance, the treatment range was determined as 15-25 μg/L for a 10-year-old patient with less than 1 BMI z-score after the 3-month risperidone administration.

In conclusion, Risperidone is a promising treatment for ASD patients due to its tolerable adverse effects and efficacy.

2.2. Systems Biology

Systems biology is an indispensable area that connects parts of biological systems and employs various and extensive experimental and computational techniques [55]. These methodologies provide necessary data about the activities of these biological systems (Cell, tissue, and organ) and their interrelationships. As the first step of developing computational models that can predict metabolic activities in biological systems, required elements that play a role in biochemical processes should be defined and listed [56]. Then, interplays between these elements are analyzed, and genome-scale maps are created step by step. Afterward, developed networks are transformed to a mathematical form to predict the metabolic behaviors of biological systems.

2.2.1. Constrained-Based Modelling

Various complex data analysis approaches have been developed to deal with large data sets. Constraint-based modeling is one of these techniques, and it is the most common approach employed with genome-scale models [57].

Genome-scale models include metabolites and a reaction set of biological systems based on experimental data. These networks can be expressed in a mathematical form. This format is called the stoichiometric matrix, and it is known as the main element of a constraint-based model (CBM) [58]. Constraint-based modeling allows researchers to obtain insight into the activities of a metabolic network under different conditions affected by environmental and genetic changes [57].

2.2.2. Genome-Scale Metabolic Models

Genome-Scale Metabolic Models (GEMs) connect genome information of a specific biological system to metabolic reactions. Thus, genotype and phenotype can be estimated based on the gene-protein-reaction chain network. Models are based on a stoichiometric matrix (S). Columns of S represent reactions, and rows are stoichiometric coefficients of metabolites. The mass and charge balances of all reactions in the S matrix have been performed. This helps track which reactions are catalyzed by the proteins encoded by the

genes, i.e., enzymes, and which metabolites are used and produced. GEMs enable a computational analysis of a specific part of a cell or system, making changes according to the research scale, and estimating metabolic flux [59].

The first GEM was curated in 1999 for *Haemophilus influenzae* [60]. Then, model organisms such as *Escherichia Coli* [61] and *Saccharomyces cerevisiae* [62], multicellular organisms such as humans [63], and plants [64] were curated. In February 2019, a genome-scale metabolic model of 6239 organisms, 5897 bacteria, 127 archaea, and 215 eukaryotes was created by computerizing the gene-protein-reaction relationship known in the literature [65]. GEMs are essential tools for strain development for bio-based chemical and material production [66–70], for prediction of enzyme function [71, 72], for drug target of pathogens [67, 73–81], for modeling the interaction of multiple cells or organisms [82]–[88], and for understanding the pathway and mechanism of diseases [76, 89, 90–97, 98-100]. The accuracy and precision of the model curated are determined by comparing flux analysis of the models with experimental or literature data [65].

2.2.3. Genome Scaled Metabolic Models of Brain

The first human-specific genome-scale metabolic model (Recon1) containing 1496 genes, 2766 metabolites, and 3744 reactions was reconstructed in 2007 [63]. Then, Lewis et al. created a brain-specific genome-scale metabolic model (iNL403) by employing brain proteome databases [101]. iNL403 model was used to investigate Alzheimer's Disease (AD) in-depth and identify metabolically significant genes. Afterward, by expanding the model constructed previously by Çakır et al., Sertbaş et al. created iMS570 to study transcriptional alterations related to six common neurodegenerative diseases, including Parkinson's disease (PD), Alzheimer's disease (AD), schizophrenia (SCH), amyotrophic lateral sclerosis (ALS), multiple sclerosis (MS), and Huntington's disease (HD) [102, 103]. They confirmed their model by comparing the flux distribution with the experimental results. Next, Özcan and Çakır developed iMS570g by including new reactions into iMS570 and examined glioblastoma brain tumors [104]. They validated their findings by comparing both in-vitro and in-vivo works. And lastly, Martin-Jimenez et al. reconstructed a genome-scale astrocyte-specific metabolic model named MODEL 1608180000 [105].

2.2.4. Transcriptome integration

Since the human model has all metabolic reactions, it is significant to eliminate irrelevant reactions and create a tissue-specific model to examine a certain part of the human body. Therefore, various algorithms have emerged to be used in the development of tissue-specific models by integrating transcriptomics data. These techniques are divided into two classes regarding their approach [104]. While the first group utilizes context-specific omics data directly to increase the predictability of flux rates, the second group develops a context-specific model by processing the data [104]. The first group includes E-Flux [106], MADE [107], TEAM [108]. And the second group includes iMAT [109], GIMME [110], mCADRE [111], INIT [112], AdaM [113], EXAMO [114].

2.3. Physiology Based Pharmacokinetic Modeling

Physiologically based pharmacokinetic (PBPK) models are increasingly employed to accelerate and enhance the efficacy of the drug design process [115]. The idea behind PBPK modeling is to mathematically define related biochemical, physicochemical, and physiological actions that identify the pharmacokinetic feature of a compound [116]. PBPK models can explain and predict the pharmacokinetics of compounds in certain people. It can also describe these data under particular pathological cases [116]. These models have been created for various species, including humans, rats, mice, and dogs [117].

PBPK models are composed of parts corresponding to tissues in the human body, linked to the circulatory system. Information related to tissue particular to the biological system such as weight, volume or/and blood flow rate should be defined for each part of the system [117].

There are five main steps in PBPK model reconstruction. Definition of the model and then each specific part (tissue, organ) found in the system, creating model equations, specifying model parameterization, and assessing simulations and parameters [116].

3. METHODS

3.1. Reconstruction of Human Metabolic Brain Model

To better understand the mechanism of the disorder, ASD-specific brain GEM was curated. Three main brain models were used for this research: iMS570 by Sertbas et al., 2014 (570 genes, 524 metabolites, 630 reactions) [103], MODEL16081800000 by Martin-Jimenez, 2017 (3765 genes, 5007 metabolites, 5659 reactions) [105] and iNL403 by Lewis et al., 2010 (403 genes, 932 metabolites and 953 reactions) [101]. Since different groups created those models, the annotations were also different. Metabolite names were standardized by KEGG ID [33], HumanCyc ID [118], or Human Metabolome Database (HMDB) ID [119] and manually integrated into the models. Then, models were prepared for comparison.

3.1.1. Metabolic Brain Model Preparations

ASD-specific brain GEM was reconstructed by the iMS570 metabolic brain model. The reaction distribution of metabolisms is given in Figure 3.1. In addition to the main metabolisms in Figure 3.1, 59 extracellular exchange reactions and 34 transport reactions are present in iMS570. This model consists of 4 main compartments: astrocyte mitochondria (_AM), astrocyte cytosol (_A), neuron mitochondria (_NM), neuron cytosol (_N). Additionally, the reconstructed metabolic model contains intercellular space [s] to investigate astrocyte-neuron transport better and compartment annotation is slightly different from iMS570: astrocyte mitochondria (_A[m]), astrocyte cytosol (_A[c]), neuron mitochondria (_N[m]), neuron cytosol (_N[c]). Schematic representation of the reconstructed model is given in Figure 3.2.

Firstly, MODEL16081800000 was examined. This is a human astrocyte metabolic model derived from Human Metabolic Reaction (HMR) GEM for generic human cells [120]. Human astrocyte GEM consists of 8 compartments: extracellular [s], cytosol [c], mitochondria [m], endoplasmic reticulum [r], Golgi apparatus [g], lysosome [l], peroxisome [p] and nucleus [n]. Therefore, reactions and metabolites were deleted based on

compartments via the “keepCompartment” command on MATLAB-Cobra Toolbox [121], and only extracellular [s], cytosol [c], mitochondria [m], and boundary [x] metabolites and related reactions were left. The compartment-based reduced model consists of 2308 metabolites 3940 reactions (1648 transport and shuttle, 236 extracellular exchange reactions). The reaction distribution of metabolisms of the reduced model is given in Figure 3.3.

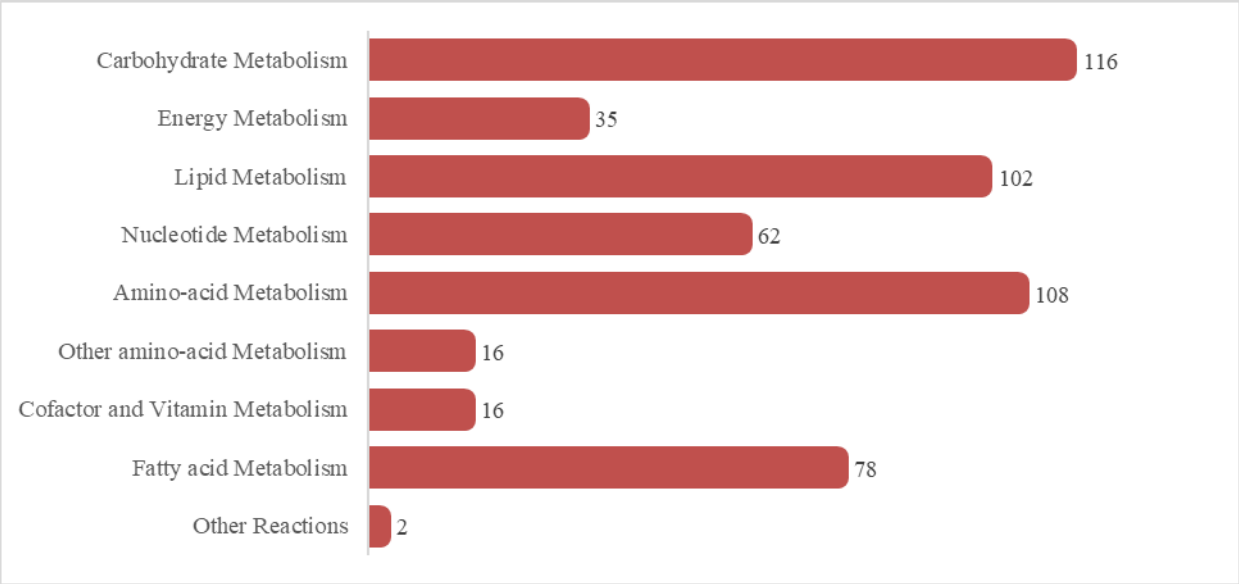

Figure 3.1. iMS570 reaction distribution of metabolisms.

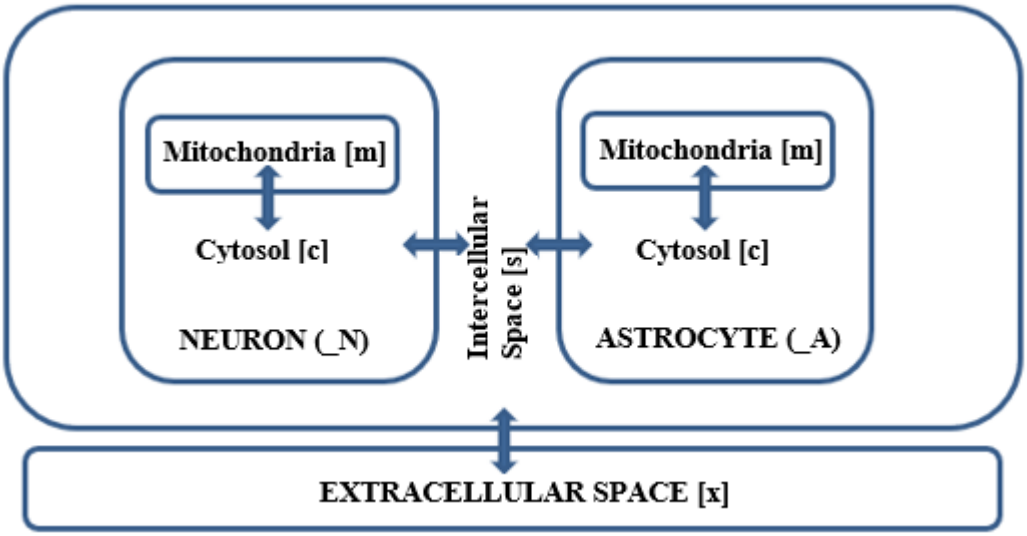

Figure 3.2. Schematic representation of the reconstructed model.

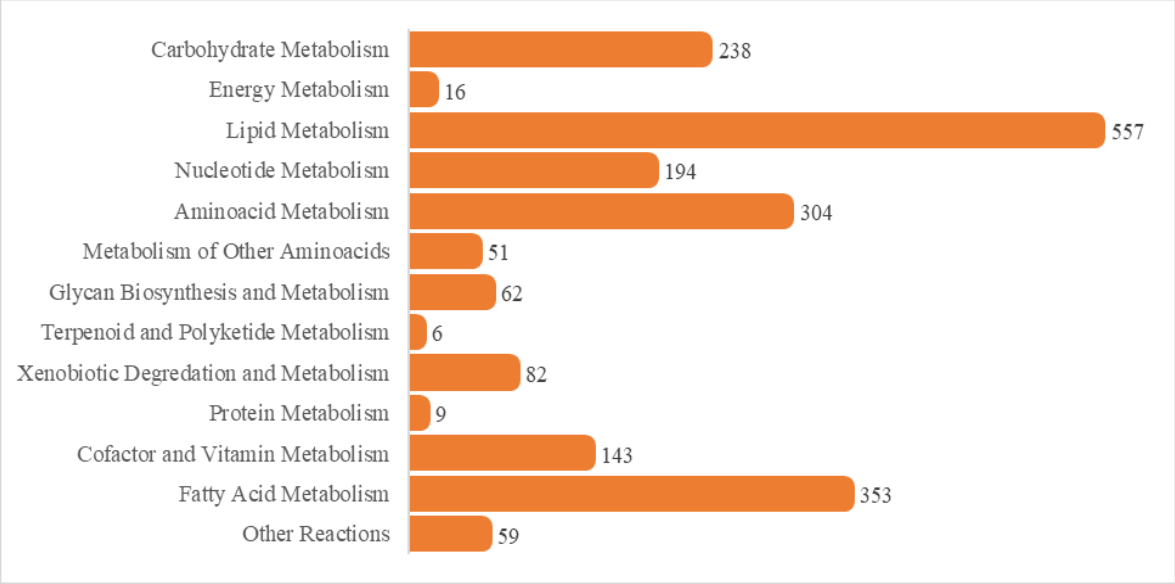

Figure 3.3. Reaction distribution of metabolisms of the compartment based reduced MODEL16081800000.

The last model prepared for comparison was iNL403. This model was curated in 2010 to investigate energy metabolism. For a healthy individual, there are three models: Glutamatergic, GABAergic, and Cholinergic. Cholinergic model does not contain ATP driven GABA secretion from interstitium to neuron cytosol; GABAergic model does not contain choline secretion, ATP driven acetylcholine secretion from interstitium to neuron cytosol and break-down of acetylcholine into acetyl and choline by acetylcholinesterase in interstitium; and Glutamergic model does not contain those all four reactions. In this model, all mentioned reactions were added to the model. iNL403 consists of astrocyte mitochondria (_A[m]), astrocyte cytosol (_A[c]), neuron mitochondria (_N[m]), neuron cytosol (_N[c]), interstitium ([I]) and endothelium and blood ([e]) compartments. Reaction distribution of metabolisms except for 311 transport and shuttle and 65 extracellular exchange reactions are given in Figure 3.4.

Different research groups reconstructed those three models (iMS570, MODEL1608180000, and iNL403). Thus, annotations of metabolites, genes, and reactions; reaction balances of hydrogen, water, coenzyme A or other medium metabolites; subsystem annotations of the reactions differ. Before elimination of duplicate reactions between

models, standardization of those criteria was performed by information from KEGG [33], HumanCyc [118], Human Metabolome Database (HMDB) [119], HMR GEM for generic human cell [120], and Metabolic Atlas (Human1) [122, 123].

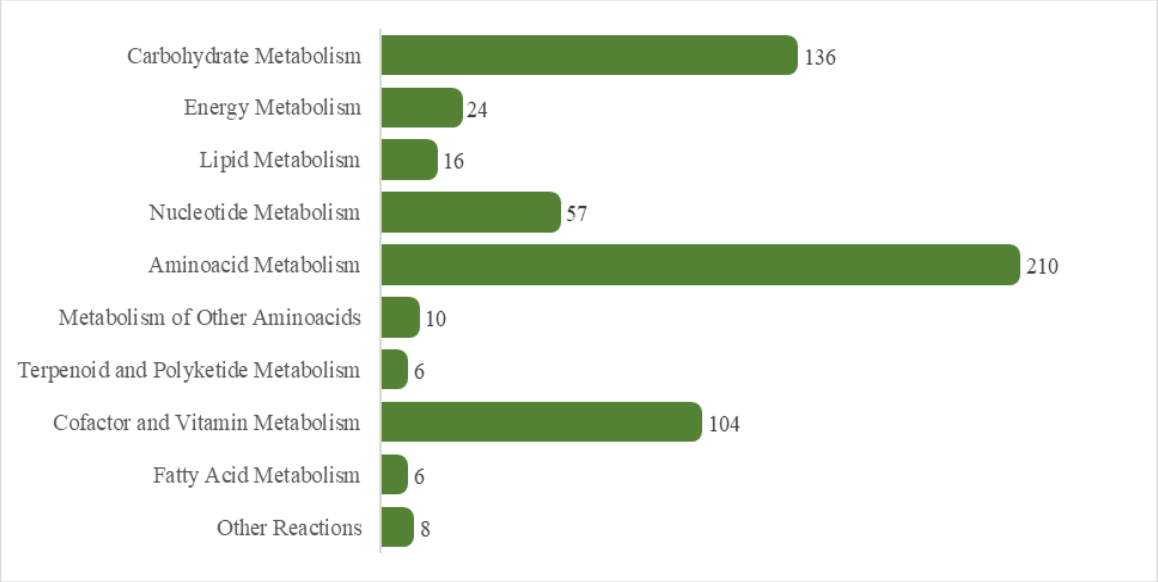

Figure 3.4. iNL403 reaction distribution of metabolisms.

3.1.2. Comparison of Metabolic Brain Models

The first attempt to compare models was to use a computational tool instead of a manual approach. For this purpose, the “compareCbModels” command was used by the modelBorgifier module of Cobra Toolbox. However, the manual comparison has been made due to code-related problems such as incompatibility of the positions of hydrogen and water molecules (such as present in one model and not in the other, or the difference in direction), which are in duplicate reactions in different models and the inadequacy of the module due to the size of the compared models.

Since it would be more efficient to make the manual comparison on a single integrated model, the three models mentioned were combined with the "mergeTwoModels" command. Since the command allows the combination of only two models, first MODEL1608180000 and iMS570 were combined, then the combined model merged with iNL403. This model has 5644 reactions, 3107 metabolites, and 1055 genes. The label part has been added to the

model struct to follow the sources of the reactions in the integrated model. The reactions with values in the S matrix regardless of direction were found and examined with the "checkDuplicateRxn" command to reduce the manual load. Examination of the combined model was made through the excel file. All reactions' EC numbers, gene, and metabolism nomenclature were uniformized to eliminate duplicate reactions.

3.1.3. Flux Balance Analysis

After eliminating duplicate reactions, transport, shuttle, and extracellular exchange reactions (2254 reactions) were investigated thoroughly; for this purpose, Flux Balance Analysis (FBA) was performed.

FBA is a mathematical method to analyze the flux of metabolites across a metabolic network. Stoichiometric matrix S has the size of m x n, where m represents metabolites and n represents reactions. Stoichiometric coefficients in this matrix state whether the metabolite is consumed (negative coefficient) or produced (positive coefficient). Flux vector v, length of n, stands for flux through reactions within the system. And concentration vector x, length of m, represents concentrations of metabolites. When the system is at steady-state (dx/dt=0),

$$Sv = 0. \tag{3.1}$$

Since there will be more reactions than metabolites (n>m), i.e., more unknown variables than equations, there will be no unique solution. In FBA, an objective function Z is maximized or minimized according to intention, with constraints on flux vector, v, and an optimal solution is found [124].

For FBA analysis of the combined model, equality constraints were determined based on iMS570 and iNL403 with the literature comparison. Constraints are given in Table 3.1. As objective functions, reactions in Table 3.2 are maximized.

For FBA, the "optimizeCbModel" function of the Cobra Toolbox was used on MATLAB. Based on the FBA results, it has been noticed that there is an undesirable loop in transport reactions of some metabolites which have zero influx are not produced in the cell,

and fluxes of those reactions are in the range of ±1000. The reason for this loop is the transport of the same metabolite via multiple ways: diffusion, or transportation between mitochondria-cytoplasm and cytoplasm-intercellular space with the help of ions such as hydrogen and sodium, calcium, or by shuttle reactions. Increased number of reactions causes computational burden, thus unhealthy results. Since transport reactions are essential for ASD, it is tried to delete/silence as few reactions as possible.

Table 3.1. Constraints for the combined model.

Reaction	Lower bound	Upper bound	Reference
L-3-amino-isobutanoate[s] <=>	-0.00023	1000	[125], [126]
GABA[s] <=>	-0.0018	0	[127], [128]
Acetate[s] <=>	-0.0013	1000	[129]
Acetoacetate[s] <=>	-0.012	-0.0015	[101]
acetaldehyde[s] <=>	-0.0014	1000	[130]
Arginine[s] <=>	-0.004	0	[127], [128]
Asparagine[s] <=>	-0.0009	0.0037	[127], [128]
BHB[s] <=>	-0.016	-0.001	[101]
Cysteine[s] <=>	-0.0086	0.0033	[127], [128]
Glucose[s] <=>	-0.29	-0.196	[101]
Glutamine[s] <=>	-0.013	0.025	[127], [128]
Glutamate[s] <=>	-0.0044	0.0047	[127], [128]
Glycine[s] <=>	-0.0053	0.0086	[127], [128]
Isoleucine[s] <=>	-0.0041	0.0004	[127], [128]
Lactate[s] <=>	-0.0058	0.079	[127], [128]
Leucine[s] <=>	-0.0062	0.0011	[127], [128]

Table 3.1. Constraints for the combined model. (cont.)

Reaction	Lower bound	Upper bound	Reference
Lysine[s] <=>	-0.0005	0.011	[127], [128]
O2[s] <=>	-2.256	-1.351	[101]
Ornithine[s] <=>	-0.0048	0.0041	[127], [128]
PE-LD pool[s] <=>	-5.00E-05	1000	[131]
proline[s] <=>	-0.0079	0.0066	[127], [128]
Phosphatidyl_serine[s] <=>	-5.00E-05	1000	[131]
Pyruvate[s] <=>	-0.0058	0.007	[127], [128]
sarcosine[s] <=>	-0.0053	0.0086	[132], [133]
Serine[s] <=>	-0.011	0.0016	[127], [128]
Valine[s] <=>	-0.011	0.005	[127], [128]
trans-4-hydroxy-L-proline_A[m] <=>	-5.00E-05	5.00E-05	[134]–[136]
N,N-Dimethylglycine_A[c] <=>	-0.0053	0.0086	[137]
Tyrosine_A[m] <=>	-0.0014	0.0037	[127], [128]
trans-4-hydroxy-L-proline_N[m] <=>	-5.00E-05	5.00E-05	[134]–[136]
N,N-Dimethylglycine_N[c] <=>	-0.0053	0.0086	[137]
Tyrosine_N[m] <=> Tyrosine_N[c]	-0.0014	0.0037	[127], [128]
ATP_A[m] + Bicarbonate_A[m] + Pyruvate_A[m] -> ADP_A[m] + Hc_A[m] + Oxoloacetate_A[m] + phosphate_A[m]	0	0.1	[102]

After transport reaction deletion, since the model should have interconnected reactions and strong gene-protein-reaction interaction, some metabolites and reactions were deleted. First, isomers and dead-end metabolites and reactions are deleted.

Table 3.2. Objective functions of the combined model.

Reactions	Function
Lactate_A[c] + NAD_A[c] <=> Hc_A[c] + NADH_A[c] + Pyruvate_A[c]	Lactate dehydrogenase
Lactate_A[m] + NAD_A[m] <=> Hc_A[m] + NADH_A[m] + Pyruvate_A[m]	Lactate dehydrogenase
NAD_N[c] + Lactate_N[c] <=> Hc_N[c] + NADH_N[c] + Pyruvate_N[c]	Lactate dehydrogenase
NAD_N[m] + Lactate_N[m] <=> Hc_N[m] + NADH_N[m] + Pyruvate_N[m]	Lactate dehydrogenase
ADP_A[c] + Hc_A[c] + Phosphoenol_pyruvate_A[c] -> ATP_A[c] + Pyruvate_A[c]	Pyruvate kinase

3.1.4. Autism-Specific Reaction Addition

The reconstructed model has five compartments, mitochondria, and cytosol of astrocyte and neuron and intercellular space. Therefore, some genes in Table 2.2 were selected based on compartments. Out of 89 genes, 48 were elected. After the ones with no EC number were eliminated, 29 genes remained: B3GALT1, B3GALT6, DYRK1A, EXT1, GAL3ST2, GALNTL5, HDAC4, HS3ST5, KAT2B, KDM5B, LARGE1, MIB1, NCOA1, NSD1, POMGNT1, PPP5C, PTEN, SGSH, SMPDL3b, SPAST, ST8SIA2, TEK, TLK2, TMLHE, TRAF7, TRIM23, TRIO, UBR1, USP45. Only one gene, DYRK1A, exists on the model. The addition of other genes would cause dead-end metabolites or lumped reactions. Thus, autism specificity was achieved by subsystem expansion which will be explained more in the discussion section.

3.1.5. Flux Variability Analysis

With Flux Variability Analysis (FVA), minimum and maximum fluxes of reactions were calculated for further investigation, and zero flux reactions were detected. For this purpose, the flux limits of all extracellular exchange reactions were set to minimum (-1000) and maximum (1000) values, thus allowing all metabolites that could pass through the blood-

brain barrier to enter and exit the brain cells. FVA assigns each reaction as an objective function and performs Flux Balance Analysis (FBA) in the model. Fluxes pass through the minimized or maximized objective function are recorded [138–140]. For minimized and maximized version of the objective function, for n reactions, a flux vector v of size nxn and an f vector length of n are formed. If the value in the f matrix is equal to zero for the minimized and maximized objective function FBA, that reaction is blocked. The algorithm of FVA is given in Figure 3.5.

for $i = 1{:}n$ $(n\ stands\ for\ number\ of\ reactions)$

$FVAmodel.c(i) = 1;\ (when\ a\ reaction\ is\ objective\ function, c = 1)$

$minFlux(i) = optimizeCbModel(FVAmodel,' min');$

$maxFlux(i) = optimizeCbModel(FVAmodel,'max');$

end

Figure 3.5. The algorithm of Flux Variability Analysis.

3.1.6. Transcriptome Integration

Transcriptome integration tool Gene Activity Moderated by Metabolism and Expression (GIMME) helps create a context-specific metabolic model with gene expression data. There are two steps in this model: 1) Optimization of the objective function with FBA, 2) Minimization of the use of inactive reactions. Those inactive reactions are the reactions whose gene expression is below the determined threshold [141].

For this purpose, Gene Expression Omnibus (GEO) data of ASD patients were investigated. GSE28475 was chosen for transcriptome integration [142, 143]. 124 samples with 24526 rows were extracted. The average of every row was calculated, and ID annotation was translated to Entrez Gene ID. Gene up- and downregulations in the presence of ASD were investigated and noted in the GSE28475 file [144]. SHANK3 gene is reported to be downregulated [145, 146], and it is closely related to ASD; its value, 3971.6, was chosen as the threshold. Also, 30% of the average of final values, 1319.4, was chosen as the second

threshold. 18630 unique genes and their gene expression data were prepared for transcriptome analysis.

Gene Inactivity Moderated by Metabolism and Expression (GIMME) method was used for transcriptome integration. Based on the threshold value, genes were either absent, "A" or present, "P". Regarding objective function, the reconstructed model was reduced by the inconsistency score between threshold and expression with the help of Flux Balance Analysis. Reactions with minimal inconsistency were survived [110].

A second optimization was performed to reduce the GIMME model. This optimization minimizes the Euclidean norm of the internal fluxes to avoid multiple optimum solutions [103]. For both SHANK3 limited and average limited gene expression data, autism-specific brain models were reconstructed.

3.2. Human Physiology Based Pharmacokinetic Modelling of Risperidone

Risperidone is an atypical, 2nd generation antipsychotic drug and an antagonist of serotonin 5-hydroxytryptamine (5-HT2A) and dopamine D2 receptors. With inhibition of 5-HT2A and D2 receptors, serotonergic and dopaminergic activity is decreased [147]. Negative social behavior and irritation symptoms are observed in schizophrenia, mood disorders, and autism spectrum disorder [148–150]. Even though ASD is not considered a dopamine-pathway disorder, improved social behavior was observed in several studies [151, 152]. Those findings indicate dopaminergic dysfunctions. Dopamine antagonists are used for child ASD-symptom treatment, and risperidone (5-17 years) [153] and aripiprazole (6-17 years) [154] are the only FDA-approved drugs. However, the dosage is crucial, especially for children [155], due to extrapyramidal symptoms [156, 157]. PBPK modeling allows to foreseen distribution through time for various ages, weights, or populations and helps to dose management. Pharmacokinetic data and receptor occupancy calculations can be used for further computational investigation of ASD. The receptor occupancy data can be used for inhibition of dopaminergic neurotransmission in ASD-specific model to observe both effects of dopamine activity and risperidone treatment.

Human Physiology Based Pharmacokinetic Modelling (PBPK) was created by systems biology tool Open Systems Pharmacology Suite, PK-Sim (Version 9.1.2) [158]. PK-Sim is a free PBPK software tool that includes predefined features for PBPK modeling of humans, rats, and other laboratory animals. Creation of individuals and populations for different ethnicities, preterm babies, and pregnant women, for preferred age, weight, height, or body mass index is possible with the PK-Sim database for anatomical and physiological characteristics. Drugs can be simulated by creating compounds with the drug's basic physico-chemistry and ADME values. To simulate the distribution formulation of the drug and its administration protocol, e.g., oral, intravenous bolus, is described by the user. Events such as meals, smoking, or observers can also be added to the simulation. The main menu of PK-Sim is given in Figure 3.6.

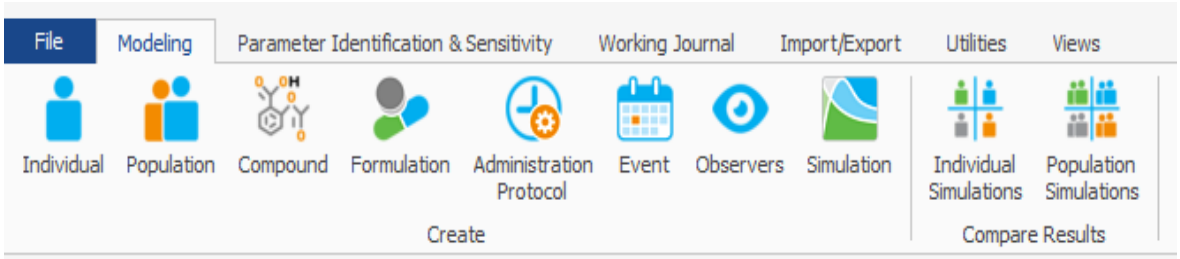

Figure 3.6. The main menu of PK-Sim.

During simulations, four individuals, eleven populations, four compounds, one formulation, two administration protocols building blocks were created.

3.2.1. Creation of a New Individual

Firstly, individuals were created. Since population simulation will be performed, individual parameters were left as default. Any information in the articles, e.g., age, weight, was used in the population creation step. Based on the papers, only ethnicity was defined in individuals. Some ethnicities' anatomical and physiological characteristics are predefined by the tool itself. During the simulations, European [159], White American [160], and Asian [161] populations were preferred regarding the experimental articles. Age, weight, height, and body-mass index (BMI) information of the populations is given in Table 3.3.

Table 3.3. Individual parameters of populations.

Populations	**Age (year)**	**Weight (kg)**	**Height (cm)**	**BMI (kg/m^2)**
European	30.00	73.00	176.00	23.57
White American	30.00	80.35	178.49	25.22
Asian	30.00	60.03	169.96	20.78

Risperidone is metabolized to paliperidone in liver by CYP (cytochrome P450)2D6, CYP3A4 and CYP3A5 [162], [163]. Therefore, expressions of those metabolic enzymes were added to the individual. PK-Sim provides to add enzymes by the query. For CYP2D6, CYP3A4 and CYP3A5, there are three possibilities: microarray expression data from ArrayExpress (European Information Institute), Expressed Sequence Tags from UniGene (National Center for Biotechnology Information), and Reverse transcription-polymerase Chain Reaction (RT-PCR) derived gene expression from literature. Due to its better accuracy of human plasma PK profiles, the RT-PCR database was chosen [164, 165].

The results of the PBPK model will be used in brain GEM. Therefore, the blood-brain barrier should be included. P-glycoprotein (P-gp) modulates drug transport for some antipsychotics, e.g., risperidone and paliperidone [166]. Accordingly, as transport protein, P-gp was added manually, and its relative expression in the blood-brain barrier was set to 1.00. European, White American, and Asian individuals were created for reference concentration of 1.00 µmol/l, and one European individual was created for reference concentration of 4.00 µmol/l to investigate the effect of P-gp concentration in the BBB [165, 167–169].

Dopamine D2 receptor occupancy (RO) of antipsychotics is well investigated. D2 receptors were considered for this research by adding D2R as a protein-binding partner. For its reference, concentration was determined as 0.40 nmol/l [170] for all individuals, and its localization was recorded as interstitial space. D2 receptor relative expression in the brain was set to 1.0.

3.2.2. Compound Creation of Risperidone and Paliperidone

To model risperidone and its metabolite paliperidone, several articles were investigated for PBPK parameters [165, 171–177]. According to the simulations, several values were found for the same parameter; the best fits are tabulated in Table 3.4.

PK-Sim's absorption, Distribution, Metabolism, and Excretion (ADME) interface provides calculation methods for specific intestinal permeability, partition coefficients, and cellular permeabilities. Only partition coefficients calculation changed to the Berezhkovskiy method since it is the most accurate risperidone and paliperidone [178]. The others remained as PK-Sim Standard.

D2 receptor binding parameters were added from the "Add Protein Binding Partner" tab under the "Specific Binding" distribution section. The dissociation rate constant at the D2 receptor, $k_{off, D2,}$ and affinity (dissociation constant) at the receptor, $K_{d, D2}$, of risperidone and paliperidone are given in Table 3.4 [176]. Risperidone or paliperidone-specific binding to the D2 receptor is described as reversible protein-substrate interaction in PK-Sim.

Under Metabolism, CYP enzymes are bound with risperidone to metabolize paliperidone. The most effective CYP enzyme for this process is reported as CYP2D6, and parameters of its two subtypes, CYP2D6.1 and CYP2D6.10, were available [175]. Thus, two risperidone compounds with only CYP2D6 enzyme kinetic differences were created. The process type for calculation is "in vitro metabolic rate in the presence of recombinant CYPs/enzymes – Michaelis-Menten." The maximum rate of the enzyme, V_{max}, and Michaelis-Menten constant, K_m, of risperidone and paliperidone is tabulated in Table 3.4. Total hepatic clearance for risperidone was not calculated because the metabolism of risperidone is assumed to be performed by CYP enzymes [175]. After simulations, for total hepatic clearance, CLHepatic, of Paliperidone was stated as 1.04 mL/min/kg by Wong et al. In this research, two paliperidone compound was created with two $CL_{Hepatic}$ value, 1.04 mL/min/kg and half 0.52 mL/min/kg. Clearance was calculated as a first-order elimination process.

Transport&Excretion section has three sections under Transport Proteins, Renal Clearances, and Biliary Clearance. Only transport proteins and the renal clearances section were used for paliperidone. P-gp was added as transport protein with the process type "In vitro active transport (vesicular assay)-Michaelis-Menten." The maximum rate of P-gp, V_{max}, and Michaelis-Menten constant, K_m, risperidone, and paliperidone can be found in Table 3.4.

Table 3.4. Basic physico-chemistry and ADME parameters of risperidone and paliperidone.

Parameters	**Risperidone**	**Paliperidone**
Lipophilicity (logP)	2.50 [171]	2.40 [172]
Fraction unbound	0.10 [174]	0.21 [174]
Molecular weight (g/mol)	410.50 [172]	426.50 [172]
Compound type	Base [172]	Base [172]
pKa1	8.80 [171]	8.20 [172]
Solubility (mg/L)	0.29 [165]	0.22 [165]
Solubility Reference pH	7.60 [165]	7.00 [165]
$k_{off, D2R}$ (1/s)	0.005 [176]	0.005 [176]
$K_{d, D2R}$ (nM)	7.24 [176]	6.17 [176]
$V_{max, P\text{-}gp}$ (pmol/min/pmol)	2.86 [177]	10.00 [165]
$K_{m, P\text{-}gp}$ (µM)	12.40 [177]	12.40 [165]
$CL_{Hepatic}$ (mL/min/kg)	-	1.04 [165]
CL_{Renal} (mL/min/kg)	0 [165]	0.54 [174]
$V_{max, CYP2D6.1}$ (pmol/min/pmol)	2.3 [175]	-
$K_{m, CYP2D6.1}$ (µM)	1.1 [175]	-
$V_{max, CYP2D6.10}$ (pmol/min/pmol)	0.10 [175]	-
$K_{m, CYP2D6.10}$ (µM)	6.70 [175]	-
$V_{max, CYP3A4}$ (pmol/min/pmol)	15.00 [175]	-
$K_{m, CYP3A4}$ (µM)	61.00 [175]	-
$V_{max, CYP3A5}$ (pmol/min/pmol)	15.00 [175]	-
$K_{m, CYP3A5}$ (µM)	200.00 [175]	-

3.2.3. Population Creation

Experimental data from seven articles were collected for population simulations [179–185]. Articles of Canovas et al. and Kumar et al. do not have free access; therefore, related data for comparison were extracted from the article of Wong et al. There was no information besides the number of volunteers participating in the experiment. Therefore, age was assumed to be 25. All participants were assumed to be male for Canovas et al. Khorana et al. Seven populations were created by the age, weight, height, and population distribution data from articles. The population demographics can be found in Table 3.3.

For ethnicity comparison, as can be seen from Table 3.3, two other populations, White American and Asian, were created with 30 individuals at 25-year-old. The population generated for Canovas et al. was set as a European population example.

To compare individual numbers, the European population with 100 25-year-old males was generated, compared with the Canovas' population again. Another individual has been created to investigate the effect of P-gp reference concentration. For this purpose, a population of 30 persons at 25-year-old was generated.

There are two more populations for receptor occupancy analysis. The article for receptor occupancy analysis has one female of 8 schizophrenic volunteers from age 18 to 52 [186]. One population was generated based on that information. The only difference of the other population is age was set to 25 years for simulation purposes.

3.2.4. Formulation and Administration Protocols

Risperidone formulation was simulated via Weibull function with a dissolution time of 10 minutes and dissolution shape of 0.92 [173].

Two administration protocols were defined: plasma concentration analysis and receptor occupancy analysis. Plasma concentration protocol consists of one time 2 mg oral dose and 100 hours of simulation. Receptor occupancy protocol consists of a 3 mg oral dose twice a day for 28 days, then a 1.5 mg oral dose twice a day for 14 days.

3.2.5. Simulations

18 simulations were created to analyze. 7 simulations were performed based on Table 3.5. The simulation based on Canovas et al. was determined as a European baseline for comparison. The remaining 2 ethnicities, White American and Asian, were simulated, too.2 simulations were created to analyze the effect of individual count in a population. Thus, population simulation with 100 persons and individual simulation was performed. 1 individual simulation was designed to investigate the CYP2D6 enzyme effect, and 1 individual was simulated for the paliperidone total hepatic clearance effect. 1 European population was simulated to investigate P-GP reference concentration. The remaining two population simulations were generated for receptor occupancy analysis for two CYP2D6 subtypes.

Table 3.5. Population demographics.

Populations		Belotto et al. [179]	Boonleang et al. [180]	Canovas et al. [181]	Gutierrez et al. [182]	Khorana et al. [183]	Kumar et al. [184]	Liu et al. [185]
Ethnicity		Brazilian White American	Thai Asian	Spanish European	Belgian European	Thai Asian	Indian Asian	Chinese Asian
Age (years)	Range	18-58	20.62-44.1	25	18-45	25	24-31	19.2-27.1
	Mean	32±12	28.18±8.27				26.8±2.4	22.9±2.7
Weight (kg)	Range	50-103	55.03-76.02				62-82	52.0-78.0
	Mean	70.4±11.9	62.43±4.76				70.7±6.8	63.2±7.0

Table 3.5. Population demographics. (cont.)

Populations		Belotto et al. [179]	Boonleang et al. [180]	Canovas et al. [181]	Gutierrez et al. [182]	Khorana et al. [183]	Kumar et al. [184]	Liu et al. [185]
Ethnicity		Brazilian White American	Thai Asian	Spanish European	Belgian European	Thai Asian	Indian Asian	Chinese Asian
Height (cm)	Range	156-180						162-187
	Mean	167±8						171.3±6.1
BMI (kg/m^2)	Range		18.99-24.91					
	Mean		21.76±2.07					
Female		11	0	0	0	0	0	0
Male		11	22	30	23	23	20	24

4. RESULTS AND DISCUSSION

4.1. Reconstruction of Human Metabolic Brain Model

The reaction distribution of metabolisms of the reconstructed model is given in Figure 4.1. Reaction distribution was performed based on KEGG Pathway Database. The final model consists of 1638 reactions (445 transport, 146 exchange, and 10 shuttle reactions out of 601), 1358 metabolites (715 unique regardless of the compartment), and 756 genes.

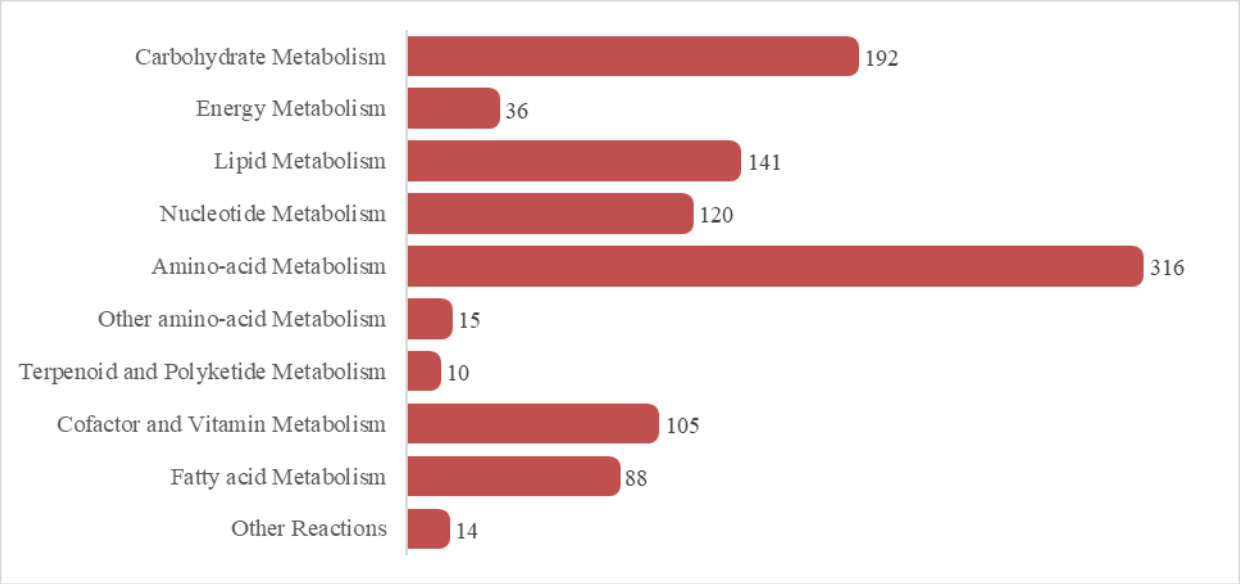

Figure 4.1. Reaction distribution of metabolisms of the reconstructed model.

4.1.1. Model Expansion

Carbohydrate metabolism is one of the most interesting metabolisms related to ASD. It can be controlled through diet, especially commonly used Ketogenic Diet (high fat, low carbohydrate), and this metabolic therapy aids in relieving some ASD symptoms [187]. In the model, carbohydrates metabolism consists of the following metabolisms and pathways:

- Glycolysis / Gluconeogenesis
- Tricarboxylic acid cycle and glyoxylate/dicarboxylate metabolism

- Pentose phosphate pathway
- Starch and sucrose metabolism
- Pyruvate metabolism
- Butanoate metabolism
- C5-branched dibasic acid metabolism
- Inositol phosphate metabolism
- Propanoate metabolism

In the presence of ASD, hypermetabolism of glucose and increased lactate production were reported [188]–[195]. This process is not only related to carbohydrate metabolism, but the chain of reactions starts here. To better investigate ASD, 76 carbohydrate metabolism reactions were added to the iMS570 model. iMS570 omits "C5-branched dibasic acid metabolism. The reconstructed model has 9 reactions for this metabolism. There is no change for the "Pentose phosphate pathway." Reaction additions about metabolism and pathways are as follows: Glycolysis / Glucogenesis, 18 reactions; Tricarboxylic acid cycle and glyoxylate/dicarboxylate metabolism, 12 reactions; Starch and sucrose metabolism, 9 reactions; Pyruvate metabolism, 12 reactions; Butanoate metabolism, 7 reactions; Propanoate metabolism, 11 reactions. The reconstructed model can provide better insight into ASD with carbohydrate metabolism expansion.

Oxidative stress, reactive oxygen species pathway, and their reaction with fatty acids are reported to be related to autism spectrum disorder [196–202]. Subsystems under "Energy Metabolism" are given below:

- Oxidative phosphorylation
- ROS detoxification
- Sulfur metabolism

Oxidative phosphorylation reactions were expanded from 10 to 17 as ROS detoxification reactions. Additionally, 2 sulfur metabolism reactions were added to the system. This expansion will aid in investigating especially transcriptome changes that occur in the presence of ASD.

The human brain's dry weight consists of 60% lipids [203]. Thus, any lipid metabolism malfunction alters signaling, plasma membrane integrity, and functions [204–206]. Therefore, cholesterol metabolism (15 reactions added) and glycerophospholipid metabolism (6 reactions added) were expanded. Bile acid biosynthesis and steroid metabolism reactions were added to the reconstructed model.

Some studies found nucleotide metabolism related to ASD based on urine findings [207, 208]. To investigate nucleotide metabolism alterations in the brain, reactions were doubled.

Dysregulation in amino-acid metabolism, antioxidant, vitamin, and cofactor metabolism is observed in ASD [209, 210]. Therefore, amino-acid metabolism and cofactor and vitamin metabolism were expanded from 121 reactions to 316 reactions and 16 reactions to 105 reactions, respectively. There was no pathway addition for amino-acid metabolism. However, under cofactor and vitamin metabolism, folate and porphyrin subsystems were expanded and "Vitamin B12 Metabolism", "Vitamin C Metabolism," "Vitamin D metabolism," "Biotin Metabolism," "Nicotinate and Nicotinamide Metabolism," "CoA Synthesis" and "Ubiquinone Synthesis" subsystems were added to the model.

As mentioned above, fatty acid metabolism and its signaling pathway are crucial for the brain, and its relation with autism spectrum disorder is thoroughly investigated [196-202]. Therefore, 10 more reactions were added to fatty acid metabolism to improve integrity within.

iMS570 transport reactions were designed as direct transport from neuron to astrocyte or astrocyte to neuron. With the addition of intercellular space [s], transport reactions increased. Besides diffusion, ATP-driven or channel-gated transports were also considered for the reconstructed model. Thus, 37 transport reactions were updated to 445. Increase in reactions and metabolism expansions; metabolites were also increased. Concerning that, exchange/demand reactions were expanded to 146 from 59.

4.1.2. Flux Variability Analysis

According to the results of FVA, the blocked reaction/total reaction ratio is less than 10% for the *E.coli* model iAF1260 [211], 25-26% for the iNL403 model [101] and 40% for the iMS570 model [103]. In the combined brain model, 409 out of 1638 reactions were blocked, thus making the rate equal to 25%, which is a small value for a model of this scale.

4.1.3. Transcriptome Data Integration

Transcriptome data were integrated into the reconstructed metabolic brain model based on down-regulation of the SHANK3 gene with an expression value of 1319.4 and a threshold of 30% of the gene expression average with a value of 36.8. After minimizing the internal fluxes, two autism-specific metabolic brain models were reconstructed. Comparison to healthy brain literature resting-state fluxes is given in Table 4.1.

Table 4.1. Comparison of transcriptome integrated models to healthy brain literature resting-state fluxes.

%Flux Ratio	ASD model with SHANK3 threshold	ASD model with 30%AVE threshold	Literature for Healthy resting state	References
Lactate release (R347/R33)	32.9	32.9	3-9	[212–215]
Glutamate/Glutamine cycle (R1638/ R33)	127.5	127.5	40-80	[216–218]
Astrocyte relative oxidative metabolism (R218/(R218+R699))	100.0	100.0	30	[216, 219, 220]
Total PPP ((R760+R758)/R33)	1.2	47.5	3-6	[221, 222]
Pyruvate carboxylase (R408/ R33)	14.3	12.7	10	[216, 219, 223]

The threshold for SHANK3 gene expression is relatively higher than the threshold for 30% of the average. Therefore, the reduced model of the SHANK3 threshold has lower reactions and metabolites. The SHANK3 model consists of 846 reactions and 996 metabolites, whereas in the 30%AVE (30% of gene expression average) model, there are 1153 reactions and 1178 metabolites. Therefore, the reaction distribution of the two models is different from each other. The ratios of the SHANK3 model to 30%AVE model are for Glycolysis/Glucogenesis reactions 39 to 26, for Pentose phosphate pathway reactions 17 to 16, Tricarboxylic acid cycle and glyoxylate/dicarboxylate metabolism reactions 32 to 18, Oxidative phosphorylation reactions 9 to 7 and ROS detoxification reactions 9 to 1. The significant difference between the total pentose phosphate pathway ratio (Table 4.1) can be explained by this difference in reaction distribution.

The objective functions are lactate dehydrogenase reactions and astrocyte pyruvate kinase reactions due to elevated lactate production in the presence of ASD [188–195]. Thus, lactate release is above healthy brain resting-state flux. Relative oxidative metabolism in astrocyte is above 3-fold of a healthy state. Mitochondrial dysfunction and increased citrate synthase were observed in ASD [224], and transcriptome analysis results are compatible with these experimental data. An increase in Glutamergic neurotransmission is associated with ASD. Glutamate/Glutamine cycle concerning glucose uptake increased for both integrated models (Table 4.1). Glutamergic dysfunction findings are consistent with ASD literature [225].

4.2. Physiology Based Pharmacokinetic Modelling

4.2.1. Effect of Population Density

PK-Sim helps to create populations, and the PK parameters of populations are the mean average. To investigate the effect of the number of people in the population, three European simulations at age 25 were performed: Individual, 30 people, 100 people. Basic physico-chemistry and ADME parameters of risperidone and paliperidone were described in Table 3.4 with CYP2D6.10 enzyme kinetics and 1.0 µM P-gp reference concentration. Figure 4.2 shows that the maximum concentration of risperidone and paliperidone for the individual is less than for populations. Since populations show the mean average, it is logical

to diverge from one person's calculations. For the maximum concentration time, a very steep difference can be observed for paliperidone in Figure 4.3. Even though $t_{1/2}$ (Figure 4.4) is not as diverse as t_{max}, individual PK parameters outstand population parameters. It may be caused by BMI differences between simulations or unfinished absorption of risperidone in the individual simulation. Unfinished absorption can result in a higher half-life for risperidone and corrupted calculations for paliperidone since it is risperidone's metabolite.

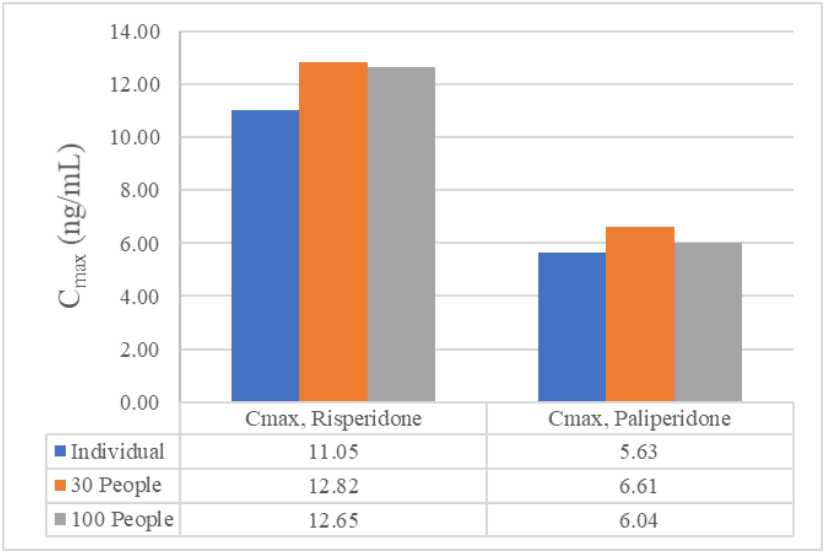

	Cmax, Risperidone	Cmax, Paliperidone
Individual	11.05	5.63
30 People	12.82	6.61
100 People	12.65	6.04

Figure 4.2. C_{max} values of risperidone and paliperidone for individual, 30 people, and 100 people populations.

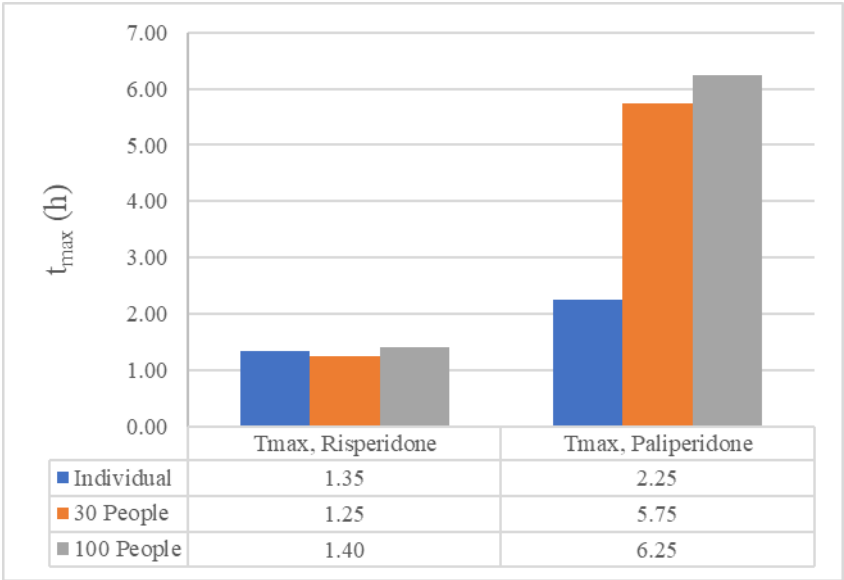

	Tmax, Risperidone	Tmax, Paliperidone
Individual	1.35	2.25
30 People	1.25	5.75
100 People	1.40	6.25

Figure 4.3. t_{max} values of risperidone and paliperidone for individual, 30 people, and 100 people populations.

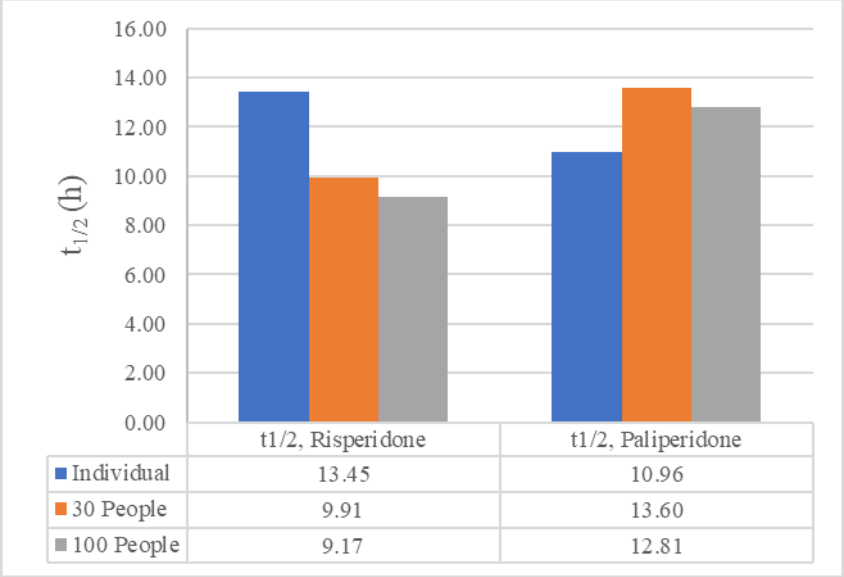

Figure 4.4. $t_{1/2}$ values of risperidone and paliperidone for individual, 30 people, and 100 people populations.

4.2.2. Effect of CYP2D6 Enzyme Kinetics

The effect of different CYP2D6 enzyme kinetics was investigated through 25 years old European individual simulations. For CYP2D6.1, the maximum rate of reaction is higher (2.3 pmol/min/pmol vs. 0.10 pmol/min/pmol), and substrate (risperidone) concentration to achieve half of the maximum rate is lower (1.1 µM vs. 6.70 µM) than CYP2D6.10. Therefore, a higher risperidone/paliperidone ratio is expected from CYP2D6.10 simulations since less paliperidone will be produced per risperidone consumed. CYP2D6.10 seems to have a lower affinity towards paliperidone, so it will require more risperidone concentration to achieve maximum rate, most probably due to competitive inhibitors [226].

When Figure 4.5 is investigated, it can be seen that the C_{max} ratio of Risperidone to Paliperidone is higher for CYP2D6.10 as expected. Additionally, $C_{max,\ Risperidone}$ is higher for CYP2D6.10, whereas $C_{max,\ Paliperidone}$ is lower. This is the result of low affinity. Risperidone to paliperidone conversion is slower for CYP2D6.10 therefore, there is more risperidone left and less paliperidone produced.

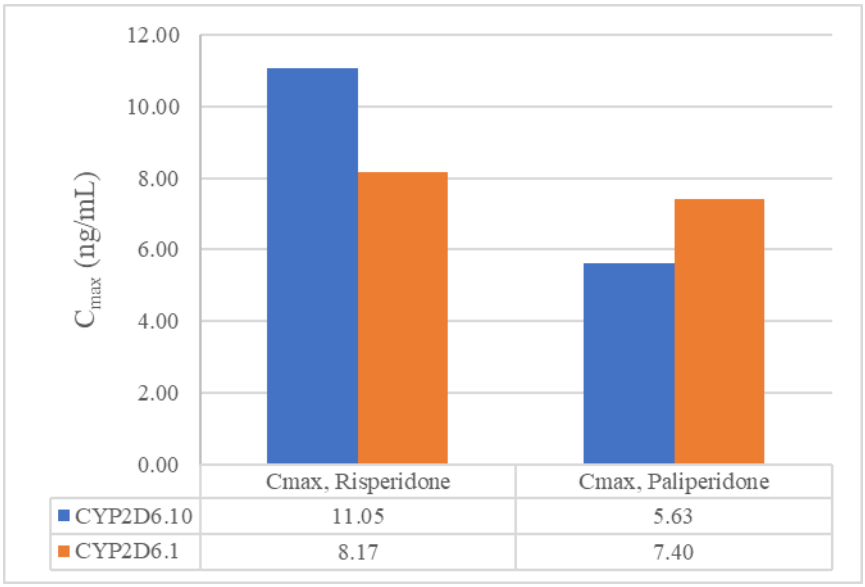

Figure 4.5. C_{max} values of risperidone and paliperidone for enzyme kinetics of CYP2D6.1 and CYP2D6.10.

Reaching the maximum concentration level is slower for CYP2D6.10 due to, again, low affinity. In Figure 4.6, there is a more significant difference for paliperidone because of the lower V_{max}/K_m ratio. The results in Figure 4.7 were also expected. There will be more risperidone needed per paliperidone production with low affinity; thus, the half-life of risperidone will be longer for CYP2D6.10. The half-life of paliperidone is longer for CYP2D6 simply because more paliperidone is produced to be cleared off.

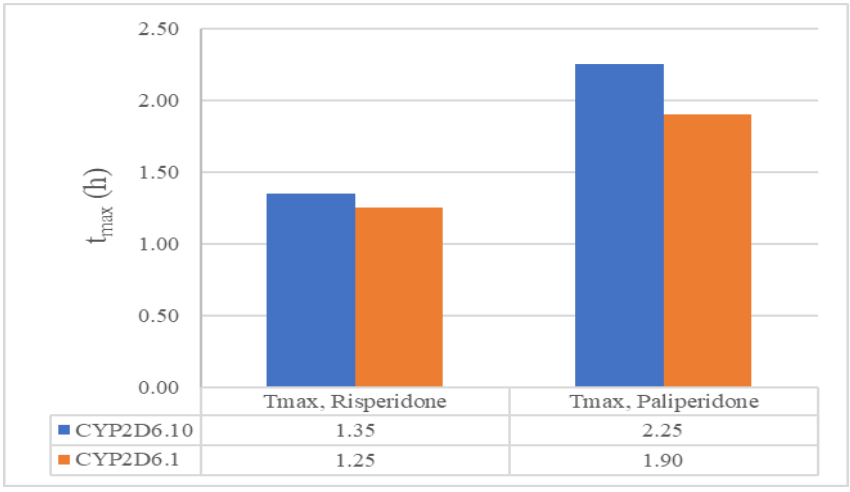

Figure 4.6. t_{max} values of risperidone and paliperidone for enzyme kinetics of CYP2D6.1 and CYP2D6.10.

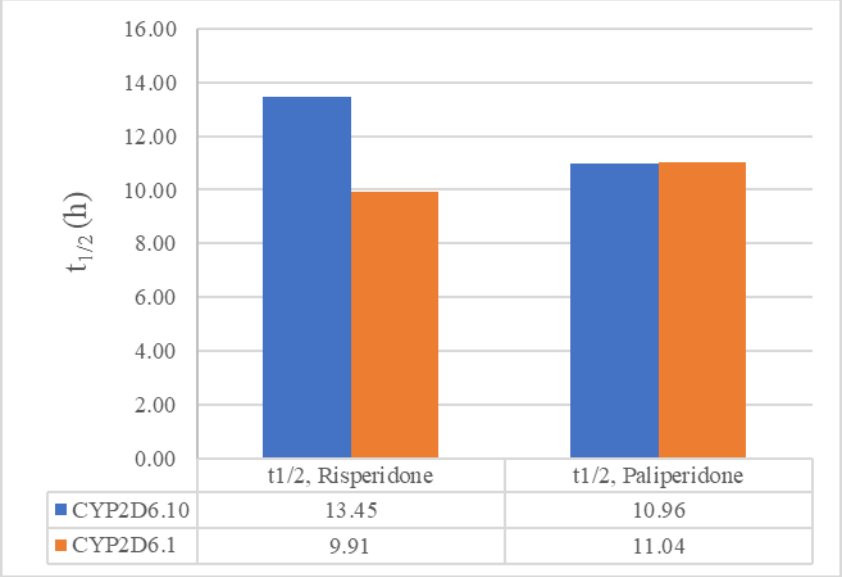

Figure 4.7. $t_{1/2}$ values of risperidone and paliperidone for enzyme kinetics of CYP2D6.1 and CYP2D6.10.

4.2.3. Effect of Ethnicities

PK-Sim provides ethnicity-driven physiological and anatomical investigations. For this purpose, European, White American, and Asian populations were simulated at age 25. As recall Table 3.3, BMIs of those populations are 23.57 kg/m^2, 25.22 kg/m^2, and 20.78 kg/m^2, respectively.

Risperidone is a highly lipophilic drug, and lipophilic drugs result in lower plasma concentrations. For higher BMI, the dosage needs to be higher for those drugs [227]. Figure 4.8 shows higher risperidone and thus paliperidone concentrations for the Asian population since BMI is the lowest and risperidone will not bind to fat tissue but circulate. t_{max} values given in Figure 4.9 show a longer time to reach the highest concentration of paliperidone for White Americans. This might be slower conversion to the metabolite since distribution is slower for higher BMI. The highest $t_{1/2}$ belongs to the Asian population, as expected in Figure 4.10. The unexpected delay in t_{max} of the Asian population may be caused by CYP2D6 polymorphisms [228, 229].

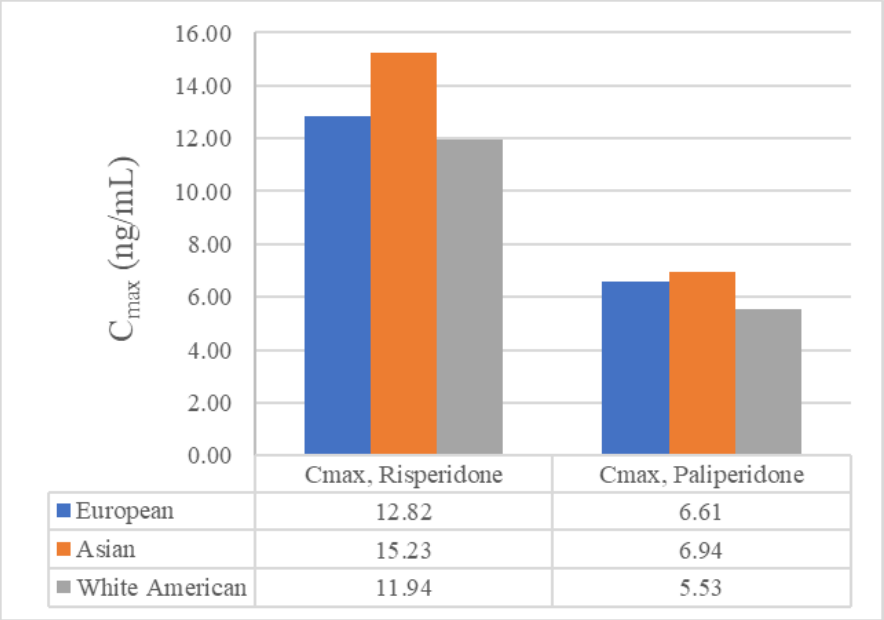

Figure 4.8. C_{max} values of risperidone and paliperidone for European, White American, and Asian populations.

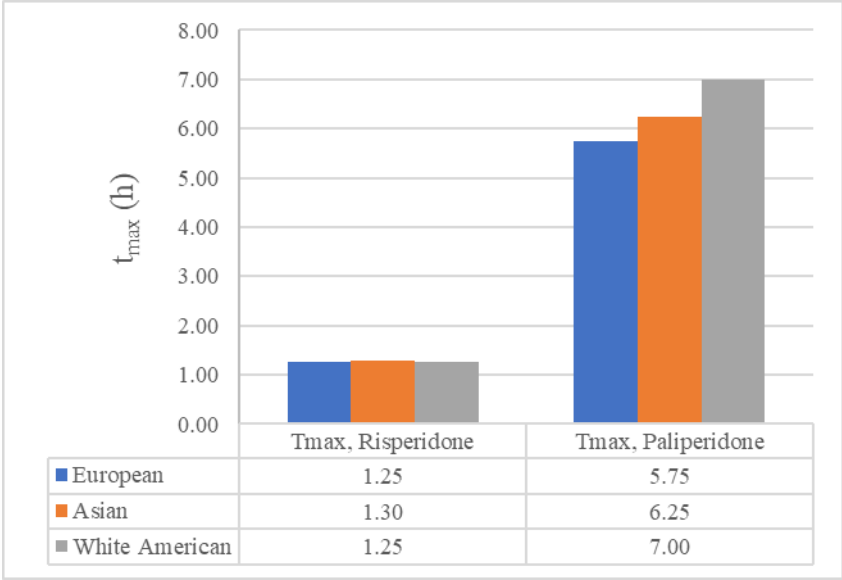

Figure 4.9. t_{max} values of risperidone and paliperidone for European, White American, and Asian populations.

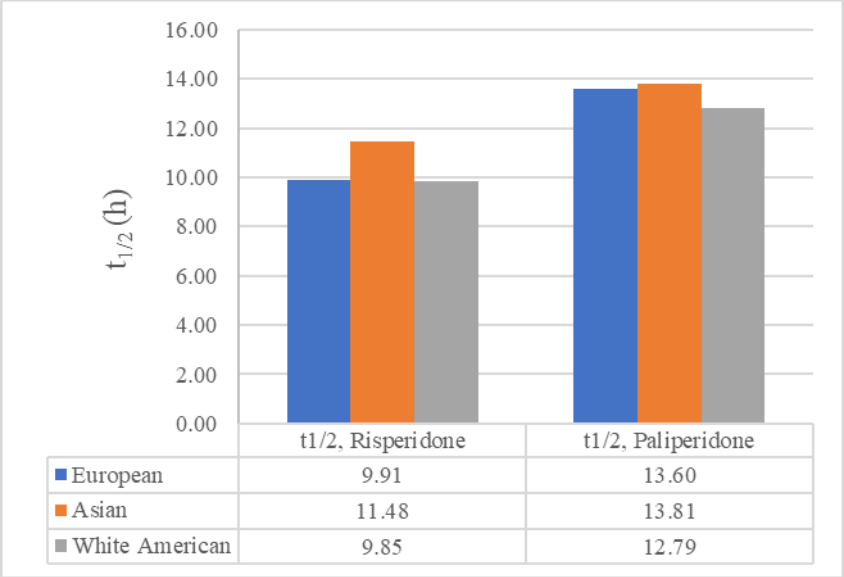

Figure 4.10. $t_{1/2}$ values of risperidone and paliperidone for European, White American, and Asian populations.

4.2.4. Effect of Hepatic Clearance of Paliperidone

Effect of hepatic clearance of paliperidone was investigated via a 25-year-old European individual with $CL_{Hepatic,\ Paliperidone}$ value with 1.04 mL/min/kg and its half 0.52 mL/min/kg. This change did not affect risperidone values since paliperidone is the end metabolite. When hepatic clearance of paliperidone decreases, C_{max}, $t_{max,}$ and $t_{1/2}$ values are increased, as shown in Figure 4.11, Figure 4.12, and Figure 4.13. When paliperidone is cleared from the liver as half as before, its concentration, time to reach this concentration, and time to remain in high concentrations increase.

4.2.5. Effect of P-GP Concentration

P-gp transport protein in the PBPK model was expressed in the blood-brain barrier and, paliperidone and risperidone are substrates/inhibitors of P-gp with moderate to strong affinity [230]. Increased concentration of P-gp leads to an increased influx of risperidone and paliperidone into the brain, which causes lower plasma concentration. Figure 4.14 demonstrates the maximum concentration that can be achieved in peripheral venous blood plasma concentrations.

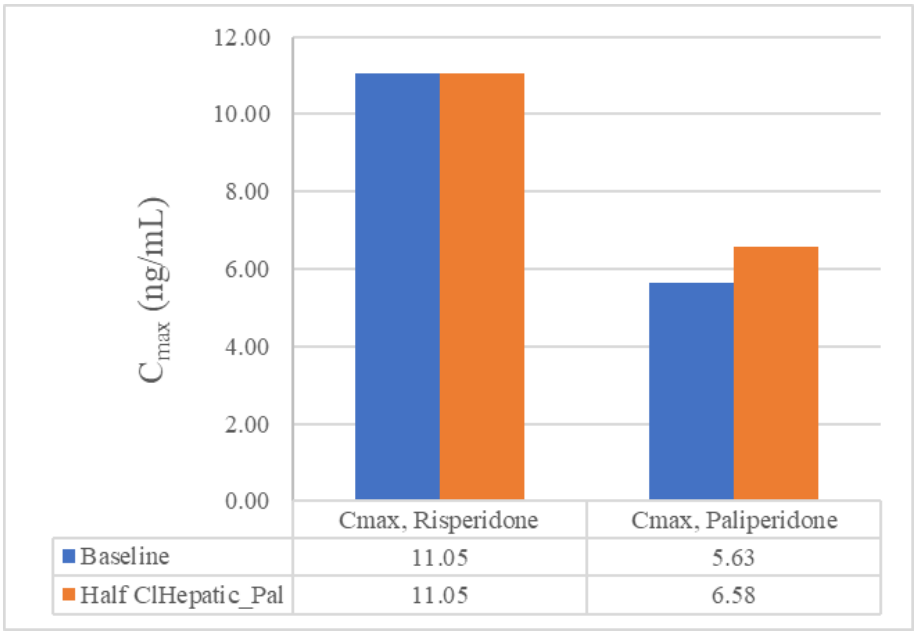

Figure 4.11. C_{max} values of risperidone and paliperidone for baseline and half $CL_{Hepatic,\ Paliperidone}$.

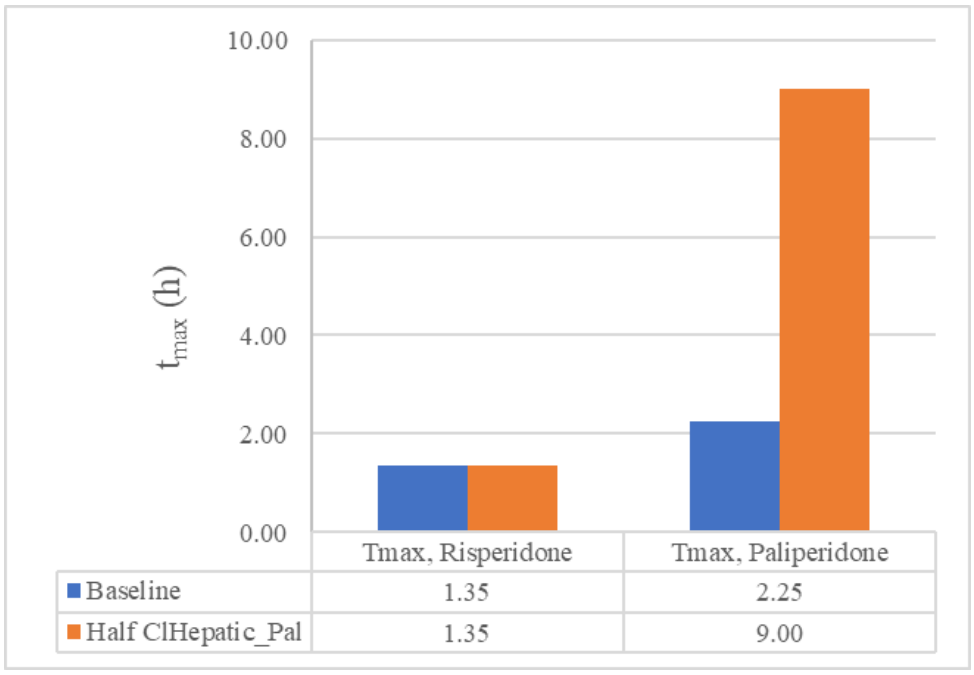

Figure 4.12. t_{max} values of risperidone and paliperidone for baseline and half $CL_{Hepatic,Paliperidone}$.

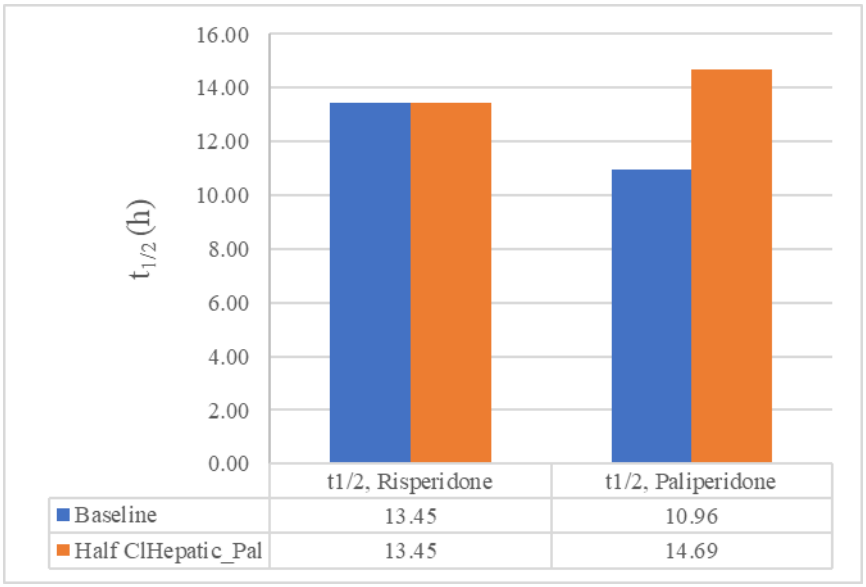

Figure 4.13. $t_{1/2}$ values of risperidone and paliperidone for baseline and half $CL_{Hepatic,Paliperidone}$.

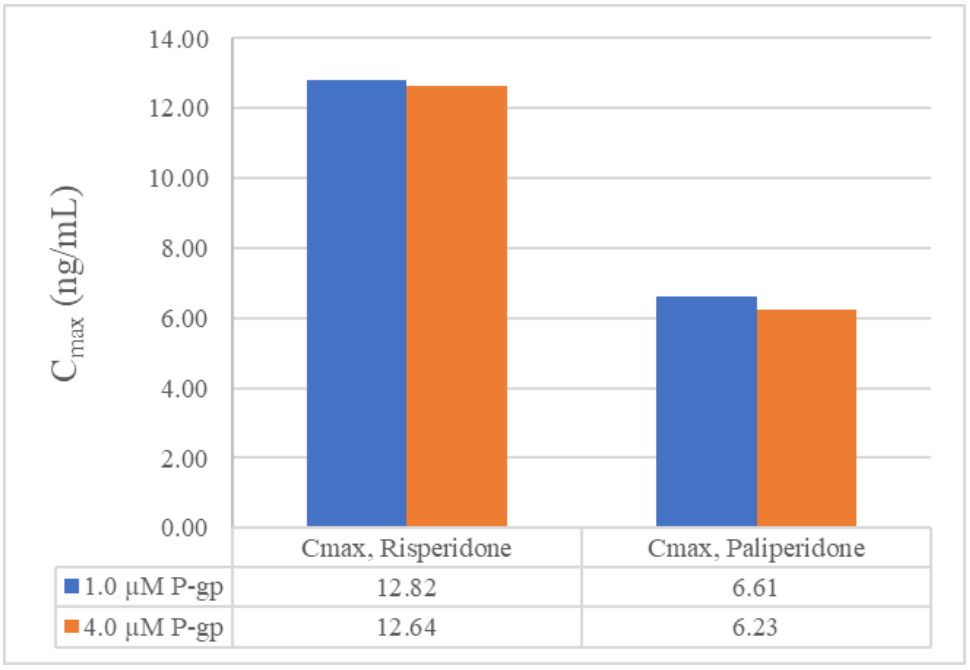

Figure 4.14. C_{max} values of risperidone and paliperidone for P-gp concentration of 1.0 µM and 4.0 µM.

In Figure 4.15, t_{max} values and in Figure 4.6, $t_{1/2}$ values of risperidone and paliperidone are higher for a higher concentration of P-gp transport protein. Because the parent drug and its metabolite transport through BBB to reach the highest concentration in plasma lags.

According to Table 3.4, V_{max}/K_m is higher for paliperidone. It means paliperidone has a higher affinity to P-gp than risperidone. It may be the reason for a slightly more significant impact on paliperidone.

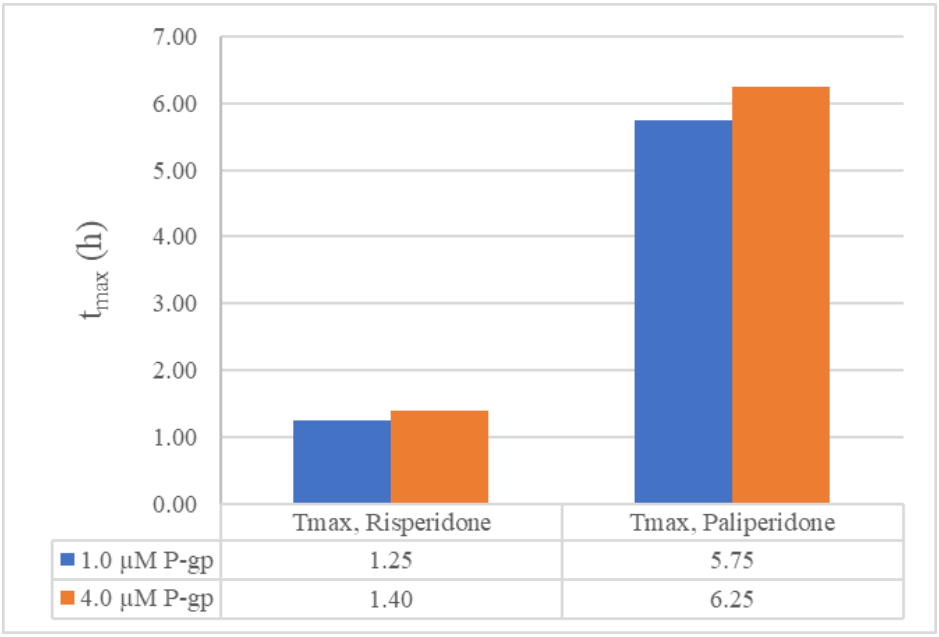

Figure 4.15. t_{max} values of risperidone and paliperidone for P-gp concentration of 1.0 µM and 4.0 µM.

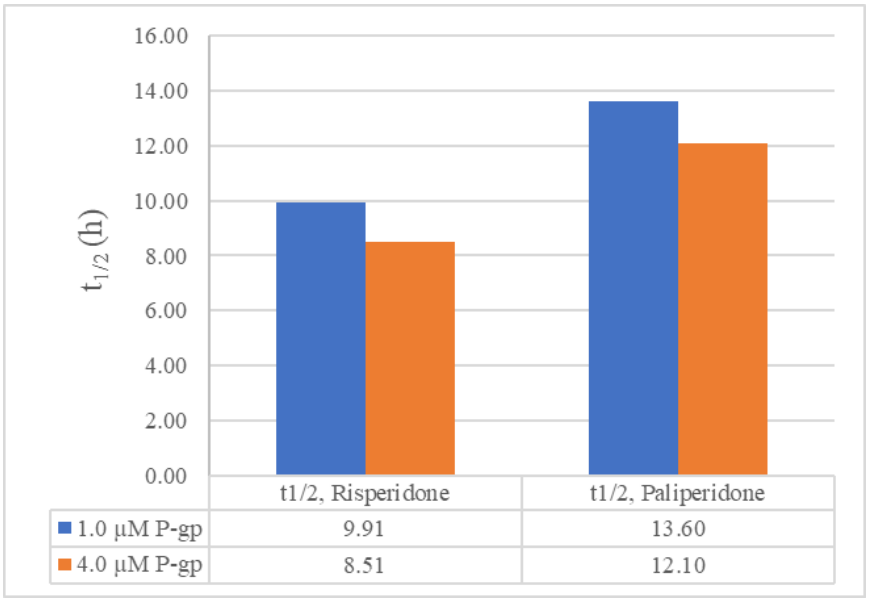

Figure 4.16. $t_{1/2}$ values of risperidone and paliperidone for P-gp concentration of 1.0 µM and 4.0 µM.

4.2.6. Comparison/Validation with Experimental Data in Articles

The articles whose demographic information is given in Table 3.5 were simulated. C_{max} values of risperidone have the closest value for Canovas et al. [181]. However, the risperidone/paliperidone ratio is underestimated experimental data from the articles. This may have been caused by CYP2D6 polymorphism. This polymorphism results in a higher plasma concentration of risperidone [229]. Additionally, metabolizer types were not specified in the articles, generally. There could be poor metabolizers that can increase the risperidone to paliperidone ratio [231].

The lower risperidone to the 9-hidroxyrisperidone ratio that characterizes the ultra-rapid metabolizers phenotype may explain the lower propensity of this phenotype to induce weight gain because of the differences in the affinity of these compounds for the receptors that might be involved in weight regulation, such as 5-HT2.

The most significant Risperidone/Paliperidone ratio divergence is Belotto et al. [179]. Only in this article is paliperidone way higher than risperidone. According to the trial simulations, enzyme kinetics (especially V_{max}, K_m values of CYP enzymes) and population significantly impact population PK parameters. The ethnicity was not stated in the article; it is only known that the study was held in Brazil. The diversity of the sample group may have caused a significant difference between the parent drug and its metabolite.

Asian studies Khorana et al., Kumar et al., and Liu et al. are best in alliance with literature data. CYP2D6.10 has a high frequency among Asians. Especially, Khorana et al. have the trend of CYP2D6.10 because of the risperidone/paliperidone ratio. Additionally, the t_{max} of paliperidone is higher for Asian studies. Half-lives of risperidone are slightly higher, half-lives of paliperidone are lower than the literature value. The comparison graphics can be found in Figure 4.17, Figure 4.18, and Figure 4.19.

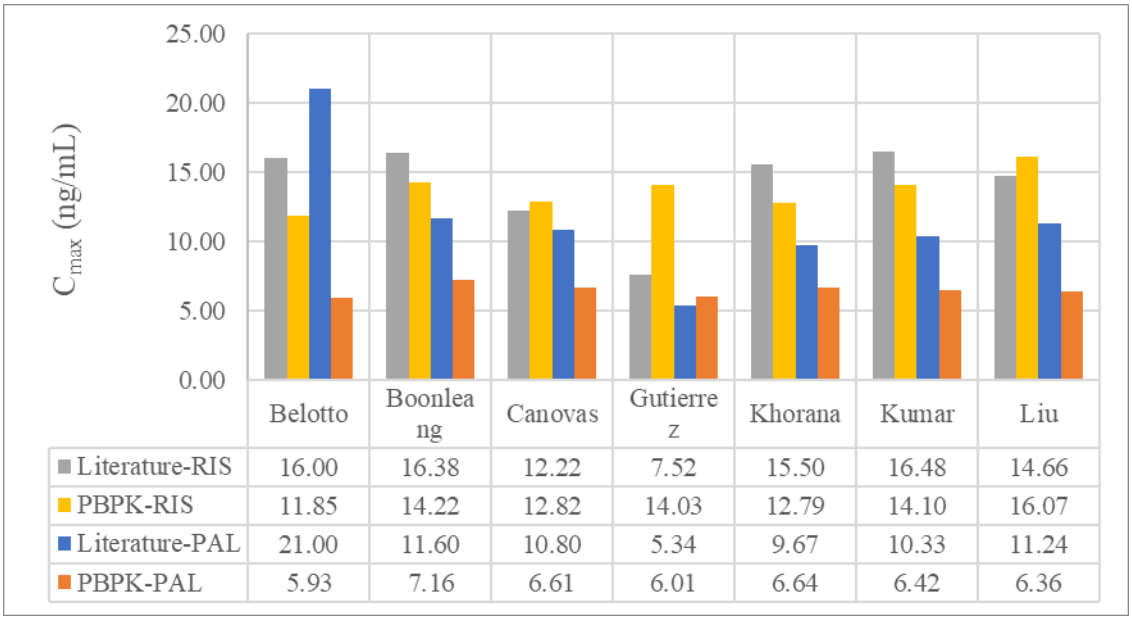

	Belotto	Boonleang	Canovas	Gutierrez	Khorana	Kumar	Liu
Literature-RIS	16.00	16.38	12.22	7.52	15.50	16.48	14.66
PBPK-RIS	11.85	14.22	12.82	14.03	12.79	14.10	16.07
Literature-PAL	21.00	11.60	10.80	5.34	9.67	10.33	11.24
PBPK-PAL	5.93	7.16	6.61	6.01	6.64	6.42	6.36

Figure 4.17. C_{max} values of risperidone and paliperidone of research articles and their PBPK calculations.

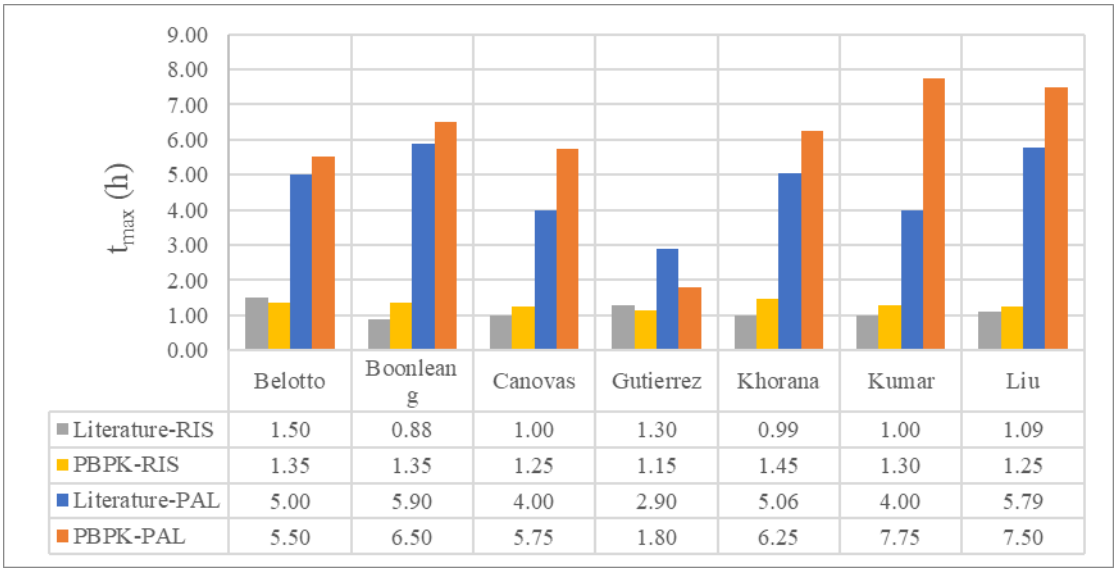

	Belotto	Boonleang	Canovas	Gutierrez	Khorana	Kumar	Liu
Literature-RIS	1.50	0.88	1.00	1.30	0.99	1.00	1.09
PBPK-RIS	1.35	1.35	1.25	1.15	1.45	1.30	1.25
Literature-PAL	5.00	5.90	4.00	2.90	5.06	4.00	5.79
PBPK-PAL	5.50	6.50	5.75	1.80	6.25	7.75	7.50

Figure 4.18. t_{max} values of risperidone and paliperidone of research articles and their PBPK calculations.

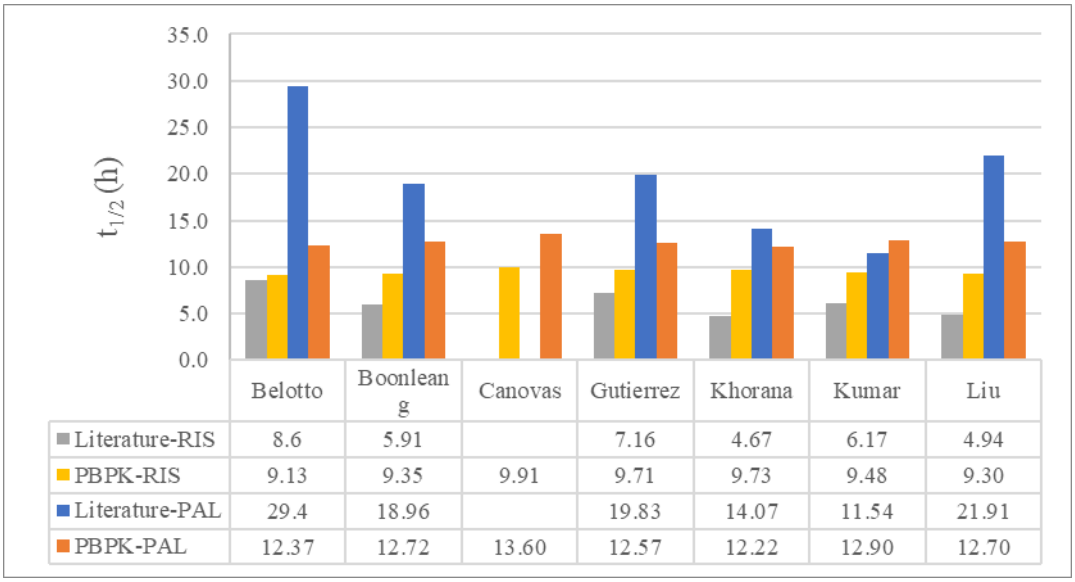

	Belotto	Boonleang	Canovas	Gutierrez	Khorana	Kumar	Liu
Literature-RIS	8.6	5.91		7.16	4.67	6.17	4.94
PBPK-RIS	9.13	9.35	9.91	9.71	9.73	9.48	9.30
Literature-PAL	29.4	18.96		19.83	14.07	11.54	21.91
PBPK-PAL	12.37	12.72	13.60	12.57	12.22	12.90	12.70

Figure 4.19. $t_{1/2}$ values of risperidone and paliperidone of research articles and their PBPK calculations.

4.2.7. Receptor Occupancy

Receptor occupancy simulations were performed based on Nyberg et al. [186]. Twice a day total of 6 mg oral risperidone was prescribed for the first 28 days, and then twice a day total of 3 mg oral risperidone was taken for another 14 days. The examinations were performed on the 28th and 42nd days, 3.5-4 hours after the morning dose. Therefore, data from days 27.17 and 41.17 were collected since day 0 was the start of the treatment for PBPK simulations. To investigate the CYP2D6 enzyme kinetics' effect, two simulations were executed.

Table 4.2. The concentration of active moiety of literature data and PBPK simulations.

	Concentration of Active Moiety (ng/mL)	
	Day 28	Day 42
CYP2D6.10	40.96	22.04
CYP2D6.1	29.30	18.45
Literature (Range)	34.8 (27.4-42.6)	17.9 (12.0-22.6)

The concentration of active moiety (risperidone+paliperidone) is in the range of literature for both simulations as can be seen from Table 4.2. Deviation of the day 42 results from a patient who dropped the study. Receptor occupancy of active moiety simulation results is tabulated in Table 4.3. Receptor occupancy of simulation CYP2D6.1 was underestimated. Since the patients have schizophrenia, genetic variations, D2 receptor availability, and the effect of other medications can alter receptor occupancy results. In either case, both CYP2D6.1 and CYP2D6.10 are promising simulations for ASD integration.

Table 4.3. Receptor Occupancy of active moiety of literature data and PBPK simulations.

	Receptor Occupancy %	
	Day 28	Day 42
CYP2D6.10	84	67
CYP2D6.1	69	55
Literature (Range)	82 (79-85)	72 (53-78)

Receptor occupancy results can be used to manipulate the SLC6A3 gene, which encodes dopamine transporter. Since dopaminergic neurotransmission was increased in the presence of ASD, as mentioned earlier, related to PBPK RO results, SLC6A3 gene downregulation can be performed based on transcriptome analysis data to observe risperidone's effect on the autism-specific brain.

4.3. Receptor Occupancy Integration to Autism-Specific Metabolic Brain Model

SLC6A3 gene decodes dopamine sink from astrocyte and neuron. Receptor occupancy integration was performed by limiting reactions coded by the SLC6A3 gene, "HMR_9092" and "HMR_9092_N" by 0.16. In Table 4.3, receptor occupancy at day 28 for CYP2D6.10 was 84%. Then, the remaining receptors should be 16%. Flux ratio comparison with autism-specific metabolic brain model is given in Table 4.4.

Table 4.4. Flux ratio comparison of autism-specific brain model to the healthy state literature value.

%Flux Ratio	Autism-specific	RO constrained	Literature
Lactate release (R347/R33)	32.9	32.9	3-9
Glutamate/Glutamine cycle (R1638/ R33)	127.5	18.3	40-80
Astrocyte relative oxidative metabolism (R218/(R218+R699))	100.0	70.8	30
Total PPP ((R760+R758)/R33)	47.5	21.5	3-6
Pyruvate carboxylase (R408/ R33)	12.7	5.08	10

After receptor occupancy integration, lactate release did not change however glutamate/glutamine cycle flux decreased below the healthy resting state value. This adverse effect may be related to the excess effective dose. A decrease in dopamine resulted in a decline in the glutamine/glutamate cycle. Antipsychotics could not fix the mitochondrial dysfunction, as expected. On the other hand, it relieves the hypermetabolism, as seen from flux ratio decrements for astrocyte relative oxidative metabolism, total PPP, and pyruvate carboxylase.

5. CONCLUSIONS AND RECOMMENDATIONS

Autism spectrum disorder is a complex developmental condition with increasing prevalence. The lack of cause-targeted medication treatment encourages researchers to investigate the mechanism of the disorder. This research aims to reconstruct a metabolic brain model extended with autism-specific genes and reactions. iMS570 brain GEM is enriched with iNL403 and MODEL1608180000. The reconstructed model contains 1638 reactions, 1358 metabolites, and 756 genes with a 25% blockage rate calculated with FVA. The reconstructed model is objected to being integrated with transcriptome data to investigate the brain under autism-like system conditions. The data for transcriptome analysis is GSE28475, which was prepared with 18630 unique genes and their gene expression data. Two threshold values are chosen according to the SHANK3 expression value and 30% of the total average of the mean expression of the samples. Transcriptome integration of those thresholds resulted in mitochondrial and glutaminergic dysfunction. Energy metabolism is highly affected by abnormalities of ASD transcriptome.

To simulate the importance of dosage and its effect on the brain, the risperidone Physiology Based Pharmacokinetic model is executed. Risperidone is an antipsychotic, and it is used for symptomatic medical treatment of ASD. Ethnicity, CYP2D6 enzyme kinetics, paliperidone total hepatic clearance, individual count in a population, and P-gp concentration effects are investigated with one time 2 mg oral dose of Risperidone. Individual count simulations are performed with an individual, 30 and 100 people European population of a 25-year-old male. Absorption of risperidone is unfinished in individual simulations; therefore, individual simulations' results differed from population simulations. Risperidone half-life is significantly high (13.45 hours vs. 9.91 hours and 9.14 hours).

CYP2D6.1 and CYP2D6.10 simulations are executed with a 25-year-old European male with a 2 mg single oral dose of risperidone. CYP2D6.10 has a lower V_{max}/K_m ratio, which leads to low affinity and slow conversion. $C_{max,\ Risperidone}/\ C_{max,\ Paliperidone}$ is higher for CYP2D6.10 (11.05 ng/ML/5.63 ng/ML) where CYP2D6.1 is 8.17 ng/mL/7.40 ng/mL. t_{max} values of CYP2D6.10 simulations are also higher.

Ethnicity with the lowest BMI, 20.78 kg/m^2, Asian populations have the highest plasma concentrations since risperidone is lipophilic. Delay in t_{max} of Asian population may be caused by CYP2D6 polymorphisms, and $t_{1/2}$ is the highest within ethnicities, White American and Asian.

Total hepatic clearance changes only affected paliperidone values. An increase in hepatic clearance of paliperidone results in a decrease of C_{max}, $t_{max,}$ and $t_{1/2}$ values. The rise in reference concentration of P-gp also leads to lower C_{max} but higher t_{max} because of the increased influx of the drugs through BBB.

Then, to compare and validate our modelling results, PBPK model simulations are performed using the experimental data on ASD in articles. Risperidone/paliperidone concentration ratios are found closer to Asian studies, and t_{max} and $t_{1/2}$ are in the upper half of the range. Those findings imply the importance of CYP enzymes kinetics. The clearance of paliperidone from the liver is assumed linear based on the parameters found in the literature. However, actual clearance can be through Michaelis-Menten kinetics. The receptor occupancy of the active moiety (risperidone plus paliperidone) is simulated for a chronic oral dose of risperidone for 8 people. Treatment is 3 mg risperidone twice a day for 24 days and 1.5 mg risperidone twice a day for 14 days. The results are compatible with the literature value range. Calculated receptor occupancy and plasma concentrations are underestimated. Since the literature data belongs to schizophrenic patients, this underestimation is validated.

The genome-scale autistic brain model developed within the framework of this thesis study enables us to observe changes in dopamine D2 receptors in the presence of antipsychotics. Autism-specific brain model shows glutaminergic and mitochondrial dysfunctions. The dopamine receptor occupancy of antipsychotic drugs (risperidone) can be simulated by the down-regulation of the dopamine receptor genes (SLC6A3). 84% receptor occupancy simulation indicates excessive drug dose due to drastic decrease in glutaminergic

neurotransmission. It also reduces mitochondrial dysfunction effects but does not neutralize, as expected.

Further improvements to the thesis could be made on the brain model. Expansions based on ASD-related genes may be performed after transcriptome integration, analysis, and validation of the current reconstructed brain model. It was not desirable in the course of this thesis due to enhanced computer load and complexity of addition and connection of dead-end metabolites. Weighted gene expression transcriptome analysis can result in more accurate fluxes such as Integrative Network Inference for Tissues (INIT) algorithm. Also, the integration of dopamine D2 receptor occupancy information can be performed through this weighted gene expression transcriptome analysis algorithm.

REFERENCES

1. Chaste, P. and M. Leboyer. "Autism Risk Factors: Genes, Environment, and Gene-Environment Interactions", *Dialogues in Clinical Neuroscience*. Vol. 14(3), pp. 281-292, 2012.

2. Sontheimer, H. *Chapter 11 - Neurodevelopmental Disorders*. Academic Press; pp. 319-347, 2015.

3. Grzadzinski, R., M. Huerta and C. Lord. "DSM-5 and Autism Spectrum Disorders (ASDs), pp. An Opportunity for Identifying ASD Subtypes", *Molecular Autism*, Vol. 4(1), No. 12, 2013.

4. Baio, J., L. Wiggins, D. L. Christensen, M. J. Maenner, J. Daniels, Z. Warren, M. Kurzius-Spencer, W. Zahorodny, C. R. Rosenberg, T. White, M. S. Durkin, P. Imm, L. Nikolaou, M. Yeargin-Allsopp, L. C. Lee, R. Harrington, M. Lopez, R. T. Fitzgerald, A. Hewitt, S. Pettygrove, J. N. Constantino, A. Vehorn, J. Shenouda, J. Hall-Lande, K. van Naarden Braun and N. F. Dowling. "Prevalence of Autism Spectrum Disorder Among Children Aged 8 Years — Autism and Developmental Disabilities Monitoring Network, 11 Sites, United States, 2014", *MMWR Surveill Summaries*, Vol. 67(6), p. 1, 2018.

5. Buescher, A.V.S., Z. Cidav, M. Knapp and D.S. Mandell. "Costs of Autism Spectrum Disorders in the United Kingdom and the United States", *JAMA Pediatrics*, Vol. 168(8), pp. 721-728, 2014.

6. Rakap, S., B. Birkan and S. Kalkan. "Türkiye'de Otizm Spektrum Bozukluğu ve Özel Eğitim", *Tohum Otizm Vakfı*, 2017.

7. Szatmari, P. and M.B. Jones. "IQ and the Genetics of Autism", *Journal of Child Psychology and Psychiatry*, Vol. 32(6), pp. 897-908, 1991.

8. Bailey, A.J. "The Biology of Autism", *Psychological Medicine,* Vol. 23(1), pp. 7-11, 1993.

9. Folstein, S. and M. Rutter. "Infantile Autism: A Genetic Study of 21 Twin Pairs", *Journal of Child Psychology and Psychiatry,*Vol. 18(4), pp. 297-321, 1977.

10. Folstein, S. E. and J. Piven. "Etiology of Autism: Genetic Influences", *Pediatrics*. Vol. 87(5 Pt 2), pp. 767-773, 1991.

11. Veenstra-Vanderweele, J., and E. H. Cook Jr. "Genetics of childhood disorders: XLVI. Autism, Part 5: Genetics of Autism.", *Journal of the American Academy of Child & Adolescent Psychiatry,* Vol. 42(1), pp. 116-118, 2003.

12. Bailey, A., A. Le Couteur, I. Gottesman, P. Bolton, E. Simonoff, E. Yuzda and M. Rutter. "Autism as a Strongly Genetic Disorder: Evidence from a British Twin Study". *Psychological Medicine,* Vol. 25(1), pp. 63-77, 1995.

13. Miles, J.H. "Autism Spectrum Disorders-A genetics review". *Genetics in Medicine,* Vol. 13(4), pp. 278-294, 2011.

14. Buxbaum, J.D. "Multiple Rare Variants in the Etiology of Autism Spectrum Disorders", *Dialogues in Clinical Neuroscience,* Vol. 11(1), pp. 35-43, 2009.

15. Wang, K., H. Zhang, D. Ma, M. Bucan, J. T. Glessner, B.S. Abrahams, D. Salyakina, M. Imielinski, J. P. Bradfield, P. M. A. Sleiman, C. E. Kim, C. Hou, E. Frackelton, R. Chiavacci, N. Takahashi, T. Sakurai, E. Rappaport, C. M. Lajonchere, J. Munson, A. Estes, O. Korvatska, J. Piven, L. I. Sonnenblick, A. I. A. Retuerto, E. I. Herman, H. Dong, T. Hutman, M. Sigman, S. Ozonoff, A. Klin, T. Owley, J. A. Sweeney, C. W. Brune, R. M. Cantor, R. Bernier, J. R. Gilbert, M. L. Cuccaro, W. M. McMahon, J. Miller, M. W. State, T. H. Wassink, H. Coon, S. E. Levy, R. T. Schultz, J. I. Nurnberger, J. L. Haines, J. S. Sutcliffe, E. H. Cook, N. J. Minshew, J. D. Buxbaum, G. Dawson, S. F. A. Grant, D. H. Geschwind, M. A. Pericak-Vance, G. D. Schellenberg and H. Hakonarson. "Common Genetic Variants on 5p14.1 Associate with Autism Spectrum Disorders", *Nature,* Vol. 459(7246), pp. 528-533, 2009.

16. Jamain, S., H. Quach, C. Betancur, M. Rastam, C. Colineaux, I. C. Gillberg, Paris Autism Research International Sibpair Study and T. Bourgeron. "Mutations of the X-Linked Genes Encoding Neuroligins NLGN3 and NLGN4 are Associated with Autism", *Nature Genetics,* Vol. 34(1), pp. 27-29, 2003.

17. Laumonnier, F., F. Bonnet-Brilhault, M. Gomot, R. Blanc, A. David, M. P. Moizard, M. Raynaud, N. Ronce, E. Lemonnier, P. Calvas, B. Laudier, J. Chelly, J. P. Fryns, H. H. Ropers, B. C. J. Hamel, C. Andres, C. Barthelemy, C. Moraine and S. Briault. "X-linked Mental Retardation and Autism are Associated with a Mutation in the NLGN4 Gene, a Member of the Neuroligin Family", *The American Journal of Human Genetics,* Vol. 74(3), pp. 552-557, 2004.

18. Durand, C. M., C. Betancur, T. M. Boeckers, J. Bockmann, P. Chaste, F. Fauchereau, G. Nygren, M. Rastam, I. C. Gillberg, H. Anckarsaeter, E. Sponheim, H. Goubran-Botros, R. Delorme, N. Chabane, M. C. Mouren-Simeoni, P. de Mas, E. Bieth, B. Rogé, D. Héron, L. Burglen, C. Gillberg, M. Leboyer and T. Bourgeron. "Mutations in the Gene Encoding the Synaptic Scaffolding Protein SHANK3 are Associated with Autism Spectrum Disorders", *Nature Genetics,* Vol. 39(1), pp. 25-27, 2007.

19. Moessner, R., C. R. Marshall, J. S. Sutcliffe, J. Skaug, D. Pinto, J. Vincent, L. Zwaigenbaum, B. Fernandez, W. Roberts, P. Szatmari and S. W. Scherer. "Contribution of SHANK3 Mutations to Autism Spectrum Disorder", *The American Journal of Human Genetics,* Vol. 81(6), pp. 1289-129, 2007.

20. Folstein, S. E., B. Rosen-Sheidley. "Genetics of Austim: Complex Aetiology for a Heterogeneous Disorder", *Nature Reviews Genetics,* Vol. 2(12), pp. 943-955, 2001.

21. Wu, S., M. Jia, Y. Ruan, J. Liu, Y. Guo, M. Shuang, X. Gong, Y. Zhang, X. Yang and D. Zhang. "Positive Association of the oxytocin Receptor Gene (OXTR) with Autism in the Chinese Han Population", *Biological Psychiatry,* Vol. 58.1, pp. 74-77, 2005.

22. Hehr, U., G. Uyanik, C. Gross, M. C. Walter, A. Bohring, M. Cohen, B. Oehl-Jaschkowitz, L. M. Bird, G. M. Shamdeen, U. Bogdahn, G. Schuierer, H. Topaloglu, L. Aigner, H. Lochmüller and J. Winkler. "Novel POMGnT1 Mutations Define

Broader Phenotypic Spectrum of Muscle–Eye–Brain Disease", *Neurogenetics,* Vol. 8(4), pp. 279-288, 2007.

23. Van der Zwaag, B., L. Franke, M. Poot, R. Hochstenbach, H. A. Spierenburg, J. A. Vorstman, E. van Daalen, M. V. de Jonge, N. E. Verbeek, E. H. Brilstra, R. van 't Slot, R. A. Ophoff, M. A. van Es, H. M. Blauw, J. H. Veldink, J. E. Buizer-Voskamp, F. A. Beemer, L. H. van den Berg, C. Wijmenga, H. K. P. van Amstel, H. van Engeland, J. P. H. Burbach and W. G. Staal. "Gene-Network Analysis Identifies Susceptibility Genes Related to Glycobiology in Autism", *PLoS One,* Vol. 4(5), No. e5324, 2009.

24. Yu, T. W., M. H. Chahrour, M. E. Coulter, S. Jiralerspong, K. Okamura-Ikeda, B. Ataman, K. Schmitz-Abe, D. A. Harmin, M. Adli, A. N. Malik, A. M. D'Gama, E. T. Lim, S. J. Sanders, G. H. Mochida, J. N. Partlow, C. M. Sunu, J. M. Felie, J. Rodriguez, R. H. Nasir, J. Ware, R. M. Joseph, R. S. Hill, B. Y. Kwan, M. Al-Saffar, N. M. Mukaddes, A. Hashmi, S. Balkhy, G. G. Gascon, F. M. Hisama, E. LeClair, A. Poduri, O. Oner, S. Al-Saad, S. A. Al-Awadi, L. Bastaki, T. Ben-Omran, A. S. Teebi, L. Al-Gazali, V. Eapen, C. R. Stevens, L. Rappaport, S. B. Gabriel, K. Markianos, M. W. State, M. E. Greenberg, H. Taniguchi, N. E. Braverman, E. M. Morrow and C. A. Walsh. "Using Whole-Exome Sequencing to Identify Inherited Causes of Autism", *Neuron,* Vol. 77(2), pp. 259-273, 2013.

25. De Rubeis, S., X. He, A. P. Goldberg, C. S. Poultney, K. Samocha, A. Ercument Cicek, Y. Kou, L. Liu, M. Fromer, S. Walker, T. Singh, L. Klei, J. Kosmicki, S. C. Fu, B. Aleksic, M. Biscaldi, P. F. Bolton, J. M. Brownfeld, J. Cai, N. G. Campbell, A. Carracedo, M. H. Chahrour, A. G. Chiocchetti, H. Coon, E. L. Crawford, L. Crooks, S. R. Curran, G. Dawson, E. Duketis, B. A. Fernandez, L. Gallagher, E. Geller, S. J. Guter, R. S. Hill, I. Ionita-Laza, P. Jimenez Gonzalez, H. Kilpinen, S. M. Klauck, A. Kolevzon, I. Lee, J. Lei, T. Lehtimäki, C. F. Lin, A. Ma'ayan, C. R. Marshall, A. L. McInnes, B. Neale, M. J. Owen, N. Ozaki, M. Parellada, J. R. Parr, S. Purcell, K. Puura, D. Rajagopalan, K. Rehnström, A. Reichenberg, A. Sabo, M. Sachse, S. J. Sanders, C. Schafer, M. Schulte-Rüther, D. Skuse, C. Stevens, P. Szatmari, K. Tammimies, O. Valladares, A. Voran, L. S. Wang, L. A. Weiss, A. J.

Willsey, T. W. Yu, R. K. C. Yuen, The DDD Study, Homozygosity Mapping Collaborative for Autism, UK10K Consortium, The Autism Sequencing Consortium, E. H. Cook, C. M. Freitag, M. Gill, C. M. Hultman, T. Lehner, A. Palotie, G. D. Schellenberg, P. Sklar, M. W. State, J. S. Sutcliffe, C. A. Walsh, S. W. Scherer, M. E. Zwick, J. C. Barrett, D. J. Cutler, K. Roeder, B. Devlin, M. J. Daly and J. D. Buxbaum. "Synaptic, Transcriptional and Chromatin Genes Disrupted in Autism", *Nature*, Vol. 515(7526), pp. 209-215, 2014.

26. Li, H., T. Yamagata, M. Mori, M. Y. Momoi. "Association of Autism in Two Patients with Hereditary Multiple Exostoses Caused by Novel Deletion Mutations of EXT1", *Journal of Human Genetics*, Vol. 47(5), pp. 262-265, 2002.

27. Kamien, B., J. Harraway, B. Lundie, L. Smallhorne, V. Gibbs, A. Heath and J. M. Fullerton. "Characterization of a 520 Kb Deletion on Chromosome 15q26.1 Including ST8SIA2 in a Patient with Behavioral Disturbance, Autism Spectrum Disorder, and Epilepsy", *American Journal of Medical Genetics Part A*, Vol. 164(3), pp. 782-788, 2014.

28. Anney, R., L. Klei, D. Pinto, R. Regan, J. Conroy, T. R. Magalhaes, C. Correia, B. S. Abrahams, N. Sykes, A. T. Pagnamenta, J. Almeida, E. Bacchelli, A. J. Bailey, G. Baird, A. Battaglia, T. Berney, N. Bolshakova, S. Bölte, P. F. Bolton, T. Bourgeron, S. Brennan, J. Brian, A. R. Carson, G. Casallo, J. Casey, S. H. Chu, L. Cochrane, C. Corsello, E. L. Crawford, A. Crossett, G. Dawson, M. de Jonge, R. Delorme, I. Drmic, E. Duketis, F. Duque, A. Estes, P. Farrar, B. A. Fernandez, S. E. Folstein, E. Fombonne, C. M. Freitag, J. Gilbert, C. Gillberg, J. T. Glessner, J. Goldberg, J. Green, S. J. Guter, H. Hakonarson, E. A. Heron, M. Hill, R. Holt, J. L. Howe, G. Hughes, V. Hus, R. Igliozzi, C. Kim, S. M. Klauck, A. Kolevzon, O. Korvatska, V. Kustanovich, C. M. Lajonchere, J. A. Lamb, M. Laskawiec, M. Leboyer, A. Le Couteur, B. L. Leventhal, A. C. Lionel, X. Q. Liu, C. Lord, L. Lotspeich, S. C. Lund, E. Maestrini, W. Mahoney, C. Mantoulan, C. R. Marshall, H. McConachie, C. J. McDougle, J. McGrath, W. M. McMahon, N. M. Melhem, A. Merikangas, O. Migita, N. J. Minshew, G. K. Mirza, J. Munson, S. F. Nelson, C. Noakes, A. Noor, G. Nygren, G. Oliveira, K. Papanikolaou, J. R. Parr, B. Parrini, T. Paton, A. Pickles, J. Piven, D. J.

Posey, A. Poustka, F. Poustka, A. Prasad, J. Ragoussis, K. Renshaw, J. Rickaby, W. Roberts, K. Roeder, B. Roge, M. L. Rutter, L. J. Bierut, J. P. Rice, J. Salt, K. Sansom, D. Sato, R. Segurado, L. Senman, N. Shah, V. C. Sheffield, L. Soorya, I. Sousa, V. Stoppioni, C Strawbridge, R. Tancredi, K. Tansey, B. Thiruvahindrapduram, A. P. Thompson, S. Thomson, A. Tryfon, J. Tsiantis, H. Van Engeland, J. B. Vincent, F. Volkmar, S. Wallace, K. Wang, Z. Wang, T. H. Wassink, K. Wing, K. Wittemeyer, S. Wood, B. L. Yaspan, D. Zurawiecki, L. Zwaigenbaum, C. Betancur, J. D. Buxbaum, R. M. Cantor, E. H. Cook, H. Coon, M. L. Cuccaro, L. Gallagher, D. H. Geschwind, M. Gill, J. L. Haines, J. Miller, A. P. Monaco, J. I. Nurnberger Jr, A. D. Paterson, M. A. Pericak-Vance, G. D. Schellenberg, S. W. Scherer, J. S. Sutcliffe, P. Szatmari, A. M. Vicente, V. J. Vieland, E. M. Wijsman, B. Devlin, S. Ennis and J. Hallmayer. "A Genome-Wide Scan for Common Alleles Affecting Risk for Autism", *Human Molecular Genetics,* Vol. 19(20), pp. 4072-4082, 2010.

29. Sanders, S. J., X. He, A. J. Willsey, A. G. Ercan-Sencicek, K. E. Samocha, A. E. Cicek, M. T. Murtha, V. H. Bal, S. L. Bishop, S. Dong, A. P. Goldberg, C. Jinlu, J. F. Keaney III, L. Klei, J. D. Mandell, D. Moreno-De-Luca, C. S. Poultney, E. B. Robinson, L. Smith, T. Solli-Nowlan, M. Y. Su, N. A. Teran, M. F. Walker, D. M. Werling, A. L. Beaudet, R. M. Cantor, E. Fombonne, D. H. Geschwind, D. E. Grice, C. Lord, J. K. Lowe, S. M. Mane, D. M. Martin, E. M. Morrow, M. E. Talkowski, J. S. Sutcliffe, C. A. Walsh, T. W. Yu, Autism Sequencing Consortium, D. H. Ledbetter, C. L. Martin, E. H. Cook, J. D. Buxbaum, M. J. Daly, B. Devlin, K. Roeder and M. W. State. "Insights into Autism Spectrum Disorder Genomic Architecture and Biology from 71 Risk Loci", *Neuron*, Vol. 87(6), pp. 1215-1233, 2015.

30. Satterstrom, F.K., J. A. Kosmicki, J. Wang, M. S. Breen, S. De Rubeis, J. Y. An, M. Peng, R. Collins, J. Grove, L. Klei, C. Stevens, J. Reichert, M. S. Mulhern, M. Artomov, S. Gerges, B. Sheppard, X. Xu, A Bhaduri, U. Norman, H. Brand, G. Schwartz, R. Nguyen, E. E. Guerrero, C. Dias, Autism Sequencing Consortium, iPSYCH-Broad Consortium, C. Betancur, E. H. Cook, L. Gallagher, M. Gill, J. S. Sutcliffe, A. Thurm, M. E. Zwick, A. D. Børglum, M. W. State, A. E. Cicek, M. E. Talkowski, D. J. Cutler, B. Devlin, S. J. Sanders, K. Roeder, M. J. Daly and J. D Buxbaum. "Large-Scale Exome Sequencing Study Implicates Both Developmental

and Functional Changes in the Neurobiology of Autism", *Cell,* Vol. 180(3), pp. 568-584, 2020.

31. Uhlen, M., L. Fagerberg, B. M. Hallström, C. Lindskog, P. Oksvold, A. Mardinoglu, A. Sivertsson, C. Kampf, E. Sjöstedt, A. Asplund, I. Olsson, K. Edlund, E. Lundberg, S. Navani, C. Al-Khalili Szigyarto, J. Odeberg, D. Djureinovic, J. O. Takanen, S. Hober, T. Alm, P. H. Edqvist, H. Berling, H. Tegel, J. Mulder, J. Rockberg, P. Nilsson, J. M. Schwenk, M. Hamsten, K. von Feilitzen, M. Forsberg, L. Persson, F. Johansson, M. Zwahlen, G. von Heijne, J. Nielsen and F. Ponten. "Tissue-based Map of the Human Proteome", *Science,* Vol. 347(6220), No. 1260419, 2015.

32. The UniProt Consortium. "UniProt: The Universal Protein Knowledgebase in 2021", *Nucleic Acids Research,* Vol. 49(D1), pp. D480-D489, 2021.

33. Kanehisa, M. and S. Goto. "KEGG: Kyoto Encyclopedia of Genes and Genomes", *Nucleic Acids Research,* Vol. 28(1), pp. 27-30, 2000.

34. Gardener, H., D. Spiegelman and S. L. Buka. "Prenatal Risk Factors for Autism: Comprehensive Meta-Analysis", *The British Journal of Psychiatry*, Vol. 195(1), pp. 7-14, 2009.

35. Goines, P. E. and P. Ashwood. "Cytokine Dysregulation in Autism Spectrum Disorders (ASD), pp. Possible Role of the Environment", *Neurotoxicology and Teratology,* Vol. 36, pp. 67-81, 2013.

36. Sandin, S., D. Schendel, P. Magnusson, C. Hultman, P. Suren, E. Susser, T. Grønborg, M. Gissler, N. Gunnes, R. Gross, M. Henning, M. Bresnahan, A. Sourander, M. Hornig, K. Carter, R. Francis, E. Parner, H. Leonard, M. Rosanoff, C. Stoltenberg and A. Reichenberg. "Autism Risk Associated with Parental Age and with Increasing Difference in Age Between the Parents", *Molecular Psychiatry*. Vol. 21(5), pp. 693-700, 2016.

37. Ornoy, A., L. Weinstein-Fudim and Z. Ergaz. "Prenatal Factors Associated with Autism Spectrum Disorder (ASD)", *Reproductive Toxicology,* Vol. 56, pp. 155-169,

2015.

38. Lyall, K., R. J. Schmidt and I. Hertz-Picciotto, *Chapter 2.7 - The Environment in Autism Spectrum Disorders*. Academic Press, 2013.

39. Berger, B. E., A. M. Navar-Boggan and S. B. Omer. "Congenital Rubella Syndrome and Autism Spectrum Disorder Prevented by Rubella Vaccination-United States, 2001-2010", *BMC Public Health*, Vol. 11(1), pp. 1-5, 2011.

40. Sakamoto, A., H. Moriuchi, J. Matsuzaki, K. Motoyama and M. Moriuchi. "Retrospective Diagnosis of Congenital Cytomegalovirus Infection in Children with Autism Spectrum Disorder But No Other Major Neurologic Deficit", *Brain and Development,* Vol. 37(2), pp. 200-205, 2015.

41. Finegan, J. A. and B. Quarrington. "Pre-. Peri-, and Neonatal Factors and Infantile Autism", *Journal of Child Psychology and Psychiatry,* Vol. 20(2), pp. 119-128, 1979.

42. Edelson, S. B. and D. S. Cantor. "Autism: Xenobiotic Influences", *Toxicology and Industrial Health*, Vol. 14(6), pp. 799-811, 1998.

43. Modahl, C., L. A. Green, D. Fein, M. Morris, L. Waterhouse, C. Feinstein and H. Levin. "Plasma Oxytocin Levels in Autistic Children", *Biological Psychiatry,* Vol. 43(4), pp. 270-277, 1998.

44. Carlsson, M. L. "Hypothesis: Is Infantile Autism a Hypoglutamatergic Disorder? Relevance of Glutamate – Serotonin Interactions for Pharmacotherapy" *Journal of Neural Transmission,* Vol. 105(4), pp. 525-535, 1998.

45. Lombard, J. "Autism: A Mitochondrial Disorder?" *Medical Hypotheses,* Vol. 50(6), pp. 497-500, 1998.

46. Frye, R. E., S. Melnyk and D. F. MacFabe. "Unique Acyl-Carnitine Profiles are Potential Biomarkers for Acquired Mitochondrial Disease in Autism Spectrum Disorder", *Translational Psychiatry*. Vol. 3, No. e220, 2013.

47. Frye, R. E., S. Rose, J. Slattery and D. F. MacFabe. "Gastrointestinal Dysfunction in Autism Spectrum Disorder: The Role of the Mitochondria and the Enteric Microbiome", *Microbial Ecolology in Health and Disease*. Vol. 26, No. 27458, 2015.

48. Maneeton, N., B. Maneeton, S. Putthisri, P. Woottiluk, A. Narkpongphun and M. Srisurapanont. "Risperidone for Children and Adolescents with Autism Spectrum Disorder: A Systematic Review", *Neuropsychiatric Disease Treatment*, Vol. 14, pp. 1811-1820, 2018.

49. Won, E. K., J. P. Park, Y. R. Lee, Y. Y. Nam, H. J. Min and Y. Kim. "Risperidone Monotherapy in Children and Adolescents with Autism Spectrum Disorders : A Naturalistic Study", *Journal of the Korean Academy of Child and Adolescent Psychiatry*. Vol. 26(4), pp. 273-278, 2015.

50. Sharma, A. and S. R. Shaw. "Efficacy of Risperidone in Managing Maladaptive Behaviors for Children with Autistic Spectrum Disorder: A Meta-Analysis", *Journal of Pediatric Health Care*. Vol. 26(4), pp. 291-299, 2012.

51. Williamson, E., N. A. Sathe, J. C. Andrews, S. Krishnaswami, M. L. McPheeters, C. Fonnesbeck, K. Sanders, A. Weitlauf and Z. Warren. "Medical Therapies for Children with Autism Spectrum Disorder—An Update", Comparative Effectiveness Review No. 189. (Prepared by the Vanderbilt Evidence-based Practice Center under Contract No. 290-2015-00003-I.) AHRQ Publication No. 17-EHC009-EF. Rockville, MD: Agency for Healthcare Research and Quality, 2017. www.effectivehealthcare.ahrq.gov/reports/final.cfm, accessed on January 5, 2022.

52. Miral, S., O. Gencer, F. N. Inal-Emiroglu, B. Baykara, A. Baykara and E. Dirik. "Risperidone Versus Haloperidol in Children and Adolescents with Autistic Disorder", *European Child and Adolescent Psychiatry*. Vol. 17(1), pp. 1-8, 2008.

53. Gencer, O., F. N. Inal-Emiroglu, S. Miral, B. Baykara, A. Baykara and E. Dirik. "Comparison of Long-Term Efficacy and Safety of Risperidone and Haloperidol in Children and Adolescents with Autistic Disorder", *European Child and Adolescent Psychiatry*, Vol. 17(4), pp. 217-225, 2008.

54. Kloosterboer, S. M., B. C. de Winter, C. G. Reichart, M. E. Kouijzer, M. M. de Kroon, E. van Daalen, W. A. Ester, R. Rieken, G. C. Dieleman, D. van Altena, B. Bartelds, R. H. N. van Schaik, K. Nasserinejad, M. H. J. Hillegers, T. van Gelder, B. Dierckx and B. C. Koch. "Risperidone Plasma Concentrations are Associated with Side Effects and Effectiveness in Children and Adolescents with Autism Spectrum Disorder", *British Journal of Clinical Pharmacology*, Vol. 87(3), pp. 1069-1081, 2021.

55. Tavassoly, I., J. Goldfarb and R. Iyengar. "Systems Biology Primer: The Basic Methods and Approaches", *Essays in Biochemistry*, Vol. 62(4), pp. 487-500, 2018.

56. Palsson, B. Ø., *Systems Biology: Constraint-Based Reconstruction and Analysis*, Cambridge University Press, 2015.

57. Haggart, C. R., J. A. Bartell, J. J. Saucerman and J. A. Papin. *Chapter twenty-one - Whole-Genome Metabolic Network Reconstruction and Constraint-Based Modeling, Methods in Systems Biology*. Academic Press, 2011.

58. Bordbar, A., J. M. Monk, Z. A. King and B. O. Palsson. "Constraint-Based Models Predict Metabolic and Associated Cellular Functions". *Nature Reviews Genetics, Vol.* 15(2), pp. 107-120, 2014.

59. Biggs, M. B., G. L. Medlock, G. L. Kolling and J. A. Papin. "Metabolic Network Modeling of Microbial Communities", *Wiley Interdisciplinary Reviews: Systems Biology and Medicine*, Vol. 7(5), pp. 317-334, 2015.

60. Edwards, J. S. and B. O. Palsson. "Systems Properties of the Haemophilus Influenzae Rd Metabolic Genotype", *Journal of Biological Chemistry*, Vol. 274(25), pp. 17410-17416, 1999.

61. Edwards, J. S. and B. O. Palsson. "The Escherichia Coli MG1655 in Silico Metabolic Genotype: Its Definition, Characteristics, and Capabilities", *Proceedings of the National Academy of Sciences*, Vol. 97(10), pp. 5528-5533, 2000.

62. Förster, J., I. Famili, P. Fu, B. Ø. Palsson and J. Nielsen. "Genome-Scale

Reconstruction of the Saccharomyces Cerevisiae Metabolic Network", *Genome Research,* Vol. 13(2), pp. 244-253, 2003.

63. Duarte, N. C., S. A. Becker, N. Jamshidi, I. Thiele, M. L. Mo, T. D. Vo, R. Srivas and B. Ø. Palsson. "Global Reconstruction of the Human Metabolic Network Based on Genomic and Bibliomic Data", *Proceedings of the National Academy of Sciences,* Vol. 104(6), pp. 1777-1782, 2007.

64. de Oliveira Dal'Molin, C. G., L. E. Quek, R. W. Palfreyman, S. M. Brumbley and L. K. Nielsen. "AraGEM, a Genome-Scale Reconstruction of the Primary Metabolic Network in Arabidopsis", *Plant Physiology,* Vol. 152(2), pp. 579-589, 2010.

65. Gu, C., G. B. Kim, W. J. Kim, H. U. Kim and S. Y. Lee. "Current Status and Applications of Genome-Scale Metabolic Models", *Genome Biology,* Vol. 20(1), pp. 1-18, 2019.

66. Chung, B. K. S., S. Selvarasu, A. Camattari, J. Ryu, H. Lee, J. Ahn, H. Lee and D. Y. Lee. "Genome-Scale Metabolic Reconstruction and In Silico Analysis of Methylotrophic Yeast Pichia Pastoris for Strain Improvement", *Microbial Cell Factories,* Vol. 9(1), pp. 1-15, 2010.

67. Kim, H.U., T. Y. Kim and S. Y. Lee. "Genome-Scale Metabolic Network Analysis and Drug Targeting of Multi-Drug Resistant Pathogen Acinetobacter Baumannii AYE". *Molecular Biosystems,* Vol. 6(2), pp. 339-348, 2010.

68. Mishra, P., N. R. Lee, M. Lakshmanan, M. Kim, B. G. Kim and D. Y. Lee. "Genome-Scale Model-Driven Strain Design for Dicarboxylic Acid Production in Yarrowia Lipolytica", *BMC Systems Biology,* Vol. 12(2), pp. 9-20, 2018.

69. Orth, J. D., T. M. Conrad, J. Na, J. A. Lerman, H. Nam, A. M. Feist and B. O. Palsson. "A Comprehensive Genome-Scale Reconstruction of Escherichia Coli Metabolism—2011". *Molecular Systems Biology*. Vol. 7(1), No. 535, 2011.

70. Yang, J. E., S. J. Park, W. J. Kim, H. J. Kim, B. J. Kim, H. Lee, J. Shin and S. Y. Lee.

"One-Step Fermentative Production of Aromatic Polyesters from Glucose by Metabolically Engineered Escherichia Coli Strains", *Nature Communications,* Vol. 9(1), pp. 79, 2018.

71. Guzmán, G.I., J. Utrilla, S. Nurk, E. Brunk, J. M. Monk, A. Ebrahim, B. O. Palsson and A. M. Feist. "Model-Driven Discovery of Underground Metabolic Functions in Escherichia Coli", *Proceedings of the National Academy of Sciences,* Vol. 112(3), pp. 929-934, 2015.

72. Oberhardt, M. A., R. Zarecki, L. Reshef, F. Xia, M. Duran-Frigola, R. Schreiber, C. S. Henry, N. Ben-Tal, D. J. Dwyer, U. Gophna and E. Ruppin. "Systems-Wide Prediction of Enzyme Promiscuity Reveals a New Underground Alternative Route for Pyridoxal 5'-Phosphate Production in E. coli", *PLOS Computational Biology,* Vol. 12(1), No. e1004705, 2016.

73. Abdel-Haleem, A. M., H. Hefzi, K. Mineta, X. Gao, T. Gojobori, B. O. Palsson, N. E. Lewis and N. Jamshidi. "Functional Interrogation of Plasmodium Genus Metabolism Identifies Species- and Stage-Specific Differences in Nutrient Essentiality and Drug Targeting", *PLOS Computational Biology,* Vol. 14(1), No. e1005895, 2018.

74. Agren, R., A. Mardinoglu, A. Asplund, C. Kampf, M. Uhlen and J. Nielsen. "Identification of Anticancer Drugs for Hepatocellular Carcinoma Through Personalized Genome-Scale Metabolic Modeling", *Molecular Systems Biology,* Vol. 10(3), No. 721, 2014.

75. Beste, D. J. V., T. Hooper, G. Stewart, B. Bonde, C. Avignone-Rossa, M. E. Bushell, P. Wheeler, S. Klamt, A. M. Kierzek and J. McFadden. "GSMN-TB: A Web-Based Genome-Scale Network Model of Mycobacterium Tuberculosismetabolism", *Genome Biology,* Vol. 8(5), pp. 1-18, 2007.

76. Bidkhori, G., R. Benfeitas, E. Elmas, M. N. Kararoudi, M. Arif, M. Uhlen, J. Nielsen and A. Mardinoglu. "Metabolic Network-Based Identification and Prioritization of Anticancer Targets Based on Expression Data in Hepatocellular Carcinoma",

Frontiers in Physiology, Vol. 9, No. 916, 2018.

77. Josling, G. A. and M. Llinás. "Sexual Development in Plasmodium Parasites: Knowing When It's Time to Commit", *Nature Reviews Microbiology*. Vol. 13(9), pp. 573-587, 2015.

78. Kim, H. U., S. Y. Kim, H. Jeong, T. Y. Kim, J. J. Kim, H. E. Choy, K. Y. Yi, J. H. Rhee and S. Y. Lee. "Integrative Genome-Scale Metabolic Analysis of Vibrio Vulnificus for Drug Targeting and Discovery", *Molecular Systems Biology*, Vol. 7(1), No. 460, 2011.

79. Presta, L., E. Bosi, L. Mansouri, L. Dijkshoorn, R. Fani and M. Fondi. "Constraint-Based Modeling Identifies New Putative Targets to Fight Colistin-Resistant A. Baumannii Infections", *Scientific Reports*, Vol. 7(1), pp. 1-12, 2017.

80. Raškevičius, V., V. Mikalayeva, I. Antanavičiūtė, I. Ceslevičienė, V. A. Skeberdis, V. Kairys and S. Bordel. "Genome Scale Metabolic Models as Tools for Drug Design and Personalized Medicine". *PLoS One,* Vol. 13(1), No. e0190636, 2018.

81. Sigurdsson, G., R. M. T. Fleming, A. Heinken and I. Thiele. "A Systems Biology Approach to Drug Targets in Pseudomonas Aeruginosa Biofilm", *PLoS One,* Vol. 7(4), No. e34337, 2012.

82. Botero, K., S. Restrepo and A. Pinzón. "A Genome-Scale Metabolic Model of Potato Late Blight Suggests a Photosynthesis Suppression Mechanism", *BMC Genomics*, Vol. 19(8), pp. 31-44, 2018.

83. Hanemaaijer, M., B. G. Olivier, W. F. M. Röling, F. J. Bruggeman and B. Teusink. "Model-Based Quantification of Metabolic Interactions from Dynamic Microbial-Community Data", *PLoS One*, Vol. 12(3), No. e0173183, 2017.

84. Kumar, M., B. Ji, P. Babaei, P. Das, D. Lappa, G. Ramakrishnan, T. E. Fox, R. Haque, W. A. Petri, F. Baeckhed and J. Nielsen. "Gut Microbiota Dysbiosis is Associated with Malnutrition and Reduced Plasma Amino Acid Levels: Lessons from Genome-

Scale Metabolic Modeling", *Metabolic Engineering*, Vol. 49, pp. 128-142, 2018.

85. McNally, C. P. and E. Borenstein. "Metabolic Model-Based Analysis of the Emergence of Bacterial Cross-Feeding via Extensive Gene Loss", *BMC Systems Biology*, Vol. 12(1), pp. 1-14, 2018.

86. Pacheco, A. R., M. Moel and D. Segrè. "Costless Metabolic Secretions as Drivers of Interspecies Interactions in Microbial Ecosystems", *Nature Communications*, Vol. 10(1), pp. 1-12, 2019.

87. Rosario, D., R. Benfeitas, G. Bidkhori, C. Zhang, M. Uhlen, S. Shoaie and A. Mardinoglu. "Understanding the Representative Gut Microbiota Dysbiosis in Metformin-Treated Type 2 Diabetes Patients Using Genome-Scale Metabolic Modeling", *Frontiers in Physiology*, Vol. 9, No. 775, 2018.

88. Stolyar, S., S. Van Dien, K. L. Hillesland, N. Pinel, T. J. Lie, J. A. Leigh and D. A. Stahl. "Metabolic Modeling of a Mutualistic Microbial Community", *Molecular Systems Biology*, Vol. 3, No. 92, 2007.

89. Aller, S., A. Scott, M. Sarkar-Tyson and O. S. Soyer. "Integrated Human-Virus Metabolic Stoichiometric Modelling Predicts Host-Based Antiviral Targets Against Chikungunya, Dengue and Zika Viruses", *Journal of The Royal Society Interface*, Vol. 15(146), No. 20180125, 2018.

90. Asgari, Y., P. Khosravi, Z. Zabihinpour and M. Habibi. "Exploring Candidate Biomarkers for Lung and Prostate Cancers Using Gene Expression and Flux Variability Analysis", *Integrative Biology*, Vol. 10(2), pp. 113-120, 2018.

91. Björnson, E., B. Mukhopadhyay, A. Asplund, N. Pristovsek, R. Cinar, S. Romeo, M. Uhlen, G. Kunos, J. Nielsen and A. Mardinoglu. "Stratification of Hepatocellular Carcinoma Patients Based on Acetate Utilization", *Cell Reports*, Vol. 13(9), pp. 2014-2026, 2015.

92. Fuhr, L., R. El-Athman, R. Scrima, O. Cela, A. Carbone, H. Knoop, Y. Li, K.

Hoffmann, M. O. Laukkanen, F. Corcione, R. Steuer, T. F. Meyer, G. Mazzoccoli, N. Capitanio and A. Relogio. "The Circadian Clock Regulates Metabolic Phenotype Rewiring Via HKDC1 and Modulates Tumor Progression and Drug Response in Colorectal Cancer", *EBioMedicine*. Vol. 33, pp. 105-121, 2018.

93. Gámez-Pozo, A., L. Trilla-Fuertes, J. Berges-Soria, N. Selevsek, R. Lopez-Vacas, M. Diaz-Almiron, P. Nanni, J. M. Arevalillo, H. Navarro, J. Grossmann, F. G. Moreno, R. G. Rioja, G. Prado-Vázquez, A. Zapater-Moros, P. Main, J. Feliú, P. Martínez Del Prado, P. Zamora, E. Ciruelos, E. Espinosa and J. A. Fresno Vara. "Functional Proteomics Outlines the Complexity of Breast Cancer Molecular Subtypes", *Scientific Reports,* Vol. 7(1), pp. 1-13, 2017.

94. Hur, W., J. Y. Ryu, H. U. Kim, S. W. Hong, E. B. Lee, S. Y. Lee and S. K. Yoon. "Systems Approach to Characterize the Metabolism of Liver Cancer Stem Cells Expressing CD133", *Scientific Reports,* Vol. 7, pp. 1-11, 2017.

95. Marin de Mas, I., E. Aguilar, E. Zodda, C. Balcells, S. Marin, G. Dallmann, T. M. Thomson, B. Papp and M. Cascante. "Model-Driven Discovery of Long-Chain Fatty Acid Metabolic Reprogramming in Heterogeneous Prostate Cancer Cells", *PLOS Computational Biology,* Vol. 14(1), No. e1005914, 2018.

96. McGarrity, S., Ó. Anuforo, H. Halldórsson, A. Bergmann, S. Halldórsson, S. Palsson, H. H. Henriksen, P. I. Johansson and Ó. Rolfsson. "Metabolic Systems Analysis of LPS Induced Endothelial Dysfunction Applied to Sepsis Patient Stratification", *Scientific Reports,* Vol. 8(1), pp. 1-14, 2018.

97. Shubham, K., L. Vinay and P. K. Vinod. "Systems-Level Organization of Non-Alcoholic Fatty Liver Disease Progression Network", *Molecular Biosystems,* Vol. 13(9), pp. 1898-1911, 2017.

98. Steenbergen, R., M. Oti, R. Ter Horst, W. Tat, C. Neufeldt, A. Belovodskiy, T. T. Chua, W. J. Cho, M. Joyce, B. E. Dutilh and D. L. Tyrrell. "Establishing Normal Metabolism and Differentiation in Hepatocellular Carcinoma Cells by Culturing in Adult Human Serum", *Scientific Reports,* Vol. 8(1), pp. 1-14, 2018.

99. Turanli, B., C. Zhang, W. Kim, R. Benfeitas, M. Uhlen, K. Y. Arga and A. Mardinoglu. "Discovery of Therapeutic Agents for Prostate Cancer Using Genome-Scale Metabolic Modeling and Drug Repositioning", *EBioMedicine,* Vol. 42, pp. 386-396, 2019.

100. Wu, H. Q., M. L. Cheng, J. M. Lai, H. H. Wu, M. C. Chen, W. H. Liu, W. H. Wu, P. M. H. Chang, C. Y. F. Huang, A. P. Tsou, M. S. Shiao and F. S. Wang. "Flux Balance Analysis Predicts Warburg-Like Effects of Mouse Hepatocyte Deficient in Mir-122a", *PLOS Computational Biology,* Vol. 13(7), No. e1005618, 2017.

101. Lewis, N. E., G. Schramm, A. Bordbar, J. Schellenberger, M. P. Andersen, J. K. Cheng, N. Patel, A. Yee, R. A. Lewis, R. Eils, R. König and B. Ø. Palsson. "Large-Scale In Silico Modeling of Metabolic Interactions Between Cell Types in the Human Brain", *Nature Biotechnology,* Vol. 28(12), pp. 1279-1285, 2010.

102. Çakır, T., S. Alsan, H. Saybaşılı, A. Akın and K. Ö. Ülgen. "Reconstruction and Flux Analysis of Coupling Between Metabolic Pathways of Astrocytes and Neurons: Application to Cerebral Hypoxia", *T heoretical Biology and Medical Modelling,* Vol. 4(1), pp. 1-18, 2007.

103. Sertbaş, M., K. Ö. Ülgen and T. Çakır. "Systematic Analysis of Transcription-Level Effects of Neurodegenerative Diseases on Human Brain Metabolism by a Newly Reconstructed Brain-Specific Metabolic Network", *FEBS Open Bio,* Vol. 4, pp. 542-553, 2014.

104. Özcan, E. and T. Çakır. "Reconstructed Metabolic Network Models Predict Flux-Level Metabolic Reprogramming in Glioblastoma", *Frontiers in Neuroscience,* Vol. 10, No. 156, 2016.

105. Martín-Jiménez, C. A., D. Salazar-Barreto, G. E. Barreto and J. González. "Genome-Scale Reconstruction of the Human Astrocyte Metabolic Network", *Frontiers in Aging Neuroscience,* Vol. 9, No. 23, 2017.

106. Colijn, C., A. Brandes, J. Zucker, D. S. Lun, B. Weiner, M. R. Farhat, T. Y. Cheng,

D. B. Moody, M. Murray and J. E. Galagan. "Interpreting Expression Data with Metabolic Flux Models: Predicting Mycobacterium Tuberculosis Mycolic Acid Production", *PLOS Computational Biology*, Vol. 5(8), No. e1000489, 2009.

107. Jensen, P. A. and J. A. Papin. "Functional Integration of a Metabolic Network Model and Expression Data without Arbitrary Thresholding", *Bioinformatics*, Vol. 27(4), pp. 541-547, 2011.

108. Collins, S. B., E. Reznik and D. Segrè. "Temporal Expression-Based Analysis of Metabolism", *PLoS Computational Biology*, Vol. 8(11), No. e1002781, 2012.

109. Shlomi, T., M. N. Cabili, M. J. Herrgård, B. O. Palsson and E. Ruppin. "Network-Based Prediction of Human Tissue-Specific Metabolism", *Nature Biotechnology*, Vol. 26(9), pp. 1003-1010, 2008.

110. Becker, S. A. and B. O. Palsson. "Context-Specific Metabolic Networks Are Consistent with Experiments", *PLOS Computational Biology*, Vol. 4(5), No. e1000082, 2008.

111. Wang, Y., J. A. Eddy and N. D. Price. "Reconstruction of Genome-Scale Metabolic Models for 126 Human Tissues Using Mcadre", *BMC Systems Biology*, Vol. 6(1), pp. 1-16, 2012.

112. Agren, R., S. Bordel, A. Mardinoglu, N. Pornputtapong, I. Nookaew and J. Nielsen. "Reconstruction of Genome-Scale Active Metabolic Networks for 69 Human Cell Types and 16 Cancer Types Using INIT", *PLOS Computational Biology*, Vol. 8(5), No. e1002518, 2012.

113. Töpfer, N., S. Jozefczuk and Z. Nikoloski. "Integration of Time-Resolved Transcriptomics Data with Flux-Based Methods Reveals Stress-Induced Metabolic Adaptation in Escherichia Coli", *BMC Systems Biology*, Vol. 6(1), pp. 1-10, 2012.

114. Rossell, S., M. A. Huynen and R. A. Notebaart. "Inferring Metabolic States in Uncharacterized Environments Using Gene-Expression Measurements", *PLOS*

Computational Biology, Vol. 9(3), No. e1002988, 2013.

115. Schmitt, W. and S. Willmann. "Physiology-Based Pharmacokinetic Modeling: Ready To Be Used", *Drug Discovery Today: Technologies,* Vol. 2(1), pp. 125-132, 2005.

116. Khalil, F. and S. Läer. "Physiologically Based Pharmacokinetic Modeling: Methodology, Applications, and Limitations with a Focus on Its Role in Pediatric Drug Development", *Journal of Biomedicine and Biotechnology,* Vol. 2011, No. 907461, 2011.

117. Jones, H. and K. Rowland-Yeo. "Basic Concepts in Physiologically Based Pharmacokinetic Modeling in Drug Discovery and Development", *CPT Pharmacometrics and Systems Pharmacology,* Vol. 2(8), pp. 1-12, 2013.

118. Romero, P., J. Wagg, M. L. Green, D. Kaiser, M. Krummenacker and P. D. Karp. "Computational Prediction of Human Metabolic Pathways from the Complete Human Genome", *Genome Biology*. 6(1), pp. 1-17, 2005.

119. Wishart, D. S., D. Tzur, C. Knox, R. Eisner, A. C. Guo, N. Young, D. Cheng, K. Jewell, D. Arndt, S. Sawhney, C. Fung, L. Nikolai, M. Lewis, M. A. Coutouly, I. Forsythe, P. Tang, S. Shrivastava, K. Jeroncic, P. Stothard, G. Amegbey, D. Block, D. D. Hau, J. Wagner, J. Miniaci, M. Clements, M. Gebremedhin, N. Guo, Y. Zhang, G. E. Duggan, G. D. Macinnis, A. M. Weljie, R. Dowlatabadi, F. Bamforth, D. Clive, R. Greiner, L. Li, T. Marrie, B. D. Sykes, H. J. Vogel and L. Querengesser. "HMDB: the Human Metabolome Database". *Nucleic Acids Research,* Vol. 35(Database issue), pp. D521-D526, 2007.

120. Mardinoglu, A., R. Agren, C. Kampf, A. Asplund, M. Uhlen and J. Nielsen. "Genome-Scale Metabolic Modelling of Hepatocytes Reveals Serine Deficiency in Patients with Non-Alcoholic Fatty Liver Disease", *Nature Communications,* Vol. 5(1), pp. 1-11, 2014.

121. Heirendt, L., S. Arreckx, T. Pfau, S. N. Mendoza, A. Richelle, A. Heinken, H. S. Haraldsdóttir, J. Wachowiak, S. M. Keating, V. Vlasov, S. Magnusdóttir, C. Y. Ng,

G. Preciat, A. Žagare, S. H. J. Chan, M. K. Aurich, C. M. Clancy, J. Modamio, J. T. Sauls, A Noronha, A. Bordbar, B. Cousins, D. C. El Assal, L. V. Valcarcel, I. Apaolaza, S. Ghaderi, M. Ahookhosh, M. B. Guebila, A. Kostromins, N. Sompairac, H. M. Le, D. Ma, Y. Sun, L. Wang, J. T. Yurkovich, M. A. P. Oliveira, P. T. Vuong, L. P. El Assal, I. Kuperstein, A. Zinovyev, H. S. Hinton, W. A. Bryant, F. J. A. Artacho, F. J. Planes, E. Stalidzans, A. Maass, S. Vempala, M. Hucka, M. A. Saunders, C. D. Maranas, N. E. Lewis, T. Sauter, B. Ø. Palsson, I. Thiele and R. M. Fleming. "Creation and Analysis of Biochemical Constraint-Based Models Using the COBRA Toolbox V.3.0", *Nature Protocols*, Vol. 14(3), pp. 639-702, 2019.

122. Wang, H., J. L. Robinson, P. Kocabas, J. Gustafsson, M. Anton, P. E. Cholley, S. Huang, J. Gobom, T. Svensson, M. Uhlen, H. Zetterberg and J. Nielsen. "Genome-Scale Metabolic Network Reconstruction of Model Animals as a Platform for Translational Research", *Proceedings of the National Academy of Sciences*, Vol. 118(30), No. e2102344118, 2021.

123. Robinson, J. L., P. Kocabaş, H. Wang, P. E. Cholley, D. Cook, A. Nilsson, M. Anton, R. Ferreira, I. Domenzain, V. Billa, A. Limeta, A. Hedin, J. Gustafsson, E. J. Kerkhoven, L. T. Svensson, B. O. Palsson, A. Mardinoglu, L. Hansson, M. Uhlen and J. Nielsen. "An Atlas of Human Metabolism", *Science Signaling*, Vol. 13(624), No. eaaz1482, 2020.

124. Orth, J. D., I. Thiele and B.Ø. Palsson. "What is flux balance analysis?" *Nature Biotechnology*, Vol. 28(3), pp. 245-248, 2010.

125. Baños, G., P. M. Daniel, S. R. Moorhouse and O. E. Pratt. "The Requirements of the Brain for Some Amino Acids", *Journal of Physiology*, Vol. 246(3), pp. 539-548, 1975.

126. Baños, G., P. M. Daniel, S. R. Moorhouse and O. E. Pratt. "The Influx of Amino Acids into the Brain of the Rat in vivo: The Essential Compared with Some Non-Essential Amino Acids", *Proceedings of the Royal Society B: Biological Sciences*, Vol. 183(1070), pp. 59-70, 1973.

127. Lying-Tunell, U., B. S. Lindblad, H. O. Malmlund and B. Persson. "Cerebral Blood Flow and Metabolic Rate of Oxygen, Glucose, Lactate, Pyruvate, Ketone Bodies and Amino Acids", *Acta Neurologica Scandinavica,* Vol. 62(5), pp. 265-275, 1980.

128. Lying-Tunell, U., B. S. Lindblad, H. O. Malmlund and B. Persson. "Cerebral Blood Flow and Metabolic Rate of Oxygen, Glucose, Lactate, Pyruvate, Ketone Bodies and Amino Acids" *Acta Neurologica Scandinavica,* Vol. 63(6), pp. 337-350, 1981.

129. Blüml, S., A. Moreno-Torres, F. Shic, C. H. Nguy and B. D. Ross. "Tricarboxylic Acid Cycle of Glia in the In Vivo Human Brain", *NMR in Biomedicine,* Vol. 15(1), pp. 1-5, 2002.

130. Sutherland V. C., T. N. Burbridge, J. E. Adams and A. Simon. "Cerebral Metabolism in Problem Drinkers Under the Influence of Alcohol and Chlorpromazine Hydrochloride", *Journal of Applied Physiology,* Vol. 15(2), pp. 189-196, 1960.

131. Rapoport, S. I. "In Vivo Fatty Acid Incorporation into Brain Phosholipids in Relation to Plasma Availability, Signal Transduction and Membrane Remodeling" *Journal of Molecular Neuroscience,* Vol. 16(2), pp. 243-261, 2001.

132. Malandro, M.S. and M. S. Kilberg. "Molecular Biology of Mammalian Amino Acid Transporters", *Annual Review of Biochemistry*. Vol. 65(1), pp. 305-336, 1996.

133. Shafqat, S., M. Velaz-Faircloth, V. A. Henzi, K. D. Whitney, T. L. Yang-Feng, M. F. Seldin and R. T. Fremeau. "Human Brain-Specific L-Proline Transporter: Molecular Cloning, Functional Expression, and Chromosomal Localization of the Gene in Human and Mouse Genomes", *Molecular Pharmacology,* Vol. 48(2), pp. 219-229, 1995.

134. Hu, C. A., W. W. Lin and D. Valle. "Cloning, Characterization, and Expression of cDNAs Encoding Human 1-Pyrroline-5-carboxylate Dehydrogenase", *Journal Biological Chemistry,* Vol. 271(16), pp. 9795-9800, 1996.

135. Thompson, S. G., P. T. -H. Wong, S. F. Leong and E. G. McGeer. "Regional

Distribution in Rat Brain of 1-Pyrroline-5-Carboxylate Dehydrogenase and Its Localization to Specific Glial Cells", *Journal of Neurochemistry*, Vol. 45(6), pp. 1791-1796, 1985.

136. Rucklidge, G. J., G. Milne, B. A. McGaw, E. Milne and S. P. Robins. "Turnover Rates of Different Collagen Types Measured by Isotope Ratio Mass Spectrometry", *Biochimica et Biophysica Acta - General Subjects*, Vol. 1156(1), pp. 57-61, 1992.

137. Lang, H., K. Minaian, N. Freudenberg, R. Hoffmann and R. Brandsch. "Tissue Specificity of Rat Mitochondrial Dimethylglycine Dehydrogenase Expression", *Biochemical Journal*, Vol. 299(2), pp. 393-398, 1994.

138. Gudmundsson, S. and I. Thiele. "Computationally Efficient Flux Variability Analysis", *BMC Bioinformatics*. Vol. 11(1), pp. 1-3, 2010.

139. Heirendt, L., I. Thiele and R. M. T. Fleming. "Distributedfba.jl: High-Level, High-Performance Flux Balance Analysis in Julia", *Bioinformatics*, Vol. 33(9), pp. 1421-1423, 2017.

140. Thiele, I., N. Swainston, R. M. Fleming, A. Hoppe, S. Sahoo, M. K. Aurich, H. Haraldsdottir, M. L. Mo, O. Rolfsson, M. D. Stobbe, S. G. Thorleifsson, R. Agren, C. Bölling, S. Bordel, A. K. Chavali, P. Dobson, W. B. Dunn, L. Endler, D. Hala, M. Hucka, D. Hull, D. Jameson, N. Jamshidi, J. J. Jonsson, N. Juty, S. Keating, I. Nookaew, N. Le Novère, N. Malys, A. Mazein, J. A. Papin, N. D. Price, E. Selkov Sr, M. I. Sigurdsson, E. Simeonidis, N. Sonnenschein, K. Smallbone, A. Sorokin, J. H. G. M. van Beek, D. Weichart, I. Goryanin, J. Nielsen, H. V. Westerhoff, D. B. Kell, P. Mendes and B. O. Palsson. "A Community-Driven Global Reconstruction of Human Metabolism", *Nature Biotechnology*,Vol. 31(5), pp. 419-425, 2013.

141. Kim, M. K. and D. S. Lun. "Methods for Integration of Transcriptomic Data in Genome-Scale Metabolic Models", *Computational and Structural Biotechnology Journal*, Vol. 11(18), pp. 59-65, 2014.

142. Chow, M. L., H. R. Li, M. E. Winn, C. April, C. C. Barnes, A. Wynshaw-Boris, J. B.

Fan, X. D. Fu, E. Courchesne and N. J. Schork. "Genome-Wide Expression Assay Comparison Across Frozen and Fixed Postmortem Brain Tissue Samples", *BMC Genomics*, Vol. 12, pp. 1-13, 2011.

143. Chow, M. L., M. E. Winn, H. R. Li, C. April, A. Wynshaw-Boris, J. B. Fan, X. D. Fu, E. Courchesne and N. J. Schork. "Preprocessing and Quality Control Strategies for Illumina DASL Assay-Based Brain Gene Expression Studies with Semi-Degraded Samples", *Frontiers in Genetics*, Vol. 3, No. 11, 2012.

144. Ansel, A., J. P. Rosenzweig, P. D. Zisman, M. Melamed and B. Gesundheit. "Variation in Gene Expression in Autism Spectrum Disorders: An Extensive Review of Transcriptomic Studies", *Frontiers in Neuroscience*, Vol. 10, No. 601, 2017.

145. Chana, G., L. Laskaris, C. Pantelis, P. Gillett, R. Testa, D. Zantomio, E. L. Burrows, A. J. Hannan, I. P. Everall and E. Skafidas. "Decreased Expression of Mglur5 within the Dorsolateral Prefrontal Cortex in Autism and Increased Microglial Number in Mglur5 Knockout Mice: Pathophysiological and Neurobehavioral Implications", *Brain, Behavior and Immunity*, Vol. 49, pp. 197-205, 2015.

146. Yasuda, Y., R. Hashimoto, H. Yamamori, K. Ohi, M. Fukumoto, S. Umeda-Yano, I. Mohri, A. Ito, M. Taniike and M. Takeda. "Gene Expression Analysis in Lymphoblasts Derived from Patients with Autism Spectrum Disorder", *Molecular Autism*, Vol. 2(1), pp. 1-8, 2011.

147. Grant, S. and A. Fitton. "Risperidone", *Drugs*, Vol. 48(2), pp. 253-273, 1994.

148. Fenton, C. and L. J. Scott. "Risperidone", *CNS Drugs*, Vol. 19(5), pp. 429-444, 2005.

149. Kemp, D. E., F. Canan, B. I. Goldstein and R. S. McIntyre. "Long-Acting Risperidone: A Review of Its Role in the Treatment of Bipolar Disorder", *Advances in Therapy*, Vol. 26(6), pp. 588-599, 2009.

150. Pavăl, D. "A Dopamine Hypothesis of Autism Spectrum Disorder", *Developmental Neuroscience*, Vol. 39(5), pp. 355-360, 2017.

151. McDougle, C. J., L. Scahill, M. G. Aman, J. T. McCracken, E. Tierney, M. Davies, L. E. Arnold, D. J. Posey, A. Martin, J. K. Ghuman, B. Shah, S. Z. Chuang, N. B. Swiezy, N. M. Gonzalez, J. Hollway, K. Koenig, J. J. McGough, L. Ritz and B. Vitiello. "Risperidone for the Core Symptom Domains of Autism: Results from the Study by the Autism Network of the Research Units on Pediatric Psychopharmacology", *American Journal of Psychiatry*, Vol. 162(6), pp. 1142-1148, 2005.

152. McCracken, J. T., J. McGough, B. Shah, P. Cronin, D. Hong, M. G. Aman, L. E. Arnold, R. Lindsay, P. Nash, J. Hollway, C. J. McDougle, D. Posey, N. Swiezy, A. Kohn, L. Scahill, A. Martin, K. Koenig, F. Volkmar, D. Carroll, A. Lancor, E. Tierney, J. Ghuman, N. M. Gonzalez, M. Grados, B. Vitiello, L. Ritz, M. Davies, J. Robinson, D. McMahon and Research Units on Pediatric Psychopharmacology Autism Network. "Risperidone in Children with Autism and Serious Behavioral Problems", *New England Journal of Medicine*, Vol. 347(5), pp. 314-321, 2002.

153. Shea, S., A. Turgay, A. Carroll, M. Schulz, H. Orlik, I. Smith and F. Dunbar. "Risperidone in the Treatment of Disruptive Behavioral Symptoms in Children with Autistic and Other Pervasive Developmental Disorders", *Pediatrics*, Vol. 114(5), pp. e634-e641, 2004.

154. Blankenship, K., C. A. Erickson, K. A. Stigler, D. J. Posey and C. J. McDougle. "Aripiprazole for Irritability Associated with Autistic Disorder in Children and Adolescents Aged 6-17 Years", *Pediatric Health*, Vol. 4(4), pp. 375-381, 2010.

155. Aman, M. G., J. A. Hollway, C. J. McDougle, L. Scahill, E. Tierney, J. T. McCracken, L. E. Arnold, B. Vitiello, L. Ritz, A. Gavaletz, P. Cronin, N. Swiezy, C. Wheeler, K. Koenig, J. K. Ghuman and D. J. Posey. "Cognitive Effects of Risperidone in Children with Autism And Irritable Behavior", *Journal of Child and Adolescent Psychopharmacology*, Vol. 18(3), pp. 227-236, 2008.

156. West, L. and J. Waldrop. "Risperidone Use in the Treatment of Behavioral Symptoms in Children with Autism", *Journal of Pediatric Nursing*, Vol. 32(6), pp. 545-549, 2006.

157. Jesner, O. S., M. Aref-Adib and E. Coren. "Risperidone for Autism Spectrum Disorder", *Cochrane Database of Systematic Reviews,* Vol. (1), No. CD005040, 2007.

158. Willmann, S., J. Lippert, M. Sevestre, J. Solodenko, F. Fois and W. Schmitt. "PK-Sim®: A Physiologically Based Pharmacokinetic 'Whole-Body' Model", *Biosilico,* Vol. 1(4), pp. 121-124, 2003.

159. Valentin, J. "Basic anatomical and physiological data for use in radiological protection: reference values: ICRP Publication 89", *Annals of the ICRP,* Vol. 32(3-4), pp. 1-277, 2002.

160. National Center for Health Statistics Hyattsville, MD 20782, "Third National Health and Nutrition Examination Survey, (NHANES III)", 1997, http://www.cdc.gov/nchs/nhanes.htm, accessed on January 5, 2022.

161. Tanaka G. and H. Kawamura. "Anatomical and physiological characteristics for Asian reference man: Male and female of different ages: Tanaka model", Division of Radioecology, National Institute of Radiological Sciences, Hitachinaka 311-12 Japan, Report Number NIRS-M-115, 1996.

162. Fang, J., M. Bourin and G. B. Baker. "Metabolism of Risperidone to 9-Hydroxyrisperidone by Human Cytochromes P450 2D6 and 3A4". *Naunyn-Schmiedeberg's Archives of Pharmacology,* Vol. 359(2), pp. 147-151, 1999.

163. Yasui-Furukori, N., M. Hidestrand, E. Spina, G. Facciolá, M. G. Scordo and G. Tybring. "Different Enantioselective 9-Hydroxylation of Risperidone by the Two Human CYP2D6 and CYP3A4 Enzymes", *Drug Metabolism and Disposition,* Vol. 29(10), pp. 1263-1268, 2001.

164. Meyer, M., S. Schneckener, B. Ludewig, L. Kuepfer and J. Lippert. "Using Expression Data for Quantification of Active Processes in Physiologically Based Pharmacokinetic Modeling", *Drug Metabolism and Disposition,* Vol. 40(5), pp. 892-901, 2012.

165. Wong, Y. C., M. Centanni E. C. M. de Lange. "Physiologically Based Modeling Approach to Predict Dopamine D2 Receptor Occupancy of Antipsychotics in Brain: Translation from Rat to Human", *Journal of Clinical Pharmacology*, Vol. 59(5), pp. 731-747, 2019.

166. Sanchez-Covarrubias, L., L. M. Slosky, B. J. Thompson, T. P. Davis and P. T. Ronaldson. "Transporters at CNS Barrier Sites: Obstacles or Opportunities for Drug Delivery?" *Current Pharmaceutical Design*, Vol. 20(10), pp. 1422-1449, 2014.

167. Hoshi, Y., Y. Uchida, M. Tachikawa, T. Inoue, S. Ohtsuki and T. Terasaki. "Quantitative Atlas of Blood-Brain Barrier Transporters, Receptors, and Tight Junction Proteins in Rats and Common Marmose", *Journal of Pharmaceutical Sciences*, Vol. 102(9), pp. 3343-3355, 2013.

168. Shawahna, R., Y. Uchida, X. Decleves, S. Ohtsuki, S. Yousif, S. Dauchy, A. Jacob, F. Chassoux, C. Daumas-Duport, P. O. Couraud, T. Terasaki and J. M. Scherrmann. "Transcriptomic and Quantitative Proteomic Analysis of Transporters and Drug Metabolizing Enzymes in Freshly Isolated Human Brain Microvessels", *Molecular Pharmaceutics*. Vol. 8(4), pp. 1332-1341, 2011.

169. Uchida, Y., S. Ohtsuki, Y. Katsukura, C. Ikeda, T. Suzuki, J. Kamiie and T. Terasaki. "Quantitative Targeted Absolute Proteomics of Human Blood–Brain Barrier Transporters and Receptors", *Journal of Neurochemistry*, Vol. 117(2), pp. 333-345, 2011.

170. Cumming, P. "Absolute Abundances and Affinity States of Dopamine Receptors in Mammalian Brain: A Review", *Synapse*. Vol. 65(9), pp. 892-909, 2011.

171. Badhan, R. K. S., M. Chenel and J. I. Penny. "Development of a Physiologically-Based Pharmacokinetic Model of the Rat Central Nervous System" *Pharmaceutics*, Vol. 6(1), pp. 97-136, 2014.

172. Loryan, I., V. Sinha, C. Mackie, A. Van Peer, W. Drinkenburg, A. Vermeulen, D. Morrison, M. Monshouwer, D. Heald and M. Hammarlund-Udenaes. "Mechanistic

Understanding of Brain Drug Disposition to Optimize the Selection of Potential Neurotherapeutics in Drug Discovery", *Pharmaceutical Research*, Vol. 31(8), pp. 2203-2219, 2014.

173. Saibi, Y., H. Sato and H. Tachiki. "Developing In Vitro-In Vivo Correlation of Risperidone Immediate Release Tablet", *AAPS PharmSciTech*, Vol. 13(3), pp. 890-895, 2012.

174. Mannens, G., W. Meuldermans, E. Snoeck and J. Heykants. "Plasma Protein Binding of Risperidone and Its Distribution in Blood", *Psychopharmacology (Berl)*, Vol. 114(4), pp. 566-572, 1994.

175. Okubo, M., S. Morita, N. Murayama, Y. Akimoto, A. Goto and H. Yamazaki. "Individual Differences in In Vitro and In Vivo Metabolic Clearances of Antipsychotic Risperidone from Japanese Subjects Genotyped for Cytochrome P450 2D6 and 3A5", *Human Psychopharmacology Clinical and Experimental*, Vol. 31(2), pp. 93-102, 2016.

176. Sahlholm, K., H. Zeberg, J. Nilsson, S. O. Ögren, K. Fuxe and P. Århem. "The Fast-Off Hypothesis Revisited: A Functional Kinetic Study of Antipsychotic Antagonism of the Dopamine D2 Receptor", *European Neuropsychopharmacoly Journal of European College of Neuropsychopharmacoly*, Vol. 26(3), pp. 467-476, 2016.

177. Boulton, D. W., C. L. DeVane, H. L. Liston and J. S. Markowitz. "In Vitro P-Glycoprotein Affinity for Atypical and Conventional Antipsychotics", *Life Sciences*, Vol. 71(2), pp. 163-169, 2002.

178. Berezhkovskiy, L. M. "Volume of Distribution at Steady State for a Linear Pharmacokinetic System with Peripheral Elimination", *Journal of Pharmaceutical Sciences*, Vol. 93(6), pp. 1628-1640, 2004.

179. Belotto, K. C. R., N. R. B. Raposo, A. S. Ferreira and W.F. Gattaz. "Relative Bioavailability of Two Oral Formulations of Risperidone 2 Mg: A Single-Dose, Randomized-Sequence, Open-Label, Two-Period Crossover Comparison in Healthy

Brazilian Volunteers", *Clinical Therapy,* Vol. 32(12), pp. 2106-2115, 2010.

180. Boonleang, J., W. Pipatrattanaseree, C. Tanthana and W. Mahatthanatrakul. "Relative Bioavailability and Pharmacokinetic Comparison of Two 2-Mg Risperidone Tablet Formulations: A Single Dose, Randomized-Sequence, Double-Blind, 2-Way Crossover Study in Healthy Male Volunteers in Thailand", *Clinical Therapy,* Vol. 32(10), pp. 1842-1853, 2010.

181. Cánovas, M., J. Delgadillo, F. Torres, N. Rlba, J. Cebrecos, P. Pelagic and F. Cabrél. "Bioequivalence Evaluation of Two Strengths of Risperidone Tablet Formulations in Healthy Volunteers", *International Journal of Clinical Pharmacology and Therapies,* Vol. 47(2), pp. 124-131, 2009.

182. Gutierrez, R., P. I. Lee, M. L. Huang and R. Woestenborghs. "Risperidone: Effects of Formulations on Oral Bioavailability", *Pharmacotherapy,*Vol. 17(3), pp. 599-605, 1997.

183. Khorana, N., S. Maphanta, O. Lohitnavy, A. Srichaiya and J. Sayasathid. "Comparative Pharmacokinetics and Bioequivalence of Two Tablet Formulations of 2 Mg Risperidone in Healthy Thai Male Volunteers", *International Journal of Clinical Pharmacology and Therapeutics,* Vol. 49(6), pp. 409-414, 2011.

184. Siva Selva Kumar, M. and M. Ramanathan. "Concurrent Determination of Olanzapine, Risperidone and 9-Hydroxyrisperidone in Human Plasma by Ultra Performance Liquid Chromatography with Diode Array Detection Method: Application to Pharmacokinetic Study", *Biomedical Chromatography,* Vol. 30(2), pp. 263-268, 2016.

185. Liu, Y., M. Q. Zhang, J. Y. Jia, Y. M. Liu, G. Y. Liu, S. J. Li, W. Wang, L. P. Weng and C. Yu. "Bioequivalence and Pharmacokinetic Evaluation of Two Formulations of Risperidone 2 Mg : An Open-Label, Single-Dose, Fasting, Randomized-Sequence, Two-Way Crossover Study in Healthy Male Chinese Volunteers", *Drugs in R&D.* Vol. 13(1), pp. 29-36, 2013.

186. Nyberg, S., B. Eriksson, G. Oxenstierna, C. Halldin and L. Farde. "Suggested Minimal Effective Dose of Risperidone Based on PET-Measured D2 and 5-HT2A Receptor Occupancy in Schizophrenic Patients", *American Journal of Psychiatry*, Vol. 156(6), pp. 869-875, 1999.

187. Neal, E. G., H. Chaffe, R. H. Schwartz, M. S. Lawson, N. Edwards, G. Fitzsimmons, A. Whitney and J. H. Cross "The Ketogenic Diet for the Treatment of Childhood Epilepsy: A Randomised Controlled Trial", *The Lancet Neurology*, Vol. 7(6), pp. 500-506, 2008.

188. Moreno, H., L. Borjas, A. Arrieta, L. Saez, A. Prassad, J. Estevez and E. Bonilla. "Clinical Heterogeneity of the Autistic Syndrome: A Study of 60 Families", *Investigación cClínica*, Vol. 33(1), 13-31, 1992.

189. László, A., E. Horváth, E. Eck and M. Fekete. "Serum Serotonin, Lactate And Pyruvate Levels In Infantile Autistic Children", *Clinica Chimica Acta*, Vol. 229(1), pp. 205-207, 1994.

190. Oliveira, G., L. Diogo, M. Grazina, P. Garcia, A. Ataide, C. Marques, T. Miguel, L. Borges, A. M. Vicente and C. R. Oliveira. "Mitochondrial Dysfunction in Autism Spectrum Disorders: A Population-Based Study", *Developmental Medicine and Child Neurology*, Vol. 47(3), pp. 185-189, 2005.

191. Germanò, E., A. Gagliano, A. Magazù, T. Calarese, M. E. Calabro, M. Bonsignore, G. Tortorella and F. Calamoneri."Neurobiology of Autism: Study of a Sample of Autistic Children", *Minerva Pediatrica*, Vol. 58(2), pp. 109-120, 2006.

192. Correia, C., A. M. Coutinho, L. Diogo, M. Grazina, C. Marques, T. Miguel, A. Ataíde, J. Almeida, L. Borges, C. Oliveira, G. Oliveira and A. M. Vicente. "Brief Report: High Frequency of Biochemical Markers for Mitochondrial Dysfunction in Autism: No Association with the Mitochondrial Aspartate/Glutamate Carrier SLC25A12 Gene", *Journal of autism and Developmental Disorders*, Vol. 36(8), pp. 1137-1140, 2006.

193. Weissman, J. R., R. I. Kelley, M. L. Bauman, B. H. Cohen, K. F. Murray, R. L. Mitchell, R. L. Kern and M. R. Natowicz. "Mitochondrial Disease in Autism Spectrum Disorder Patients: A Cohort Analysis", *PLoS One,* Vol. 3(11), No. e3815, 2008.

194. Rossignol, D. A. and R. E. Frye. "Mitochondrial Dysfunction in Autism Spectrum Disorders: A Systematic Review and Meta-Analysis", *Molecular Psychiatry*. Vol. 17(3), pp. 290-314, 2012.

195. Khemakhem, A.M., R. E. Frye, A. El-Ansary, L. Al-Ayadhi and A. Bacha. "Novel Biomarkers of Metabolic Dysfunction is Autism Spectrum Disorder: Potential for Biological Diagnostic Markers", *Metabolic Brain Disease,* Vol. 32(6), pp. 1983-1997, 2017.

196. Chauhan, A., V. Chauhan, W. T. Brown and I. Cohen. "Oxidative Stress in Autism: Increased Lipid Peroxidation and Reduced Serum Levels of Ceruloplasmin and Transferrin - The Antioxidant Proteins", *Life Sciences,* Vol. 75(21), pp. 2539-2549, 2004.

197. James, S. J., P. Cutler, S. Melnyk, S. Jernigan, L. Janak, D. W. Gaylor and J. A. Neubrander. "Metabolic Biomarkers of Increased Oxidative Stress and Impaired Methylation Capacity in Children with Autism", *The American Journal of Clinical Nutrition*, Vol. 80(6), pp. 1611-1617, 2004.

198. Al-Gadani, Y., A. El-Ansary, O. Attas and L. Al-Ayadhi. "Metabolic Biomarkers Related to Oxidative Stress and Antioxidant Status in Saudi Autistic Children", *Clinical Biochemistry,* Vol. 42(10), pp. 1032-1040, 2009.

199. Essa, M. M., G. J. Guillemin, M. I. Waly, M. M. Al-Sharbati, Y. M. Al-Farsi, F. L. Hakkim, A. Ali and M. S. Al-Shafaee. "Increased Markers of Oxidative Stress in Autistic Children of the Sultanate of Oman", *Biological Trace Element Research,* Vol. 147(1), pp. 25-27, 2012.

200. Zoroglu, S. S., F. Armutcu, S. Ozen, A. Gurel, E. Sivasli, O. Yetkin and I. Meram.

"Increased Oxidative Stress and Altered Activities of Erythrocyte Free Radical Scavenging Enzymes in Autism", *European Archives of Psychiatry and Clinical Neuroscience*, Vol. 254(3), pp. 143-147, 2004.

201. Ming, X., T. P. Stein, M. Brimacombe, W. G. Johnson, G. H. Lambert and G. C. Wagner. "Increased Excretion of a Lipid Peroxidation Biomarker in Autism", *Prostaglandins, Leukotrienes and Essential Fatty Acids*, Vol. 73(5), pp. 379-384, 2005.

202. Essa, M. M., S. Subash, N. Braidy, S. Al-Adawi, C. K. Lim, T. Manivasagam and G. J. Guillemin. "Role of NAD+, Oxidative Stress, and Tryptophan Metabolism in Autism Spectrum Disorders", *International Journal of Tryptophan Research,* Vol. 6, No. IJTR.S11355, 2013.

203. Tamiji, J. and D. A. Crawford. "The Neurobiology of Lipid Metabolism in Autism Spectrum Disorders", *Neurosignals*, Vol. 18(2), pp. 98-112, 2010.

204. Boland, L. M., M. M. Drzewiecki, G. Timoney E. Casey. "Inhibitory Effects of Polyunsaturated Fatty Acids on Kv4/Kchip Potassium Channels", *American Journal of Physiology-Cell Physiology*, Vol. 296(5), pp. C1003-C1014, 2009.

205. Tallberg, T., J. Dabek, R. Hallamaa and F. Atroshi. "Lipidomics: The Function of Vital Lipids in Embryogenesis Preventing Autism Spectrum Disorders, Treating Sterile Inflammatory Diatheses with a Lymphopoietic Central Nervous System Component", *Journal of Lipids*, Vol. 2011, No. 137175, 2011.

206. Tierney, E., I. Bukelis, R. E. Thompson, K. Ahmed, A. Aneja, L. Kratz and R. I. Kelley. "Abnormalities of Cholesterol Metabolism in Autism Spectrum Disorders", *American Journal of Medical Genetics Part B: Neuropsychiatric Genetics*, Vol. 141(6), pp. 666-668, 2006.

207. Page, T. and M. Coleman. "Purine Metabolism Abnormalities in a Hyperuricosuric Subclass of Autism", *Biochimica et Biophysica Acta - Molecular Basis of Disease*, Vol. 1500(3), pp. 291-296, 2000.

208. Page, T., A. Yu, J. Fontanesi and W. L. Nyhan. "Developmental Disorder Associated with Increased Cellular Nucleotidase Activity", *Proceedings of the National Academy of Sciences,* Vol. 94(21), pp. 11601-11606, 1997.

209. Smith, A. M., J. J. King, P. R. West, M. A. Ludwig, E. L. Donley, R. E. Burrier and D. G. Amaral. "Amino Acid Dysregulation Metabotypes: Potential Biomarkers for Diagnosis and Individualized Treatment for Subtypes of Autism Spectrum Disorder", *Biological Psychiatry*, Vol. 85(4), pp. 345-354, 2019.

210. Ming, X., T. P. Stein, V. Barnes, N. Rhodes and L. Guo. "Metabolic Perturbance in Autism Spectrum Disorders: A Metabolomics Study", *Journal of Proteome Research,* Vol. 11(12), pp. 5856-5862, 2012.

211. Thiele, I., N. Jamshidi , R. M. T. Fleming and B. Ø. Palsson. "Genome-Scale Reconstruction of Escherichia coli's Transcriptional and Translational Machinery: A Knowledge Base, Its Mathematical Formulation, and Its Functional Characterization" *PLOS Computational Biology,* Vol. 5(3), No. e1000312, 2009.

212. Lubow, J. M., I. G. Piñón, A. Avogaro, C. Cobelli, D. M. Treeson, K. A. Mandeville, G. Toffolo and P. J. Boyle. "Brain Oxygen Utilization is Unchanged by Hypoglycemia in Normal Humans: Lactate, Alanine, and Leucine Uptake are Not Sufficient to Offset Energy Deficit", *American Journal of Physiology-Endocrinology and Metabolism*, Vol. 290(1), pp. E149-E153, 2006.

213. Madsen, P. L., N. F. Cruz, L. Sokoloff and G. A. Dienel. "Cerebral Oxygen/Glucose Ratio is Low during Sensory Stimulation and Rises above Normal during Recovery: Excess Glucose Consumption during Stimulation is Not Accounted for by Lactate Efflux from or Accumulation in Brain Tissue", *Journal of Cerebral Blood Flow and Metabolism,* Vol. 19(4), pp. 393-400, 1999.

214. Nybo, L., B. Nielsen, E. Blomstrand, K. Møller and N. Secher. "Neurohumoral Responses during Prolonged Exercise in Humans", *Journal of Applied Physiology,* Vol. 95(3), pp. 1125-1131, 2003.

215. Wahren, J., K. Ekberg, E. Fernqvist-Forbes and S. Nair. "Brain Substrate Utilisation during Acute Hypoglycaemia", *Diabetologia,* Vol. 42(7), pp. 812-818, 1999.

216. Gruetter, R., E. R. Seaquis and K. Ugurbil. "A Mathematical Model of Compartmentalized Neurotransmitter Metabolism in the Human Brain", *American Journal of Physiology-Endocrinology and Metabolism,* Vol. 281(1), pp. E100-E112, 2001.

217. Lebon, V., K. F. Petersen, G. W. Cline, J. Shen, G. F. Mason, S. Dufour, K. L. Behar, G. I. Shulman and D. L. Rothman. "Astroglial Contribution to Brain Energy Metabolism in Humans Revealed by 13C Nuclear Magnetic Resonance Spectroscopy: Elucidation of the Dominant Pathway for Neurotransmitter Glutamate Repletion and Measurement of Astrocytic Oxidative Metabolism", *Journal of Neuroscience,* Vol. 22(5), pp. 1523-1531, 2002.

218. Shen, J., K. F. Petersen, K. L. Behar, P. Brown, T. W. Nixon, G. F. Mason, O. A. C. Petroff, G. I. Shulman, R. G. Shulman and D. L. Rothman. "Determination of the Rate of the Glutamate/Glutamine Cycle in the Human Brain by In Vivo 13C NMR", *Proceedings of the National Academy of Sciences,* Vol. 96(14), pp. 8235-8240, 1999.

219. Oz, G., D. A. Berkich, P. G. Henry, Y. Xu, K. LaNoue, S. M. Hutson and R. Gruetter. "Neuroglial Metabolism in the Awake Rat Brain: CO2 Fixation Increases with Brain Activity", *Journal of Neuroscience,* Vol. 24(50), pp. 11273-11279, 2004.

220. Hertz, L., L. Peng and G. A. Dienel. "Energy Metabolism in Astrocytes: High Rate of Oxidative Metabolism and Spatiotemporal Dependence on Glycolysis/Glycogenolysis", *Journal of Cerebral Blood Flow and Metabolism,* Vol. 27(2), pp. 219-249, 2006.

221. Wiesinger, H., B. Hamprecht and R. Dringen. "Metabolic Pathways for Glucose in Astrocytes", *Glia,* Vol. 21(1), pp. 22-34, 1997.

222. Ben-Yoseph, O., D. M. Camp, T. E. Robinson and B. D. Ross. "Dynamic Measurements of Cerebral Pentose Phosphate Pathway Activity In Vivo Using [1,6-

^{13}C2,6,6-^{2}H2] Glucose and Microdialysis", *Journal of Neurochemistry,* Vol. 64(3), pp. 1336-1342, 1995.

223. Aureli, T., M. E. Di Cocco, M. Calvani and F. Conti. "The Entry of [1-13C]Glucose into Biochemical Pathways Reveals a Complex Compartmentation and Metabolite Trafficking Between Glia and Neurons: A Study by 13C-NMR Spectroscopy", *Brain Research,* Vol. 765(2), pp. 218-227, 1997.

224. Delhey, L., E. N. Kilinc, L. Yin, J. Slattery, M. Tippett, R. Wynne, S. Rose, S. Kahler, S. Damle, A. Legido, M. J. Goldenthal and R. E. Frye. "Bioenergetic Variation is Related to Autism Symptomatology", *Metabolic Brain Disease,*Vol. 32(6), pp. 2021-2031, 2017.

225. Zieminska, E., B. Toczylowska, D. Diamandakis, W. Hilgier, R. K. Filipkowski, R. Polowy, J. Orzel, M. Gorka and J. W. Lazarewicz. "Glutamate, Glutamine and GABA Levels in Rat Brain Measured Using MRS, HPLC and NMR Methods in Study of Two Models of Autism", *Frontiers in Molecular Neuroscience,* Vol. 11, No. 418, 2018.

226. Canela, E. I., G. Navarro, J. L. Beltrán and R. Franco. "The Meaning of the Michaelis-Menten Constant: K_m Describes a Steady-State", *bioRxiv,* No. 608232, 2019.

227. Barras, M. and A. Legg. "Drug Dosing in Obese Adults", *Australian Prescriber,* Vol. 40(5), pp. 189-193, 2017.

228. Gaedigk, A., K. Sangkuhl, M. Whirl-Carrillo, T. Klein and J. S. Leeder. "Prediction of CYP2D6 Phenotype from Genotype Across World Populations", *Genetics in Medicine,* Vol.19(1), pp. 69-76, 2017.

229. Puangpetch, A., N. Vanwong, N. Nuntamool, Y. Hongkaew, M. Chamnanphon and C. Sukasem. "CYP2D6 Polymorphisms and Their Influence on Risperidone Treatment", *Pharmacogenomics and Personalized Medicine,* Vol. 9, pp. 131-147, 2016.

230. Zhu, H. J., J. S. Wang, J. S. Markowitz, J. L. Donovan, B. B. Gibson and C. L. DeVane. "Risperidone and Paliperidone Inhibit P-Glycoprotein Activity In Vitro", *Neuropsychopharmacology*,Vol. 32(4), pp. 757-764, 2007.

231. Snoeck, E., A. Van Peer, G. Mannens, R. Woestenborghs, J. Heykants, M. Sack, M. Horton and R. Meibach. "Influence of Age, Renal and Liver Impairment on the Pharmacokinetics of Risperidone in Man", *Psychopharmacology (Berl)*, Vol. 122(3), pp. 223-229, 1995.

APPENDIX A: RECONSTRUCTED METABOLIC BRAIN MODEL REACTION, METABOLITE AND GENE LIST

The content is given on CD.

APPENDIX B: PHYSIOLOGY BASED PHARMACOKINETIC MODEL

The content is given on CD.

APPENDIX C: GENE EXPRESSION TRANSCRIPTOME DATA OF GSE28475

The content is given on CD.

APPENDIX D: AUTISM-SPECIFIC REDUCED METABOLIC BRAIN MODELS BY GIMME ALGORITHM REACTION, METABOLITE AND GENE LIST

The content is given on CD.